AD-A131 736 LASER INDUCED DAMAGE IN THE EYE: STUDY OF ENERGY DEPOSITION IN THE RETINA(U) UNIVERSITY OF WESTERN ONTARIO LONDON W J MCGOWAN ET AL. JUN 76 1/2

UNCLASSIFIED DAMD17-76-G-9401 F/G 6/18 NL

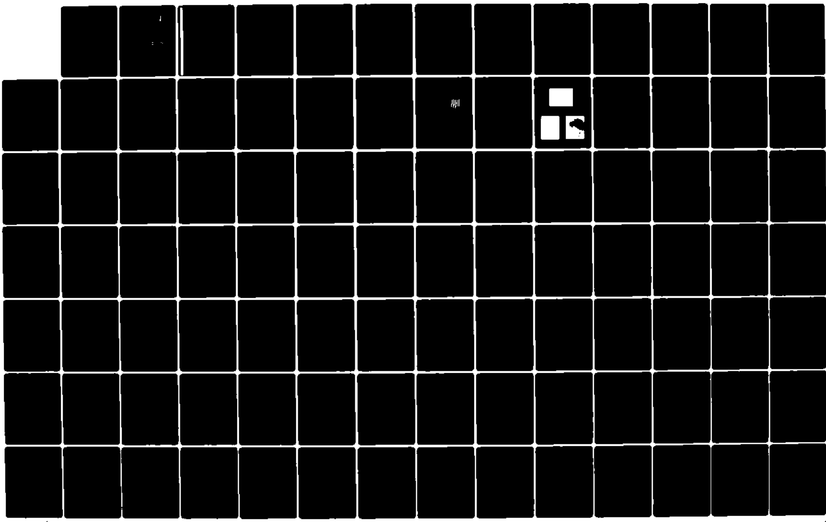

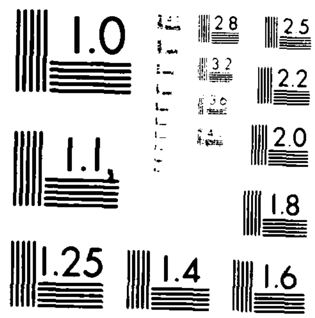

MICROCOPY RESOLUTION TEST CHART
NATIONAL

PHOTOGRAPH THIS SHEET

ADA131736

DTIC ACCESSION NUMBER

LEVEL: II

INVENTORY: I

Laser Induced Damage in the Eye

DOCUMENT IDENTIFICATION

Final, 1 Apr. '75 - 31 Mar '76

Grant DAMD17-75-G-9401

Jun. 76

DISTRIBUTION STATEMENT A
Approved for public release;
Distribution Unlimited

DISTRIBUTION STATEMENT

ACCESSION FOR		
NTIS	GRA&I	☒
DTIC	TAB	☐
UNANNOUNCED		☐
JUSTIFICATION		
BY		
DISTRIBUTION /		
AVAILABILITY CODES		
DIST	AVAIL AND/OR SPECIAL	
A		

DISTRIBUTION STAMP

DTIC
ELECTE
AUG 25 1983
S D
D

DATE ACCESSIONED

83 08 05 001

DATE RECEIVED IN DTIC

PHOTOGRAPH THIS SHEET AND RETURN TO DTIC-DDA-2

DTIC FORM OCT 79 70A

DOCUMENT PROCESSING SHEET

LASER INDUCED DAMAGE IN THE EYE

Final Report

William J. McGowan

June 1976

Supported by

US Army Medical Research and Development Command
Fort Detrick, Frederick, Maryland 21701

Contract No. DAMD17-75-G-9401

University of Western Ontario
London 72, Canada

The findings in this report are not to be construed as an Official Department of the Army position unless so designated by other authorized documents

SECURITY CLASSIFICATION OF THIS PAGE (When Data Entered)

REPORT DOCUMENTATION PAGE

READ INSTRUCTIONS BEFORE COMPLETING FORM

1. REPORT NUMBER	2. GOVT ACCESSION NO.	3. RECIPIENT'S CATALOG NUMBER
4. TITLE (and Subtitle) Laser Induced Damage in the Eye		5. TYPE OF REPORT & PERIOD COVERED Final Report 1 April 75 - 31 March 76
		6. PERFORMING ORG. REPORT NUMBER
7. AUTHOR(s) William J. McGowan		8. CONTRACT OR GRANT NUMBER(s) DAMD17-75-G-9401
9. PERFORMING ORGANIZATION NAME AND ADDRESS University of Western Ontario London 72, Canada		10. PROGRAM ELEMENT, PROJECT, TASK AREA & WORK UNIT NUMBERS 62772A.3E162772A813.00.009
11. CONTROLLING OFFICE NAME AND ADDRESS US Army Medical Research and Development Command Fort Detrick Frederick, Maryland 21701		12. REPORT DATE June 1976
		13. NUMBER OF PAGES 186 pages
14. MONITORING AGENCY NAME & ADDRESS(if different from Controlling Office)		15. SECURITY CLASS. (of this report) Unclassified
		15a. DECLASSIFICATION/DOWNGRADING SCHEDULE

16. DISTRIBUTION STATEMENT (of this Report)

Approved for public release; distribution unlimited.

17. DISTRIBUTION STATEMENT (of the abstract entered in Block 20, if different from Report)

18. SUPPLEMENTARY NOTES

19. KEY WORDS (Continue on reverse side if necessary and identify by block number)

20. ABSTRACT (Continue on reverse side if necessary and identify by block number)

DD FORM 1 JAN 73 1473 EDITION OF 1 NOV 65 IS OBSOLETE

SECURITY CLASSIFICATION OF THIS PAGE (When Data Entered)

THE UNIVERSITY OF WESTERN ONTARIO

Department of Physics and Centre for Interdisciplinary

Studies in Chemical Physics

LASER INDUCED DAMAGE IN THE EYE

STUDY OF ENERGY DEPOSITION IN THE RETINA

FINAL REPORT FOR THE PERIOD

Apr. 1/75 to Mar. 31/76

Work done by:

B. Borwein
C. Dyson
M.J. Hollenberg
A. Karkhanis
D. Lockyer
J.Wm. McGowan
J.A. Medeiros
M. Sanwal

Report written by:

J.Wm. McGowan
Principal Investigator

B. Borwein
Research Associate

J.A. Medeiros
Research Associate

M. Sanwal
Research Associate

Contract No.
U.S. Army Medical Research &
Development Command
Contracting Officer: Lt. Col. E. Woodward

June, 1976

TABLE OF CONTENTS

1. INTRODUCTION

The recent developments in high intensity light sources, particularly the laser, have focused interest and concern on damage - both accidental and therapeutic - to the human eye. The retina of the eye is particularly susceptible to light-induced damage. Considerable research has gone into a study of retinal damage and its repair. However, the major part of this work has dealt with gross damage. By contrast in our program we have tried to develop techniques that allow us to look at the electron microscopic level at damage throughout the entire retina as a function of the frequency of the bombarding radiation (its color) duration of radiation exposure and its intensity. We have also undertaken to examine electron microscopically the morphology of the retina following abuse by either laser light or other electromagnetic radiation in an attempt to understand the repair mechanisms.

Important to our understanding of damage and repair is a detailed understanding of how photoreceptors work. Our approach to this problem has been largely physical. Three years ago we began the program by accepting the trichromatic picture of color detection. However, over the last few years we have been led to the conclusion that the cones are acting as highly discriminatory dielectric waveguides, and detect color through strong dispersion of the incident spectra. If indeed all cones are created equal in local regions as is suggested by this model then radiation damage within the retina to the color discriminatory elements will be uniformly

distributed throughout, and will not be limited to the red, green or blue sensitive elements as has been proposed in the past. As for example, based upon the present model, one would expect that if the retina were to suffer an abuse brought about by an intense red light - not simply the red cones would be destroyed but rather all cones would be partially destroyed.

Accepting for the moment that the cones are dielectric waveguides we have carried out extensive calculations which have led to very specific predictions that can be tested not only in our laboratory but in many others. Our primary tool in testing this model and in causing controlled damage in the retina has been the tunable dye laser. We have been able to use light from this laser to create lesions of all sizes. We have subsequently examined the retinas with light microscopy, as well as transmission and scanning electron microscopes both at The University of Western Ontario and at the University of Calgary in Calgary, Alberta.

Our primary animal this year has remained the rabbit, although experiments have been begun with babboon eyes, quail eyes and monkey eyes. Complementing the program supported by the U.S. Army Medical Research & Development Command has been a study of the Human Eye undertaken in conjunction with the Ophthalmological community in London, Ontario. In these studies laser lesions have been placed in eyes affected with choroidal melanoma shortly before the enucleations. Subsequent to the removal parts of the retina have been made available to us for study.

With this report of our first year of operation under the U.S. Army Medical Research & Development Command we present primarily papers that have been submitted for publication, papers that are about to be submitted and those in preparation, along with abstracts of papers that we will or have presented at various congresses this year. The development of an effective multidisciplinary team has been a hard task, however, we have now reached the stage where our program is limited by the time available for detailed analysis of electron microscopic data. The superb working relationship that has developed between the team of scientists and the local ophthalmological community and the excellent cooperation we have had from the Department of Anatomy, will, we feel, bring considerable return within the next short while.

In the sections which follow we briefly outline our program as it has been carried out this year. However, the bulk of our results are summarized in the appendix, either in papers which have been published, submitted for publication or in preparation for submission.

2. DESCRIPTION OF FACILITIES AND TECHNIQUES USED

There are two principal laboratories at our disposal for these studies, one in the Physics Department where the Tunable Dye Laser is set up and through which the theoretical studies are being conducted, and the second in the Department of Anatomy. Besides these two laboratories we have at our disposal the Argon Ion Laser Photocoagulators at Victoria Hospital and St. Joseph's Hospital, electron microscopic facilities in the Departments of Clinical & Neurological Sciences and Pathology at University Hospital, and the laboratories and Scanning and Transmission Electron microscopes in the Division of Morphological Science, the Faculty of Medicine, University of Calgary.

The next few paragraphs will describe the equipment that has been used in each of these places.

2.1 FACILITIES IN THE LASER LABORATORY, THE UNIVERSITY OF WESTERN ONTARIO, DEPARTMENT OF PHYSICS

In the Laser Laboratory our main tool has been the Flashlamp Pumped Dye Laser, Synergetics Chromobeam 1050. This apparatus has been modified in such a way that it works in conjunction with a Topcon TRC-F Fundus Camera. Coupled with this apparatus is a gonioscopic animal holder designed primarily for our study of monkey eyes, although it has been successfully used for our rabbit eye studies. (Fig. 1).

The Synergetics Chromobeam 1050 Flashlamp pumped system has been useful in producing pulses of laser light that

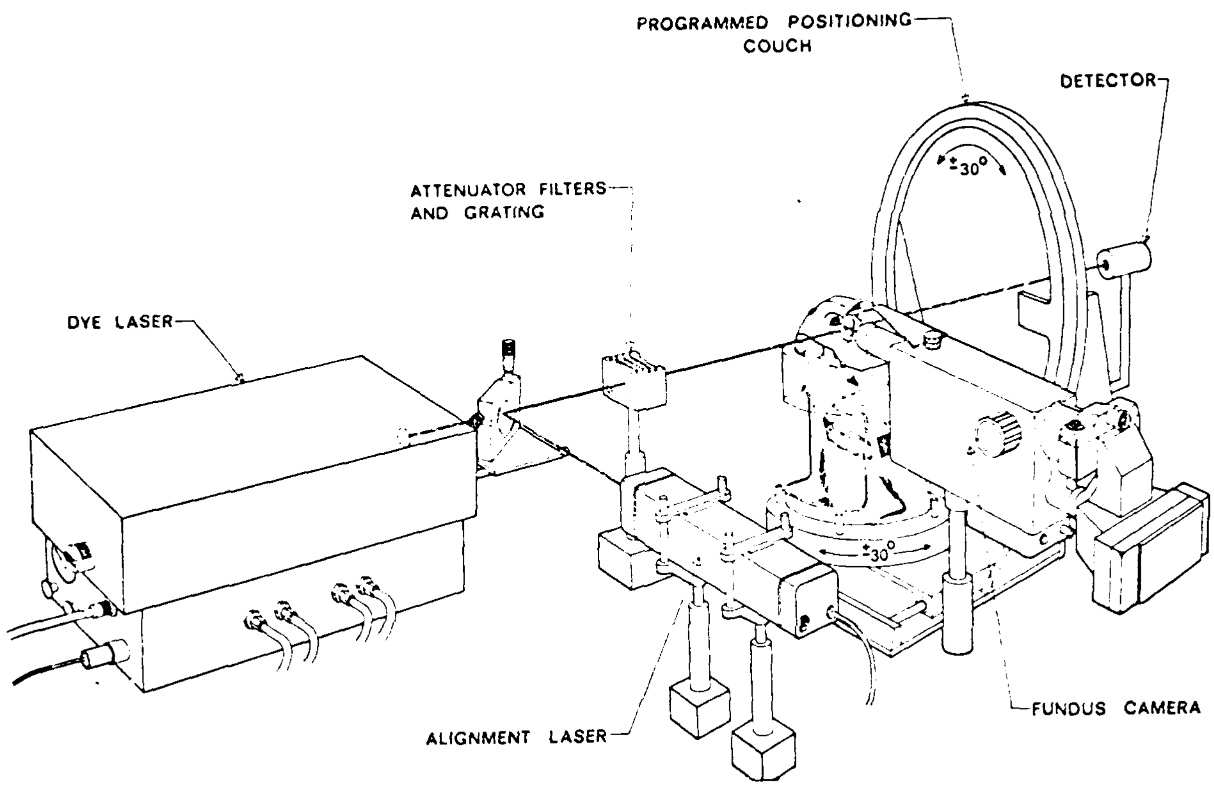

FIG. 1. Schematic diagram of the lasing apparatus. A pulsed, tunable dye laser is directed, via the fundus camera, into the eye of the subject animal. The animal holder is constructed to provide rotation independently about two orthogonal axis centered at the animal's pupil.

last about 0.5 μ sec. The second laser system is now being installed. It too will be coupled to the gonioscopic animal holder. The new system is a Control Laser 6 watt Argon Ion Laser which can be made to oscillate on a number of lines primarily in the blue-green. This system is to be used to pump a dye cell.

2.2 THE LABORATORY, ANATOMY DEPARTMENT, THE UNIVERSITY OF WESTERN ONTARIO

Because of the excellent cooperation of the A tomy Department our project has had at its disposal the foll ing optical microscopes:

Wild M20 Microscope and Camera

Bausch & Lomb Dissecting Microscope

Reichert NR241 421 Microscope

We have also been free to use the Rickert OMU2 Ultra Microtrome for which we have our own diamond knife. We also have at our disposal within the department the electron microscope facilities including:

Hitachi HHS-2 Scanning Electron Microscope

AEI 801 Transmission Electron Microscope

2.3 FACILITIES IN THE DEPARTMENTS OF OPHTHALMOLOGY

The Department of Ophthalmology at The University of Western Ontario is located primarily in three hospitals, University Hospital, Victoria Hospital and St. Joseph's Hospital. We have had excellent cooperation from all three groups, and in particular have been able to use the Argon Ion Laser Photocoagulators available in both Victoria and St. Joseph's Hospitals.

Victoria Hospital - Coherent Radiation Incorporated
Argon Ion Laser Photocoagulator

St. Joseph's Hospital - Model 150 Brit Electronics
Argon Laser Photocoagulator

2.4 LABORATORY IN THE DIVISION OF MORPHOLOGICAL SCIENCE, FACULTY OF MEDICINE, UNIVERSITY OF CALGARY

Although Prof. Martin Hollenberg is now Head of the Division of Morphological Science, University of Calgary, he had earlier on been associated with the Department of Anatomy, University of British Columbia. He has now established a new extensive laboratory system that is available for this project in Calgary, Alberta. In his laboratory he has a Cambridge 180 Scanning Electron Microscope and a Philips 300 Transmission Electron Microscope. These facilities, together with support personnel and his colleagues are available to assist with the program.

2.5 MEMBERSHIP IN THE CENTRE FOR CHEMICAL PHYSICS

On 3 May, 1973 the National Research Council of Canada announced the development of a Centre for Interdisciplinary Studies in Chemical Physics (CCP) at the University of Western Ontario. This organization was founded in response to a Canadian need for groups of established scientists from many disciplines to work together in well developed problem areas.

The Centre for Chemical Physics is designed to be an effective link between the University, government, industry,

medicine and the local community. It is constituted such that scientists, engineers, medical people, and in some instances non-scientists can work together within the institute as full members of that organization.

Perhaps the most important single program within the Centre is the Visiting Fellows program, modelled after a similar successful program at the Joint Institute for Laboratory Astrophysics, University of Colorado. This program brings to a focus specific program areas by bringing a number of experts to this University for prescribed periods.

The Visiting Fellows are drawn from the international community of established scientists, engineers and medical people, although an attempt is made each year to have at least one Visiting Fellow from a Canadian industry or government laboratory. Between three and six Visiting Fellows are scheduled to come to the University each year. They normally spend between six months and a year at the Centre. They have no formal commitment to teach, but are free to work at their own pace in conjunction with the other members of the Centre staff.

Four service groups are available to Centre members. They are: 1) Instrument Shop, 2) Electronics Shop, 3) Drafting and 4) Computing Services. There is only a minimal charge to Centre members for use of these services which are unique on the campus. Our project has made extensive use of these Centre facilities.

3. APPLICATION OF OPTICAL TRANSFORM TECHNIQUES TO LASER DAMAGE STUDIES

The conventional method employed for experimental determination of the threshold of damage to the retina by laser light consists of exposing test eyes to a large number of single shots over a wide range of incident intensities. The probability of observable damage resulting from each intensity over the whole range of exposure levels is then determined and a probit analysis enables one to evaluate that incident intensity which results in an observable lesion 50 percent of the time (the 50 percent effective dose level, ED_{50}).

There are several attendant difficulties with this method with which the experimenter must cope. Most of these problems occur because a large number of separate exposures must be carried out in order to obtain a statistically significant result. This means a large number of experimental animals must be used. This is an important problem when monkeys are the experimental animal of choice inasmuch as these animals are rapidly becoming prohibitively expensive. In addition many primate species are in danger of extinction and conservation considerations are strongly mitigating against the use of monkeys in acute experiments requiring large numbers of animals.

In addition to these considerations (which are forcing many researchers to reappraise their programs) there are some general problems of the technique which apply regardless of the experimental animal. Because of the large number of separate

exposures it is not necessarily obvious that the test eye is in a stable and unchanging state over the 1 to 2 hour exposure period. One must try to ascertain whether or not the previous exposures in a run have altered the state of the eye sufficiently to affect subsequent exposures during a given run. One also cannot be assured that the focal properties of the eye are stable over many exposures; neither can one determine whether or not all exposures in a run have the same relationship between the retinal energy density and the incident corneal energy density of the laser exposure. Furthermore, it is required that the laser output and calibration be stable over a long period while the exposures are carried out.

Virtually all of these problems can be circumvented if a large number of graded laser beams of known energy can bombard the retina at the same time. This can be and has been done in our laboratory. The technique entails passing the incident laser beam through an appropriate diffracting screen; depending on the choice of screen it is possible to tailor the pattern of focused exposures at the retinal surface in virtually any manner desired.

3.1 OPTICAL DIFFRACTION TECHNIQUES

An exact description of the scattering of light from a given diffracting object requires solution of Maxwell's equations subject to the appropriate boundary conditions. This method of solution can only be carried out for the simplest of geometries. For practical cases of interest it is necessary to use approximate methods; the accuracy of these methods can be

quite good, however. Using a scalar representation of the EM fields greatly simplifies the computations and is quite adequate if we are not interested in polarization effects and regions within a few wavelengths of the diffracting objects.

The general scalar theory leads to the Rayleigh-Sommerfield equation for the fields (Shulman, 1970). For many cases of interest this representation can be considerably simplified. A most useful approximation is that of Fraunhofer diffraction which applies whenever the incident and scattered fields can be adequately represented as plane waves. This obtains for collimated light incident on the diffracting object and observing the outgoing waves at large distances from the scattering region; equivalently the focal plane of a lens imaging the diffracting object satisfies the "great distance" criterion.

This is a standard problem in optics and is treated in many texts (see, for example, Born and Wolf, 1965). The main feature of this analysis is that the field distribution in the Faunhoffer domain is simply the Fourier transform of the field distribution in the diffracting plane. Figure 3.1 shows the geometry of interest: the physical picture is that of plane waves incident on an object, the subsequently diffracted waves are combined at the lens and appearing in the transform plane is the optical spectrum of the diffracting object resulting from interference of the scattered amplitudes.

It can be shown (Shulman, 1970) that if the area of consideration in the input plane and the back focal plane are

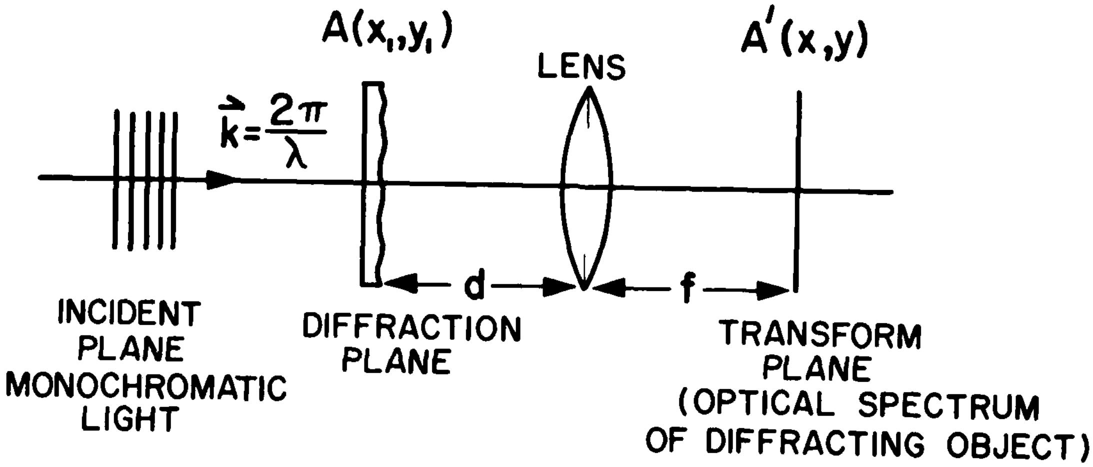

$$|A'(x,y)|^2 = \frac{|F(u,v)|^2}{\lambda^2 (d+f)^2}$$

$F(u,v)$ IS THE FOURIER TRANSFORM OF $A(x_1, y_1)$

FIG. 3.1 Diagram showing the geometry used in diffracted beam technique.

respectively restricted to domains given by

$$(x_1^2 + y_1^2)^{\frac{1}{2}} < f/5$$

and

$$(x^2 + y^2)^{\frac{1}{2}} < 0.14f$$

then the light amplitude distribution A'(x,y) in the back focal plane of a lens is accurately given by

$$A'(x,y) = \frac{-i\exp[ikR(x,y)]}{\lambda(f+d)} F(u,v) \tag{3.1}$$

where

$$u = x/\lambda f, \quad v = y/\lambda f \tag{3.2}$$

$$R(x,y) = \frac{f^2 + df + x^2 + y^2}{(f^2 + x^2 + y^2)^{\frac{1}{2}}} \tag{3.3}$$

and

$$F(u,v) = \iint A(x_1,y_1) \exp[-2\pi i(ux_1 + vy_1)] \, dx_1 \, dy_1 \tag{3.4}$$

F(u,v) is the Fourier transform (two dimensional) of the light amplitude distribution $A(x_1,y_1)$ a distance d in front of the lens. The physically measurable quantity in the transform plane is the intensity or square of the light amplitude distribution

$$|A'(x,y)|^2 = \frac{1}{\lambda^2(f+d)^2} |F(u,v)|^2 \tag{3.5}$$

The computation of the Fourier transform of many simple diffracting objects is easily evaluated. The diffraction from more complex objects can often be evaluated as combination of these simple cases where the linearity of the Fourier transform is exploited (the transform of a product or sum is the product or sum of the individual transforms). An important special case for the diffracting object is that of a transmission function consisting of a periodic array of alternately transmitting and opaque bands (diffraction grating).

A Ronchi ruling is a square wave grating with alternating opaque and transparent regions of equal width. Such a square wave train alternating between the amplitudes 0 and 1 with an angular frequency ω (2π times the grating frequency) can be written as the infinite Fourier series:

$$f(y_1) = \tfrac{1}{2}\left(1 + \frac{4}{\pi}\cos \omega y_1 - \frac{4}{3\pi}\cos 3\omega y_1 + \frac{4}{5\pi}\cos 5\omega y_1 - \ldots\right) \tag{3.3}$$

which is a series consisting of a DC term (½) equal to the mean value of the square wave amplitude and alternately the addition and subtraction of the cosine of the odd harmonics of the fundamental grating frequency. Writing the cosine as its component complex exponentials this is:

$$f(y_1) = \tfrac{1}{2} + \frac{1}{\pi} e^{i\omega y_1} + \frac{1}{\pi} e^{-i\omega y_1} - \frac{1}{3\pi} e^{i3\omega y_1} - \frac{1}{3\pi} e^{-i3\omega y_1} + \ldots \tag{3.4}$$

The Fourier transform of each of these terms gives a point in the inverse frequency space (transform plane of the lens). Thus the optical transform of a Ronchi ruling will consist of points in the focal plane of the lens corresponding to the associated frequencies; there will be a DC or zero order term of amplitude ½, and the ± odd harmonics of ω, $(2n+1)\omega$ of amplitude $1/(2n+1)\pi$. The positions of the spectral components in the transform plane are odd multiples of the quantity $y_o = \lambda f\omega/2$ when the grating is placed in the front focal plane of the lens. The scattering geometry and optical spectrum of a Ronchi ruling is shown in Figure 3.2

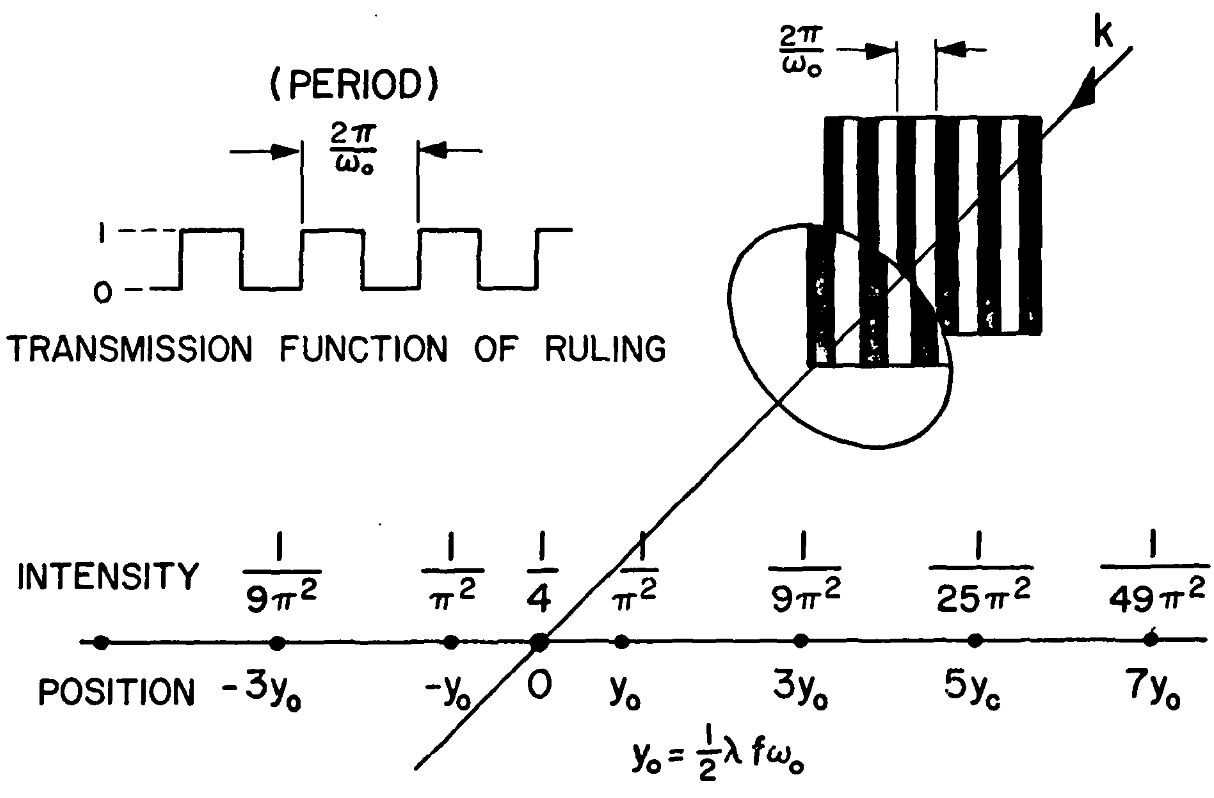

FIG. 3.2 Scattering geometry and optical spectrum of a Ronchi ruling.

Fig. 3.3 Fundus photograph of the rabbit retina taken within a few minutes of exposure to laser shots. A range of intensities of conventional single shots are evident. Note the three shots produced by a single Ronchi ruling just to the right of the large, dark burn in the center of the photograph.

Fig. 3.4 Computed intensities of a laser beam diffracted by two crossed rulings.

Fig. 3.5 A photograph of the frequency spectrum of two crossed rulings. The relative intensities of the components is given by Fig. 3.4. Note that the gratings used for this photograph are not exact Ronchi rulings since even frequency components are visible in the spectrum.

Fig. 3.6 The photo shows the spectrum of a grating of spatial frequency 2ω on the left with the dc and 1st order terms heavily over-exposed. On the right is the spectra of a grating with a spatial frequency ω and the over-exposed central orders with the spectrum of the undiffracted, focused plane wave (i.e. just the d.c. term) just to the left of this spectrum. The central spectrum is that of the two gratings superimposed parallel to each other. Proportionally less energy is in the lower diffraction orders and more in higher orders.

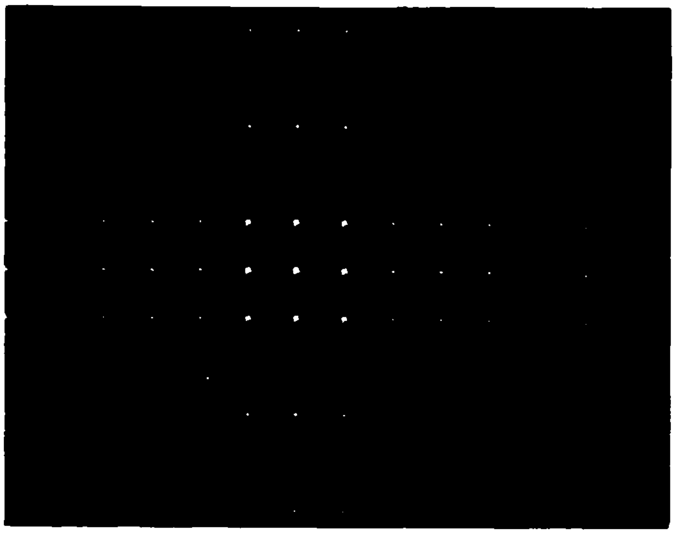

FIG. 3.5

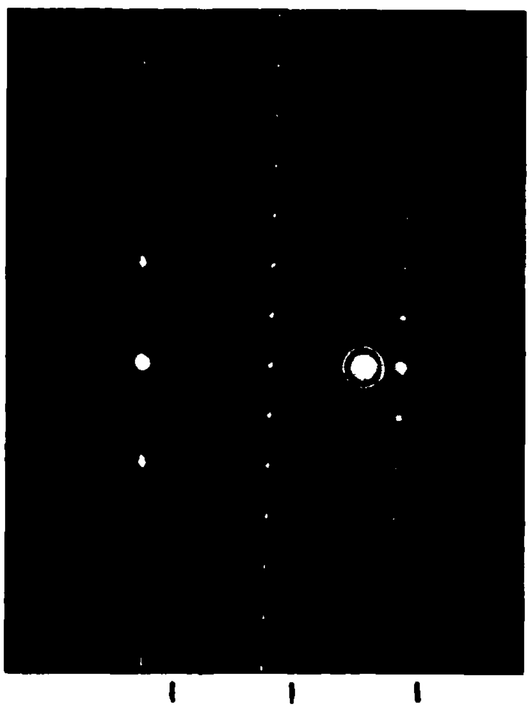

40 CPS 20x40 20CPS

FIG. 3.6

FIG. 3.3

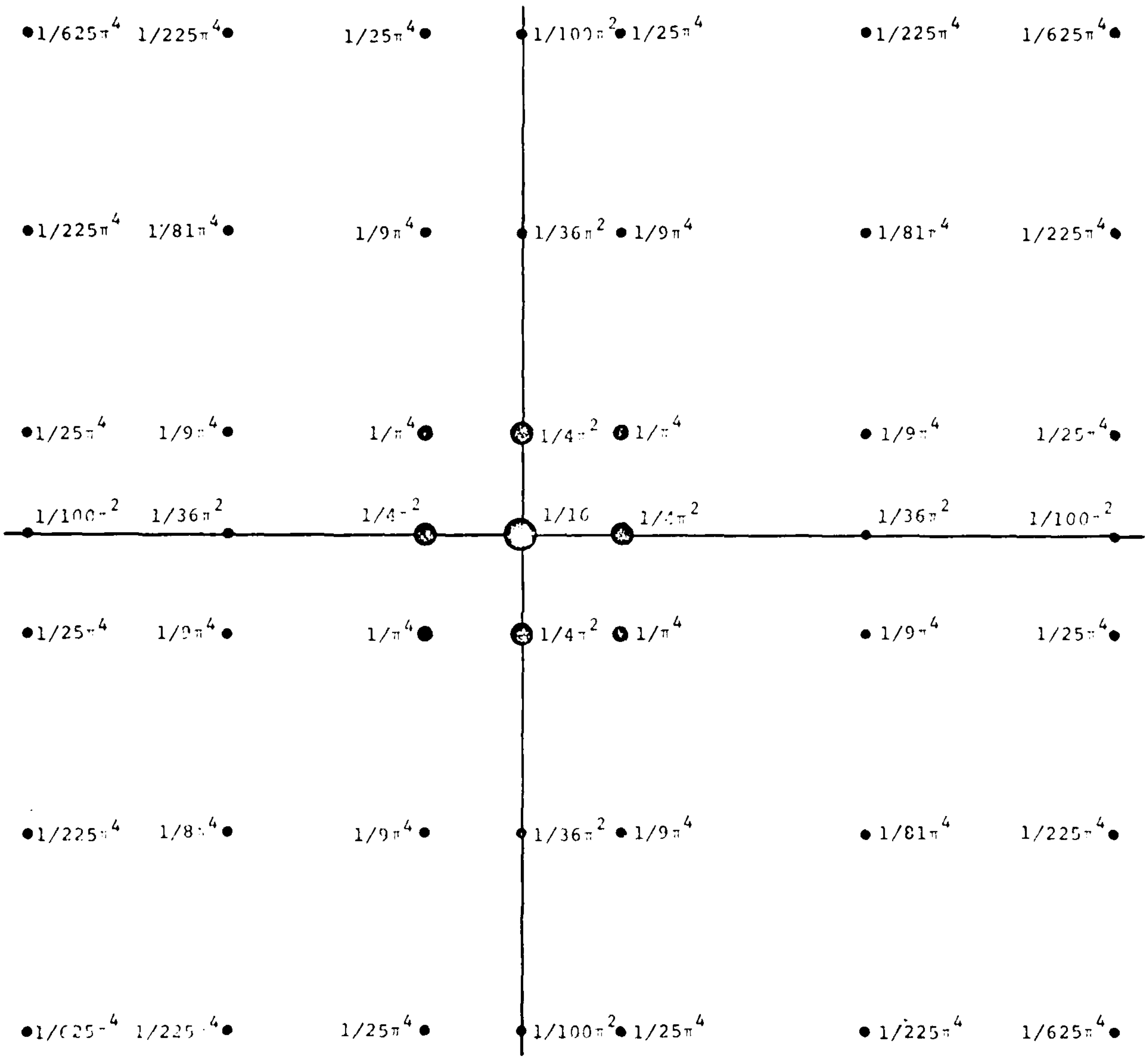

FIG. 3.4 Computed intensities of a laser beam diffracted by two crossed rulings.

Figure 3.3 is a fundus photograph of a rabbit retina which has been exposed to a large range of laser beam intensities. A linear sequence of lesions vertically oriented is visible beside the very large central lesion. This is the burn pattern resulting from diffraction of the incident laser beam through a Ronchi ruling. The D.C. and two first order terms are easily visible in this pattern. Note that in retinal damage studies it is only necessary to refract the test eye for accommodation to infinite distance, no other lenses are required. This process can be extended to two dimensions by crossing two Ronchi rulings. Fig. 3.4 shows the computed intensities and Fig. 3.5 a photograph of a laser beam diffracted by two crossed rulings. Some features worth noting in Fig. 3.5 are the presence of small amounts of even harmonics in the spectra (due to phase variations in the rulings) and ghost spots due to multiple reflections in the glass plates forming the rulings. These illustrate the difficulties that must be guarded against (and can in fact be dealt with) in this technique for laser damage measurements.

One limitation of the transmission grating technique is the relatively large amount of energy in the diffraction pattern in the zeroth and first orders. Most information on damage thresholds are obtained when there is a slowly varying gradation of intensities around the threshold level. Such a gradation is present in the higher orders of the grating spectra. The intensity of the 13th frequency component is 72% of the intensity of the 11th component; ratios for higher terms are

even larger. Unfortunately, use of light intensities high enough to put these higher orders around the threshold level is precluded in retinal damage studies. The intensity of the first two orders would be sufficient to produce catastrophic retinal damage. This difficulty can be circumvented, however. One possibility is to block the first two components in the transform plane (optical filtering) and reimage the modified transform at the retina with additional lenses.

A less cumbersome method is to use an appropriate combination of the commercially available Ronchi rulings. One simple technique is to superimpose two rulings, one of twice the frequency of the other with their rulings parallel to each other. The transmission function of this combination consists of a repeating array which is transmitting over 1/4 of its cycle and opaque over 3/4 of the cycle. This has the desired effect of decreasing the relative contribution of the lower order terms and increasing the contribution to the power spectrum of the higher frequency components. This effect is shown in Figure 3.6 . The relative intensities of the DC term and the 1st to 5th harmonic terms are in the sequence: 1.0, 0.576, 0.405, 0.182, 0, .021. This example is illustrative of the possibilities inherent in the transform technique. Other combinations can be chosen to suit particular experimental needs.

Another method is to use a grating in which the modulations are in transmitted phase only. By proper choice of the phase differential it is possible to tailor the resulting interference pattern in the transform plane to have virtually any desired distribution of energy among the diffracted orders

including even zero intensity in the zeroth order.

For a phase grating of sinusoidal modulations in transmitted phase with m (in radians) the amplitude of the phase excursion, the peak intensity of the qth order component is proportional to $[J_q(m/2)]^2$ where $J_q(m/2)$ is the Bessel function of the first kind of order q (see for example, Goodman, 1968).

Two examples of the intensity distribution in the first eight orders for peak-to-peak excursions of the phase delay given by $m/2 = 4$ and $m/2 = 6$ are shown in Figure 3.7. As may be inferred from these plots, the trend is for a higher proportion of the diffracted power to appear in higher orders for increasing phase excursions.

These phase gratings can be produced by bleaching a photographic negative of a transmission grating. The areas of greatest density of developed grains in the negative will have the greatest emulsion thickness and thus the greatest phase delay when bleached. Phase gratings have also been produced by exposing dichromated gelatin films to an appropriately modulated light distribution. Dichromated gelatin renders light amplitude information directly as modulations of the film thickness and consequently as a phase grating. The phase excursions produced by these methods can, however, be rather difficult to control.

While we have focused our attention on diffracting gratings, it should be noted that the optical transform technique is much more versatile than we have thus far implied. It is in fact possible to tailor the light distribution in a transform plane to be virtually any pattern desired. Using

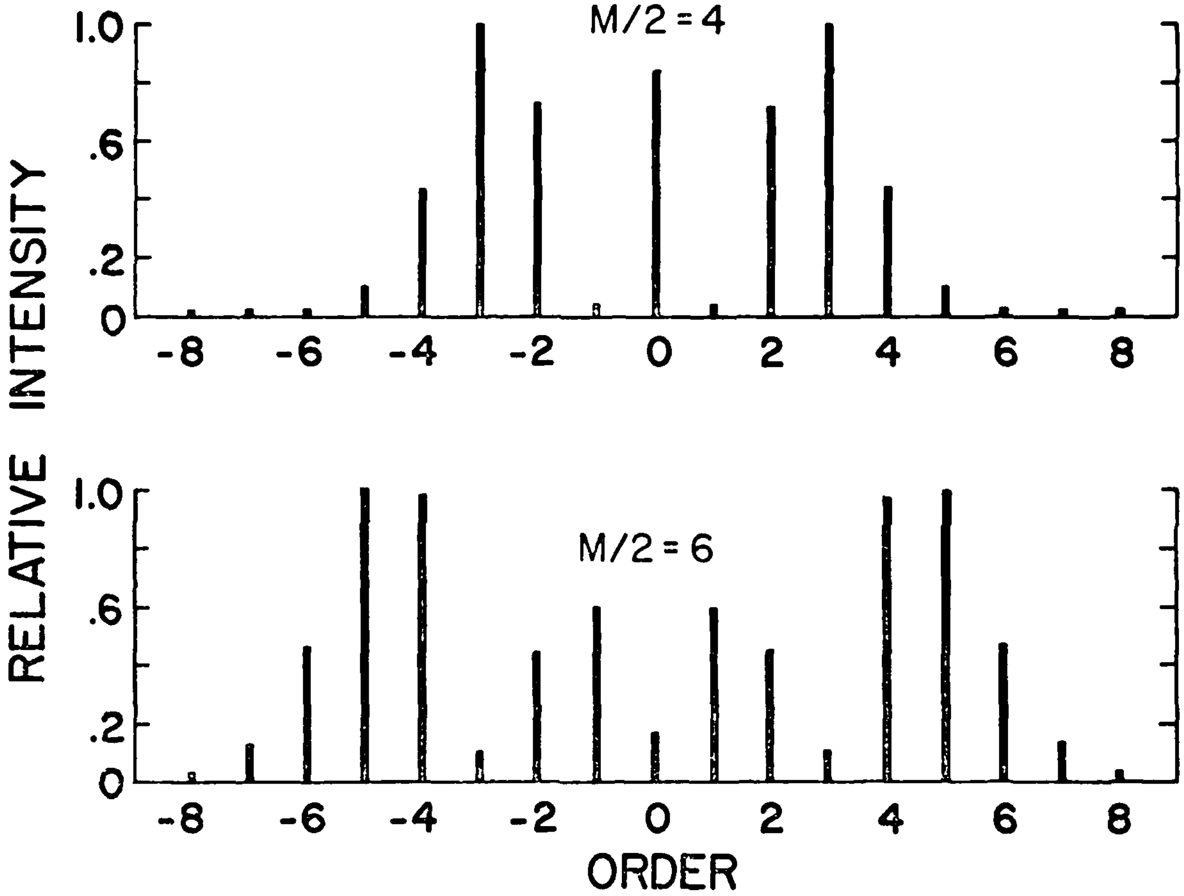

FIG. 2.7 Two examples of the intensity distribution in the first eight orders for peak-to-peak excursions of the phase delay.

techniques similar to that employed in making printed circuit boards, one can photographically produce a diffracting screen which is the optical transform of a desired pattern. A method is to draw a pattern with black dots, for example, whose area is proportional to the intensity of the transmitted radiation desired in the transform plane. This may be photographed and reduced in size and rendered in copper on glass films. The optical transform of this screen will then be the diffracting object desired; it can also be photographed and rendered as the desired diffracting screen.

4. PROPAGATION AND SPECTRAL DISPERSION OF ELECTROMAGNETIC RADIATION IN A TAPERED DIELECTRIC ROD

Our objective is to examine the light propagation characteristics of a slightly tapered cylinder with a diameter only slightly larger than the wavelength of the propagated radiation. This problem is relevant to primate foveal cones whose light sensitive portions are less than one micron in diameter. Foveal cone tapers to be inferred from light microscopic measurements (Polyak, 1941) are on the order of 0.5 degrees (full taper angle). Solving the transmission problem for a tapered cylinder (cone) is considerably more complex than for a uniform rod. Fortunately, for our purposes, exact solution of the more complex problem is not needed; for sufficiently small taper angles, light propagation in a cone is well represented in local regions by the uniform cylinder solutions. This representation will be discussed in more detail after first considering the nature of the solutions for the case of the infinite, uniform rod.

4.1 THE UNIFORM DIELECTRIC WAVEGUIDE

The geometry of interest is shown in Fig. 4.1. A dielectric cylinder of diameter d and refractive index n_1 is embedded in an infinite medium of refractive index n_2. The cylinder long axis is chosen as the Z direction and a plane wave of wavelength λ is incident with wave vector $|\vec{k}| = 2\pi/\lambda$.

For the general case of EM wave propagation in a source-free homogenous medium the fields must satisfy the wave equation

$$\left[\nabla^2 - \epsilon\mu\,(\partial^2/\partial t^2)\right] \begin{Bmatrix} \vec{E} \\ \vec{H} \end{Bmatrix} = 0 \qquad (4.1)$$

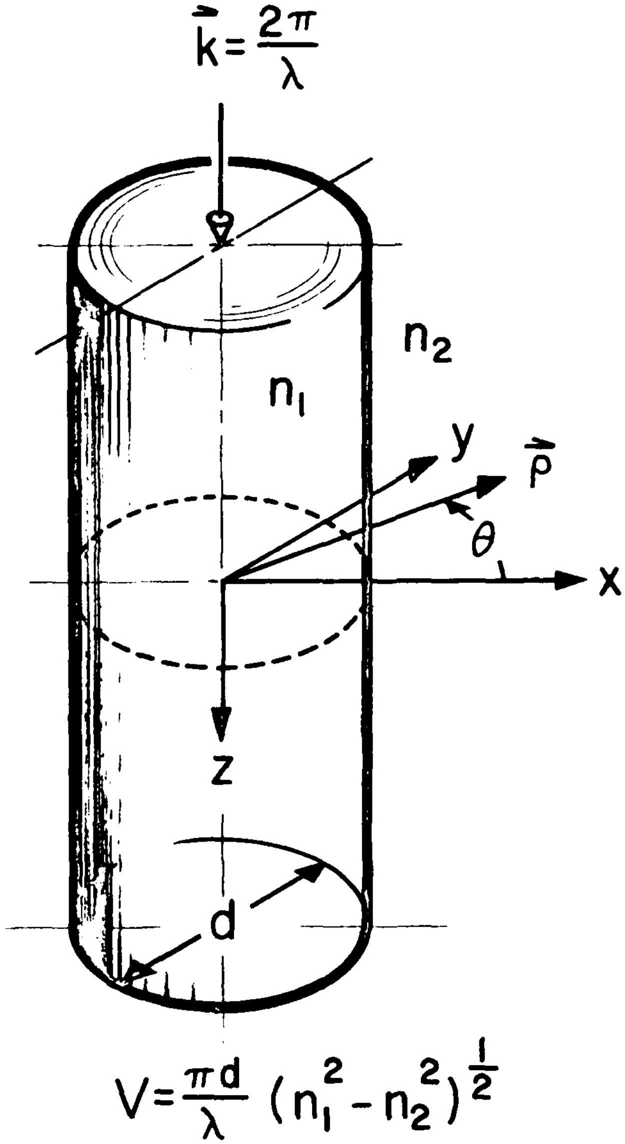

FIG. 4.1 DIELECTRIC WAVEGUIDE GEOMETRY. A cylinder of diameter d and refractive index n_1 is embedded in an infinite medium of refractive index of n_2. Light of wave vector $\vec{k}$ is incident along the z axis which is coincident with the cylinder axis. The polar coordinates ρ and θ are shown with respect to the rectangular coordinates x and y. The quantities n_1, n_2, d, and λ determine the waveguide characteristic parameter V.

where ϵ and μ are the dielectric constant and magnetic permeability of the medium. A particular solution is obtained by applying the appropriate boundary conditions.

For the dielectric rod the tangential components of the electric and magnetic fields of the radiation are required to be continuous across the rod-surround interface. We are, in addition interested in those solutions representing local confinement to the rod structure (guided waves). We thus match those solutions at the boundary for which the fields are zero at infinite radial distance (non-radiative propagation) and finite within the waveguide.

We are interested in those elementary solutions which are in the form

$$\left.\begin{matrix} \vec{E}(x,y,z,t) \\ \vec{H}(x,y,z,t) \end{matrix}\right\} = \left\{\begin{matrix} \vec{F}(x,y,h,\omega) \\ \vec{G}(x,y,h,\omega) \end{matrix}\right\} exp\ (i\omega t - ihz) \tag{4.2}$$

The general procedure consists of substituting this form for the fields in the wave equation (4.1); we must then solve for the eigenvectors $\vec{F}$ and $\vec{G}$ and the eigenvalues h. The eigenvalue equation is

$$(\nabla_T^2 + \beta^2) \left\{\begin{matrix} \vec{F}(x,y,z) \\ \vec{G}(x,y,z) \end{matrix}\right\} = 0 \tag{4.2}$$

where

$$\beta^2 = k^2 - h^2 = \omega^2\epsilon\mu - h^2 \tag{4.3}$$

is the propagation constant of the medium and the transverse Laplacian operator is

$$\nabla_T^2 = \frac{\partial^2}{\partial x^2} + \frac{\partial^2}{\partial y^2} = \frac{\partial^2}{\partial \rho^2} + \frac{1}{\rho}\frac{\partial}{\partial \rho} + \frac{1}{\rho^2}\frac{\partial^2}{\partial \phi^2}$$

where ρ and ϕ are the polar coordinates

$$\rho = (x^2 + y^2)^{\frac{1}{2}}$$

$$\phi = \tan^{-1}\ (y/x).$$

We will use the subscript 1 to refer to the values of the medium constants inside the guide and the subscript 2 for the constants outside the guide. Thus, for example, we will have inside the guide the values ε_1, k_1, n_1, [illegible]$_1$, μ_1, h_1. For dielectric media of interest $\mu_1 = \mu_2$ and we also find that $h_1 = h_2$.

The explicit form of this equation (4.2) written out in the cylindrical coordinates dictated by the geometry of the problem is, upon separation of variables [illegible] and ϕ, just Bessel's differential equation for the radial function. The eigenfunction solutions we seek are found to be Bessel functions of the first kind inside the guide and modified Bessel functions of the second kind outside the guide.

These eigenfunction solutions of the problem correspond to propagation modes of the waveguide and the number of such solutions depends on the physical parameters of the guide. These physical parameters determine the propagation characteristic in the form of the dimensionless frequency V given by the waveguide characteristic equation:

$$V = \frac{\pi d}{\lambda} \left(n_1^2 - n_2^2\right)^{\frac{1}{2}} \tag{4.4}$$

As the parameter V decreases, the number of eigenvector solutions which satisfy equation (4.2) and, consequently, the number of allowed propagation modes decreases. Large V means many propagation modes are allowed; the superposition of a large number of modes means that the interior of the guide can be uniformly illuminated. This case of a large rod (because of large V) is just the geometric optics limit.

In the more familiar metal-wall waveguide the boundary condition imposed by the vanishing of the fields within the metal result in TE (transverse electric) and TM (transverse magnetic) propagation modes. In the dielectric waveguide none of the field components are necessarily zero (although TE-like and TM-like solutions do exist). In general the solutions are hybrid in that the transverse components of both $\vec{E}$ and $\vec{H}$ are non-zero. Two kinds of mode solutions are found, the so-called HE and EH modes. We will be interested in the lowest order mode, the HE_{11} mode which is the only propagated mode for $V < 2.405$.

The analysis of Kapany and Burke (1972) is a useful and informative method of solving the waveguide problem. In solving equation (4.2) they use complex transverse field components (4.5)

$$E_{\pm} = E_x \pm iE_y$$

and upon application of the boundary conditions it is found that the solutions for the fields inside the guide are:

$$E_{\pm} = \pm\,(1 \pm \alpha)\; A\, J_{n\pm 1}\; (u\rho/\tfrac{1}{2}d)\; \exp[i(n\pm 1)\phi + i\omega t - ihz]$$

$$E_z = (2\beta_1/ih)\; A\, J_n\; (u\rho/\tfrac{1}{2}d)\; \exp[\, in\phi + i\omega t - ihz]$$

$$H_{\pm} = \pm\,(ih/\omega\mu)\; [(k_1{}^2/h^2 \pm \alpha)/(1 \pm \alpha)]\; E_{\pm} \qquad (4.6)$$

$$H_z = (ih/\omega\mu)\; \alpha E_z$$

and outside the guide the fields are equations (4.6) with the substitutions

$$J_p(up/\tfrac{1}{2}d) \rightarrow H_p(\nu p/\tfrac{1}{2}d),\ p = n-1,\ n,\ n+1$$

$$A \rightarrow A \quad uJ_n(u)/\nu H_n(\nu) \tag{4.7}$$

$$\beta_1 \rightarrow \beta_2$$

$$k_1 \rightarrow k_2$$

Where d is the diameter of the guide and A is arbitrary with AA* proportional to the power in the mode. $H_n(\nu)$ is the Hankel function and for bound modes we are interested in the case $\nu = -iq$ where q is real. We will use modified Bessel functions of the second kind, K_n, given by the substitution

$$H_n(-iq) = (-i)^{-n-1}\,(2/\pi)\,K_n(q)$$

The eigenvalues u and q are related through

$$V^2 = u^2 + q^2 = (k_1{}^2 - k_2{}^2)\,\frac{d}{4} = \left(\frac{\pi d}{\lambda}\right)^2 (n_1{}^2 - n_2{}^2) \tag{4.8}$$

α is found from the boundary conditions to be

$$\alpha = n\left[\frac{1}{u^2} + \frac{1}{q^2}\right]\left[\frac{J_n'(u)}{uJ_n(u)} + \frac{K_n'(q)}{qK_n(q)}\right]^{-1} \tag{4.9}$$

where the prime denotes differentiation with respect to the argument of the Bessel function. Now $u = \beta_1 d/2$ and $q = \beta_2\, d/2$ and these eigenvalues are determined by the lowest non-zero value of u which satisfies the eigenvalue equation, arising from the application of the boundary conditions. For HE_{nm} modes this equation is

$$\frac{J_{n-1}(u)}{J_n(u)} = \frac{-(\epsilon_1+\epsilon_2)}{2\epsilon_1}\;\frac{u}{q}\;\frac{K_n'(q)}{K_n(q)}$$

$$+\ u\left\{\frac{n}{u^2}\quad\left[\left(\frac{(\epsilon_2-\epsilon_1)}{2\epsilon_1}\;\frac{K_n'(q)}{qK_n(q)}\right)^2 + n^2\left(\frac{1}{u^2} + \frac{1}{q}\right)\left(\frac{1}{u^2} + \frac{\epsilon_2}{\epsilon_1 q^2}\right)\right]^{\frac{1}{2}}\right\}$$

$$\tag{4.10}$$

The problem consists of finding those values of u and q which satisfy this transcendental eigenvalue equation corresponding to the waveguide with physical parameters ε_1, ε_2 and V for the possible choices of mode number n (n = 0,1,2,3,...). The values of u and q are then used in equations (4.6) and (4.7) to evaluate the fields.

The power propagated by the waveguide is given by the time-averaged axial component of the Poynting vector:

$$S_z = \frac{1}{4} \mathrm{Re} \quad i(E_+H_+^* - E_-H_-^*) \tag{4.11}$$

Now the power flow inside the waveguide is given by the integration

$$P_1 = \int_0^{2\pi} \int_0^{d/2} \bar{S}_z \; \rho d\rho d\phi \tag{4.12}$$

and outside by integrating over the space exterior to the rod

$$P_2 = \int_0^{2\pi} \int_{d/2}^{\infty} \bar{S}_z \; \rho d\rho d\phi \tag{4.13}$$

(The power flow along the outside of the cylinder occurs as an evanescent surface wave whose amplitude decreases rapidly with increasing radial distance).

We will be concerned with determining that fraction of the total power propagated in the mode which is conducted inside the guide. This fraction, η, is given by P_1 and P_2 above (with total power = $P_1 + P_2$) by

$$\eta = \frac{P_1}{P_1 + P_2} = [1 + P_2/P_1]^{-1} \tag{4.14}$$

This modal efficiency, η , is particularly important for retinal

receptors since it is only the energy flux conducted within the waveguide that can be absorbed by the photopigment contained therein and thus have a physiological effect. Of course, as some of the incident radiation is absorbed within the guide there will tend to be power flow into the guide since if P_1 decreases, then P_2 also decreases in order to satisfy equation (4.15). However, for the case of interest (retinal cones) absorption of incident radiation is in general small compared to attenuation due to power transfer out of the cone as η decreases with decreasing diameter.

For the retinal cones we use the refractive index values $n_1 = 1.387$ and $n_2 = 1.347$ (Sidman, 1957, Barer, 1957) which gives $\pi(n_1^2 - n_2^2)^{1/2} = 1.04$ and $\delta = 1 - (n_2/n_1)^2 = .0568$. For foveal cones d is no larger than 0.9 micron (Polyak, 1941; Cohen, 1972; Dowling, 1965). Thus in the visible wavelength range (0.4 to 0.7 microns) an upper limit on V for the foveal cones is approximately $V < 2.34$ (using the waveguide characteristic equation $V = (\pi d/\lambda)(n_1^2 - n_2^2)^{1/2}$.)

For values of $V < 2.405$ only the HE_{11} mode can be propagated by the guiding structure (higher modes are cut off). Thus particularizing the equations above for the eigenvalues in the case of $n = 1$, and using the definition

$$\delta = 1 - k_2^2/k_1^2 = 1 - \epsilon_2/\epsilon_1 = 1 - (n_2/n_1)^2$$

we have for the eigenvalue equation of the HE_{11} mode

$$J_0/J_1 = \frac{1}{u} - (1-\delta/2)\left(\frac{uK_0}{qK_1} + \frac{u}{q^2}\right) - \left[\frac{V^2}{q^4}\left(\frac{V^2}{u^2} - \delta\right) + \frac{\delta^2}{4}\left(\frac{K_0}{qK_1} + \frac{1}{q^2}\right)^2\right]^{1/2} \tag{4.15}$$

where the arguments of J and K are understood to be u and q respectively.

This transcendental eigenvalue equation must be solved numerically. A computer program was written in which J_0, J_1, K_0, and K_1 were evaluated for trial values of u. As a function of the waveguide parameters δ and V (where V determines q through $q = (V^2 - u^2)^{\frac{1}{2}}$) input into the program, the program searched for values of u which minimized the difference between the two sides of equation (4.15) above. Through an iterative procedure which could be carried out as often as desired, the program searched through stages of progressively smaller increments of the trial values of u as the sought for eigenvalue satisfying Eqn. (4.15) is approached.

The solution of the eigenvalue problem is shown graphically in Fig. 4.2 where the two sides of Eqn. (4.15) are plotted as a function of u. The left-hand side of Eqn. (4.15) $(J_0(u)/J_1(u))$ resembles the cot u function and only the positive branch of the function is used for HE_{11} mode; only one curve is obtained for any V and δ. The more complicated right hand side of Eqn. (4.15) is a monotonically increasing function of u with zero value at u = o. Curves are plotted for $\delta = 0.1$ and Fig. 4.3 shows the dependence of the eigenvalue u on the waveguide parameter V where u/V is plotted as a function of V. As V decreases below about 1.0, u approaches V asymptotically ($u/V \to 1.0$).

In fact, u differs so little from V in this range and q consequently approaches zero so closely that the direct

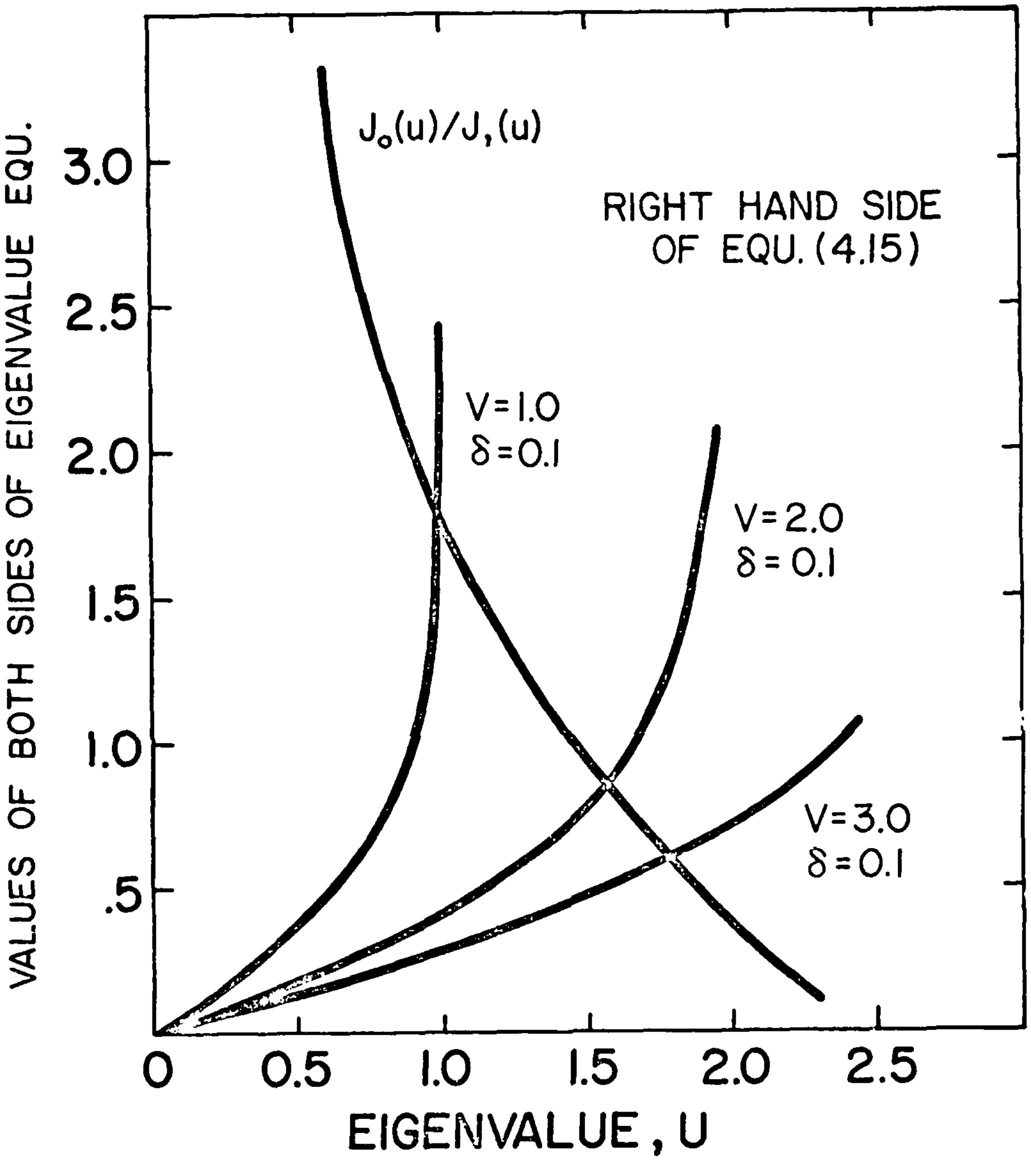

FIG. 4.2 GRAPHICAL SOLUTION OF THE EIGENVALUE EQUATION. A plot of each side of the eigenvalue equation for the HE_{11} mode is shown. The value of u at which the curves intersect is the eigenvalue for the problem with the corresponding physical parameters. There is only one curve for $J_0(u)/J_1(u)$ as a function of u. The more complicated right hand side of the eigenvalue equation depends on the choice of parameters. The plots are for δ = 0.1 and the three choices V = 1.0, 2.0, 3.0. q is related to u and V through $V^2 = u^2 + q^2$.

numerical evaluation method of the program becomes very difficult and the computer capacity is soon exceeded. While exact solution is thus not possible for small V, the fact that q approaches zero very closely may be exploited to considerably simplify solution of the eigenvalue problem resulting in a highly accurate analytic approximation.

We first note that the eigenvalue equation (4.15) reduces to a simple form for $\delta = 0$, namely

$$\frac{J_O(U)}{uJ_1(u)} = \frac{K_O(q)}{qK_1(q)} \tag{4.16}$$

which holds exactly. Moreover the eigenvalues of equation (4.15) for any non-zero δ approach those of the $\delta = 0$ case as V decreases (even for larger values of V the solution for the $\delta = 0$ case is not a bad approximation for typical values of δ encountered in many physically important situations.) As has been noted by Snyder (1969) as $u/V \to 1.0$ we may reasonably substitute V = u in equation (4.16)

$$\frac{J_O(V)}{VJ_1(V)} = \frac{K_O(q)}{qK_1(q)}\ . \tag{4.17}$$

The asymptotic small argument form for the Bessel functions of the second kind give for the right hand side of this equation ln (1.123/q). We thus obtain an analytic solution for Eqn. (4.17),

$$q = 1.123\ \exp[-J_O(V)/VJ_1(V)]. \tag{4.18}$$

The eigenvalue u is then given by $(V^2 - q^2)^{1/2}$. The results of this approximation are shown in Fig. 4.3 where it is also compared to the exact result for $\delta = 0$ and 0.1. The approxi-

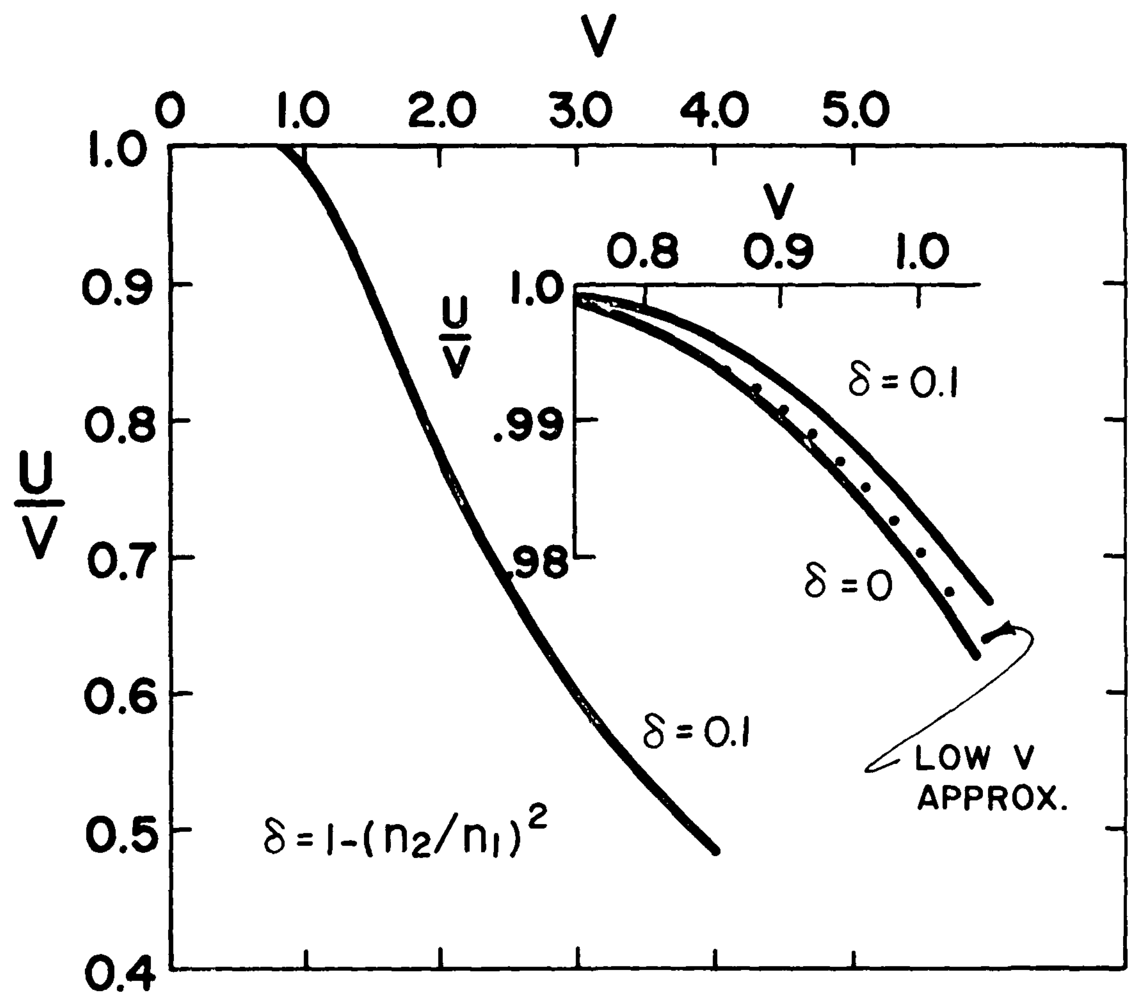

FIG. 4.3 THE EIGENVALUE SOLUTION. The eigenvalues u obtained by the numerical solution of the eigenvalue equation are plotted in the form u/V vs V. The main plot is for the choice $\delta = 0.1$. The insert shows a magnified view of the region around V = 0.9 to illustrate the dependence of the eigenvalue on the choice of δ. As V decreases, the eigenvalues for any δ converge to the value in the $\delta = 0$ case. As is evident u approaches V asymptotically as V decreases below 1.0 ($q \to 0$).

mation is very accurate below V = 0.8 where the results for all values of converge.

Once the eigenvalues are determined it is then possible to evaluate the fields via Eqns. (4.6), (4.7), (4.8) and (4.9). In our case, however, we are primarily interested in power propagation in the waveguide. Evaluating the eigenvectors through eqn. (4.12) inside and outside the guide and determining the power propagated in each region by carrying out the integrations of equations (4.13) and (4.14) we get for the ratio of power propagated in the evanescent wave to the power propagated in the interior in the HE_{11} mode

$$\frac{P}{P} = -\left[\frac{u^2}{q^2}\right] \frac{(k^2+\ \ ) \left[\frac{K_o}{K_1} - 1\right] + \ (k^2-\ \ )\left[\frac{K_o}{K_1} - 1 - \frac{4}{q^2}\right]}{(1+\ \ ) \left[\frac{J_o}{J_1} + 1\right] + \ (1-\ \ ) \left[\frac{J_o}{J_1} + 1 - \frac{4}{u^2}\right]} \qquad (4.20)$$

where the arguments of J and K are u and q respectively and:

$$k^2 = (k\ /k\ )^2 = 1 - \qquad (4.21)$$

$$= 1 - \ (u/V)^2 \qquad (4.22)$$

$$= (1-\ )/(1+\ ) \qquad (4.23)$$

$$= -\left(\frac{1}{u^2} + \frac{1}{q^2}\right) \Bigg/ \left(\frac{J_o}{uJ_1} - \frac{K_o}{qK_1} - \frac{1}{u^2} - \frac{1}{q^2}\right) \qquad (4.24)$$

With this expression we may then compute the modal efficiency through eqn. (4.15). The result is displayed in Fig. 4.4 where we have plotted η as a function of V for δ = 0.1. The inset also shows η for = 0 as well as the small V approximation. Fig. 4.5 is the same data plotted logrithmically. These plots illustrate that the general result of decreasing V

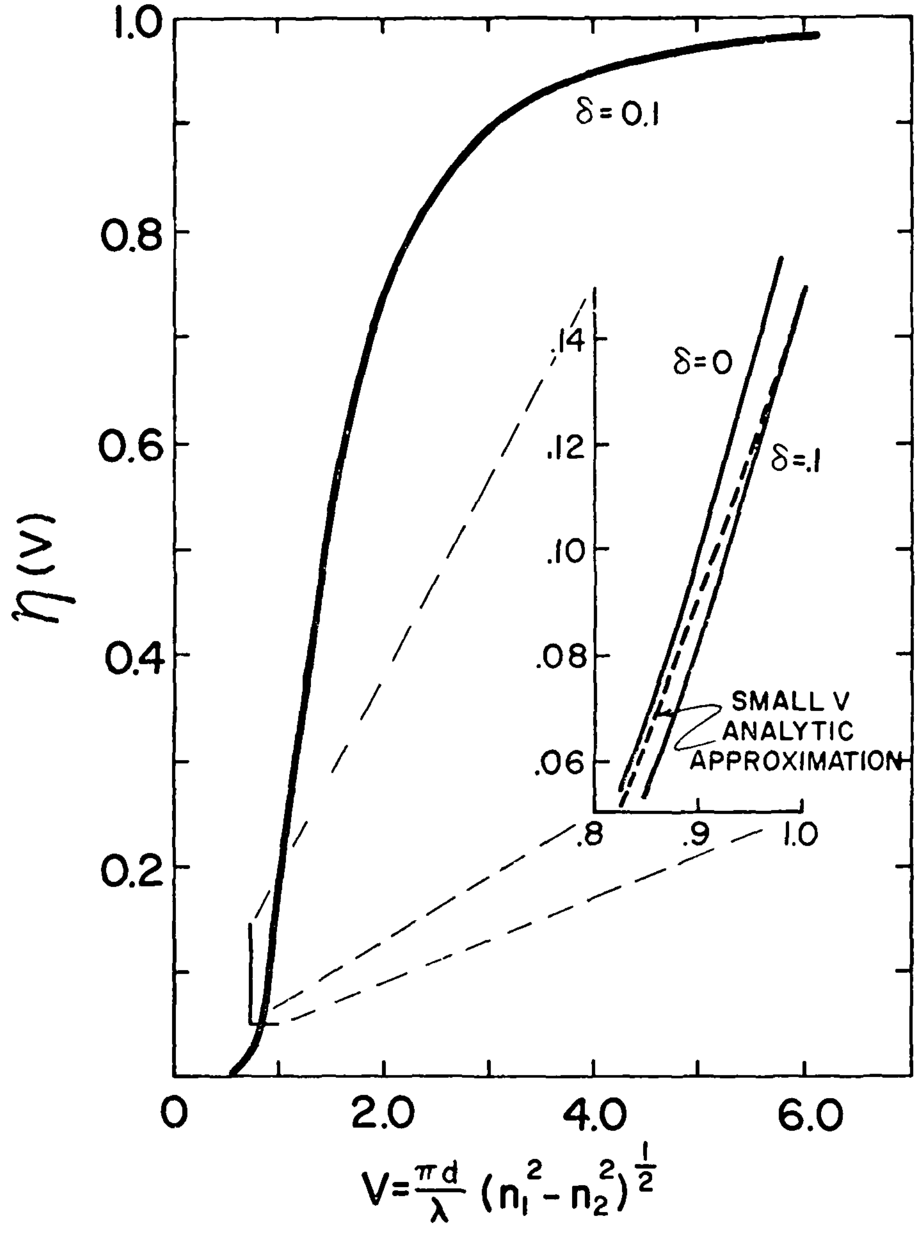

FIG. 4.4 CUT OFF CHARACTERISTICS OF THE HE_{11} MODE. The modal efficiency η is the fraction of power propagated in the mode which is conducted within the wave guide. The full curve is for a wave guide with δ = 0.1 and the inset shows an expanded view of the region 0.8 < V < 1.0 where the HE_{11} modal efficiency for the δ = 0 and δ = 0.1 case are compared with the small V analytic approximation discussed in the text. This approximation is very good in the region below V = 0.8 although it is not useable above V = 1.0.

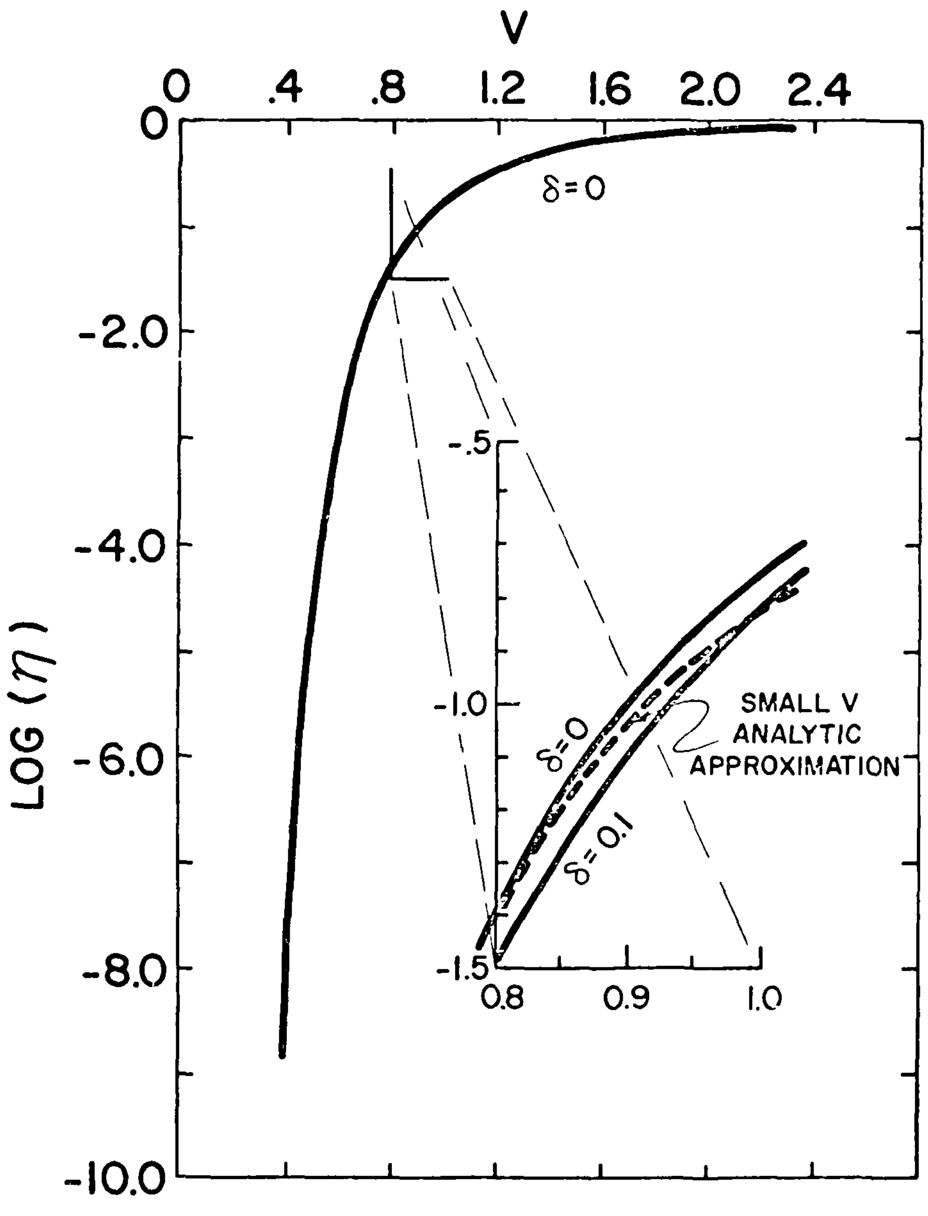

FIG. 4.5 CUT OFF CHARACTERISTICS OF THE HE_{11} MODE. The HE_{11} modal efficiency is again displayed this time as a semi-logarithmic plot to demonstrate the precipitous approach toward zero efficiency for small V. While the efficiency is thus rapidly dropping below V ~ 0.8 very acute discrimination is evidently possible since a small change in V results in a large change in the relative fraction propagated in the wave guide.

is a decrease in η, that is, the power conducted within the core of a waveguide decreases with decreasing V. While the HE_{11} mode propagation (as is shown in these plots) does not go exactly to zero for a non-zero value of V (as do the higher order modes) the power conducted within the guide gets very small (below V = 0.6). For example at V = 0.3, $\eta < 10^{-16}$.

4.2 ATTENUATION IN A CONE

Our main focus of interest is on the propagation characteristics of a conical dielectric waveguide. Exact solution of this problem is very difficult and has been investigated by Snyder (1970, 1972a, 1972b). The main result of this analysis is that the primary effect of a conical taper in a dielectric rod is the coupling of a particular propagation mode with other modes of the waveguide. In general then there is no unique propagation mode for this case: one must determine the coupling coefficients for all other possible modes including the radiation modes. The greater is the taper angle of the cone, the larger will be the coupling coefficients. For a tapered guide with V < 2.405, however, the coupling will only be to the radiation modes as the higher order propagation modes are cut off.

For small tapers where the diameter change of a guide is small over distances comparable to the wavelength of the incident radiation, Snyder (1970, 1971) has shown that at each point along the guide the radiation propagates in the same manner as in a uniform guide with the same local values of the physical parameters (in what Snyder calls local modes).

Thus the picture we use to model the foveal cones in the primate retina is that of a dielectric rod with the effect of the taper being to transfer increasing amounts of the guided radiation from within the core into the evanescent surface wave as the cone is penetrated. This effect will be wavelength dependent and it is just this behavior which is of interest. In the model of interest there is no coupling into higher order modes since $V < 2.405$ and the main effect of ignoring the mode coupling of a tapered guide is to underestimate the rate at which energy is transferred out of the guide into the radiation modes. For the case of foveal cones this effect will be quite small since the taper angle is less than 0.5 degrees and the coupling coefficients to the radiation modes will be small. Neglecting the mode coupling will err on the safe side in that we determine a lower bound for how rapidly the cone disperses the incident energy; the approximation does not qualitatively affect the wavelength dependence of the process.

In order to display the proposed model mechanism for color discrimination we compute only the transmission properties of the cones. The effect of absorption can be taken into account by using the appropriate wavelength-dependent extinction coefficient (which is related to the photopigment absorption) as the imaginary part of the refractive index of the interior of the cone. For the case of the foveal cones where the absorption is small over distances comparable to the wavelength of light the absorptionless model will sensibly portray the relevant transmission properties of the cones Snyder and Pask, (1973)

and is the representation which we evaluate here.

There are many ways in which the spectrum dispersing properties of a cone can be displayed. For a cone with a uniform taper a sensible index of the change in transmission properties of a cone is the ratio of the fraction of power left within the guide at its narrow end to that initially at the broader entrance end, η_{out}/η_{in}.

Based on the measurements summarized by Polyak (1941), the foveal cone model we employ is that of a gently tapering segment 40 microns long by 0.8 microns in diameter at proximal and 0.5 microns at the distal end. The appropriate refractive index values n_1 and n_2 are not known with any certainty. We thus plot, in Figure 4.6 the ratio η_{out}/η_{in} as a function of the inverse of the incident wavelength (which is proportional to the photon energy) for a range of choices of the refractive index difference parameter, $\pi(n_1{}^2 - n_2{}^2)^{\frac{1}{2}}$.

Our choice for the operating point of the cones must clearly be somewhere in the middle of the range of the displayed curves. The upper curves do not discriminate sufficiently between long and short wavelengths. The lower curves, on the other hand, do not propagate light with sufficient intensity to be as efficient as the cones are known to be from photopic efficiency data. In fact, the best experimental estimates for n_1 and n_2 discussed previously indicate a choice of operating point just in this optimum range. It is to be expected that $\pi(n_1{}^2 - n_2{}^2)^{\frac{1}{2}}$ is somewhat smaller than the value of 1.04 to be inferred from Sidman (1957) and Barer (1957) since it has been

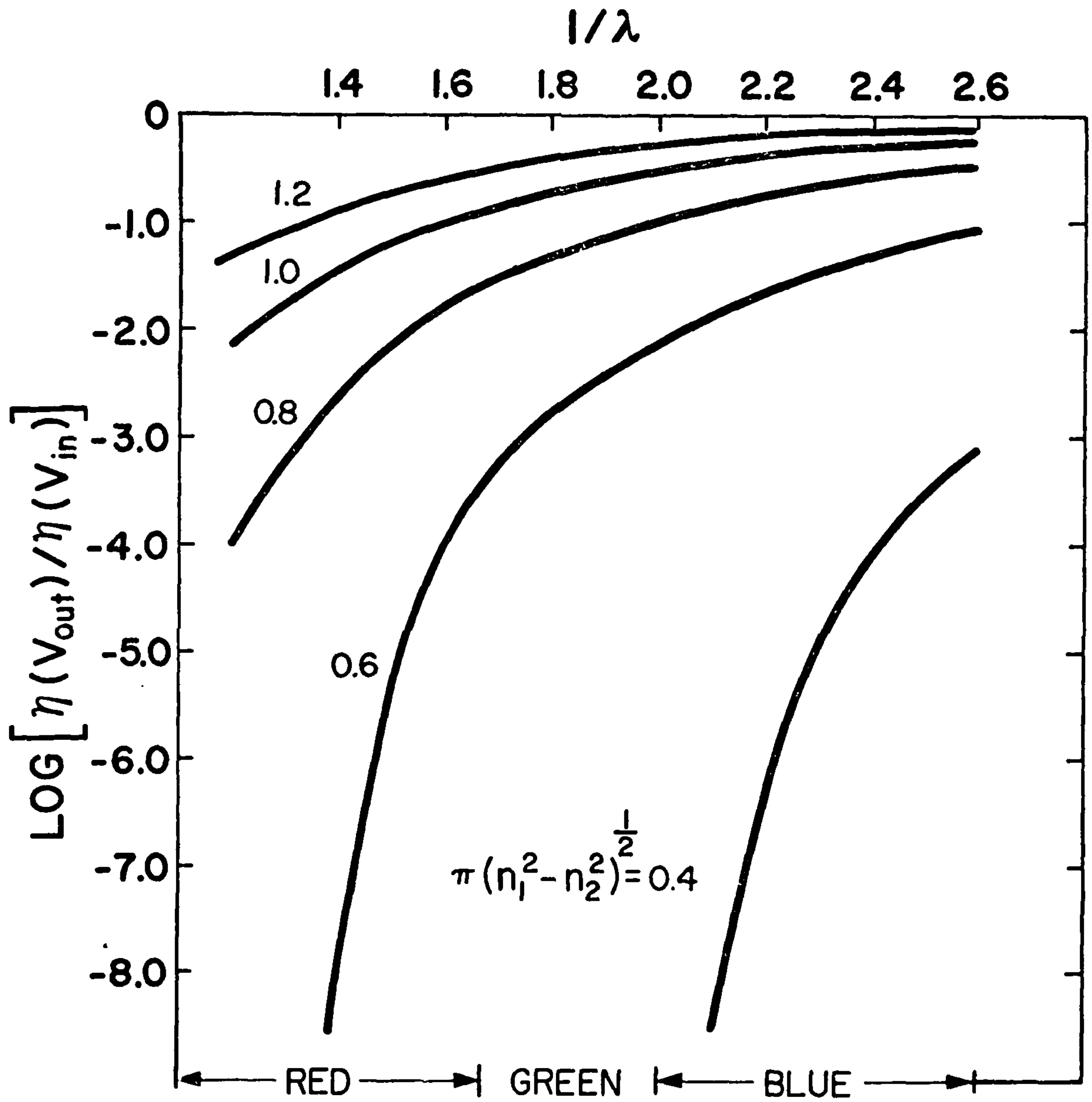

FIG. 4.6 The log of the ratio η_{out}/η_{in} as a function of the inverse of the photon wavelength (proportional to photon energy) for a range of refractive index difference parameter $\pi(n_1^2-n_2^2)^{\frac{1}{2}}$.

noted that the inter-photoreceptor space in the human eye is significantly denser (n_2 larger) than in other species, Feeney (1972).

The discrimination of a cone with $\pi(n_1^2 - n_2^2)^{1/2}$ equal to 0.7 is shown in more detail in Fig. 4.7. Here the relative modal efficiency at each point along the cone is plotted as a function of position for different input wavelengths spanning the visible spectrum. It is clear that the different colors transmit differently along the cone structure.

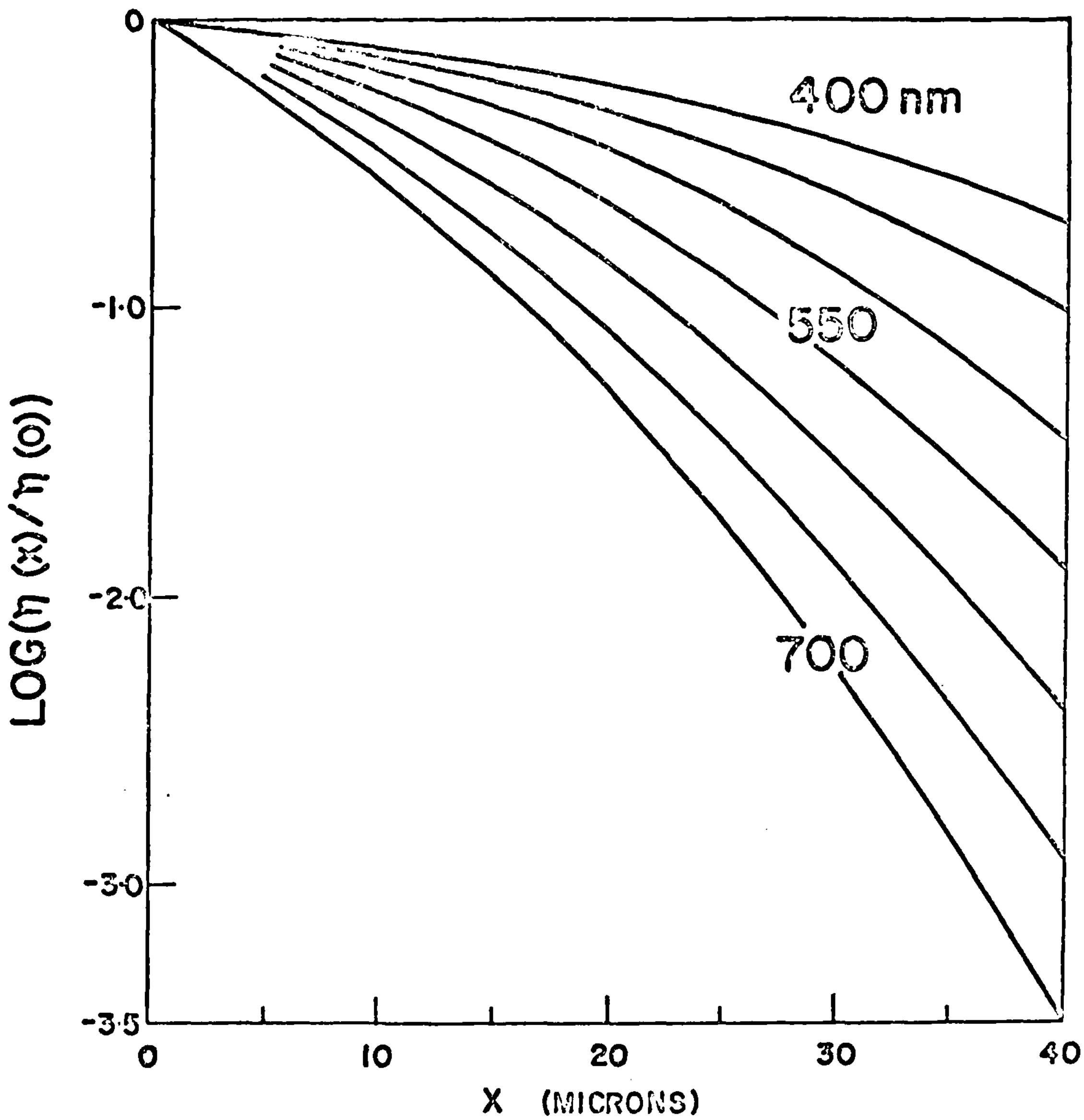

Fig. 4.7 With $\pi (n_1^2 - n_2^2)^{\frac{1}{2}} = 0.7$. The relative modal efficiency at each point along a 40μ cone given as a function of wavelength.

5. SCANNING ELECTRON MISCROSCOPIC STUDIES OF LASER LESIONS IN THE RABBIT RETINA

For the past year we have continued to study the rabbit retina, even though our studies of other retinal material have begun. Thus far in the literature there are only a few studies of vertebrate retina using scanning electron microscopy, but none have been completed on the rabbit retina, and none whatsoever of laser lesions in the retina. In the Appendices 1.2 and 1.3 we summarize our results in two papers entitled "Scanning Electron Microscopy of Normal and Lased Rabbit Retina" which has already been submitted for publication and "Scanning Electron Microscopy of Normal and Lased Rabbit Pigment Epithelium" which is prepared for publication. In appendix 2 we list the colloquia, seminars and talks which have been given on this subject.

[illegible]. THE STUDY OF THE VITREAL-RETINAL JUNCTION

We first became interested in this problem as a result of scanning electron microscopic studies of laser lesions of the rabbit retina where membranes were observed at the vitreal-retinal junction. We have begun an extended study of this membrane for different exposure intensities at various recovery times. This junction has been examined after one hour, one, two and four days and one, two, four and six weeks, together with areas in which the inner limiting membrane is mechanically disturbed. Where our initial studies had indicated that an epiretinal membrane was forming our control studies are now shedding some doubt upon this.

The lesions are being studied both with the TEM and SEM. The nature of the membrane which we have observed is of particular importance to the ophthalmologists associated with our group, since it represents an important aspect of the general problem of light damage within the eye.

7. DETAILED STUDIES OF CONES

7.1 THE TAPER OF OUTER SEGMENTS

We are presently in the process of measuring the taper of the outer segments of foveal and parafoveal cones. It is important to note that in our hypothesis of color vision the cones may have a slight taper in the foveal region. Recent measurements have suggested that foveal cones are generally said to be rod like, yet few of these studies are available in the literature. In 1965 Dowling pointed out that foveal cones studied by his group showed no taper, but as the cone outer segments are 50 to 60 μ long and less than 1 μ in diameter, his results are inconclusive since he seems to have studied them only by longitudinal transmission electron microscopic sections.

We have begun the study in which we are taking both thick and thin serial transverse sections of the cones over the entire outer segments. Both TEM and SEM are being used. We have already prepared the retina for the squirrel monkey, baboons, and humans for study. Particular attention is being given in Dr. Hollenberg's laboratory to the problem of the shrinkage of the material. It is interesting that never before have careful detailed measurements of these cone outer segments been made. Without question these measurements will be invaluable to our understanding of the operation of the retina.

7.2 OUTER SEGMENT DISC STRUCTURE

It is widely reported in the literature that cone outer segment discs of lower vertebrates are continuous with the membrane at the edge opposite the connecting cilium and the

groups of discs are continuous with each other, especially at the vitreal end. Dowling (1965) reports that only the most vitreal discs show continuity with the plasma membrane and the foveal cones of Macaca monkeys (less than one-third of their length). Cohen (1961) "The Structure of the Eye" reports that as one proceeds distally in the cone outer segments infolding becomes rarer and rarer, and finally none is observed. In this case the discs appear to be discreet units. However with lanthanum infiltration, Cohen (1972) it is apparent that some cone discs are open to extra cellular space, even in the sclera. This difference in accessibility to the extra cellular space may be important in the ionic exchange following photo-reception. This too may have an important bearing on the proposed model. Because of this we are carefully examining our high resolution photographs of the cone outer segment disc groupings to see if there is any consistency in the pattern of discs open or discrete continuous with each other within an infolding.

7.3 THE EFFECTS OF MONOCHROMATIC LASER LIGHT UPON THE CONE OUTER SEGMENT DISCS

We are presently examining SEM and TEM photographs of retina to identify specific damage in the discs caused by monochromatic light at power levels both above and below the threshold for forming ophthalmologically detectable lesions.

7.4 THE EFFECT ON THE CONE OUTER SEGMENT DISCS WHEN THE ENTIRE RETINA IS EXPOSED TO MONOCHROMATIC LIGHT

We have presently initiated a series of experiments designed to determine whether or not all discs respond in the same way to intense light. We are also examining the effect of such damage both in the foveal and anterior portions of the retina. Pourcho and Bernstein (1975) found that with prolonged osmication at 40^{o}C, the amount of osmium deposited in the outer segment disc was increased by light stimulation and decreased after lengthy dark adaptation. We have exposed Japanese quails, goldfish and guppies, to red and blue light (6 days on a 12 hour cycle) and to dark adaptation. These eyes are presently being processed by standard methods for electron microscopic studies and by prolonged osmication in order to allow us to carefully scrutinize the discs.

7.5 REAL TIME X-RAY MICROGRAPHS OF CONES DURING LIGHT EXPOSURE

In order to properly account for the Stiles-Crawford Effect of the first kind it has been suggested that the dimensions of cones change when subjected to visible radiation (Snyder & Pask 1976). After exposure the retina apparently recovers within sixty seconds. In order to study this point we have made initial contacts with scientists associated with the European Molecular Biology Organization to carry out experiments using the Synchrotron Radiation Source in Hamburg, Germany. Using the ~1 Å intense x-ray source we will attempt to make x-ray lithographs of live retinal material as a

function of time after light and dark adaptation. This new method which is soon to be described in the literature by Spiller et al make possible time resolved experiments with a resolution approaching 100 Å. The time for exposure is expected to be less than 1 second.

8. DETAILED EXAMINATION OF LASER DAMAGE IN THE HUMAN RETI

A series of experiments has been carried out in conjunction with the ophthalmological community in London, Ontario. The results of these experiments will be described in a series of papers, the first of which is given in appendix 1.4.

Through the year we have developed a superb working relationship with the London ophthalmological community which is particularly interested in laser damage to the eye. It is because of their help that we have been able to carry out these experiments.

9. NATO-AGARD LECTURE SERIES

Last Fall one of us participated in the NATO-Agard Lecture Series No. 79 on Laser Hazards and Safety in the Military Environment. The text of papers prepared for this series are given in appendices 1.5 and 1.6.

REFERENCES

1. Barer, R. (1957) "Refractometry and Interferometry of living cells". J. Opt. Soc. Am. 47, 545.
2. Born, M. and Wolf, E. (1965) Principles of Optics Pergamon Press, Oxford.
3. Cohen, A.I. (1972) "The fine structure of the extra-foveal receptors of the rhesus monkey", Exp. Eye Res. 1, 128-36.
4. Dowling, J.E. (1965) "Foveal receptors of the monkey retina: Fine Structure," Science 147, 57-9.
5. Feeney, L. (1972) "The Interphotoreceptor Space II. Histochemistry of the matrix" Develop. Biol. 32, 115-128.
6. Goodman, J.W. (1968) Introduction to Fourier Optics McGraw-Hill Book Co., N.Y.
7. Kapany, N.S. and Bruke, J.J. (1972) Optical Waveguides Academic Press, N.Y.
8. Polyak, S. (1941) The Retina, Univ. of Chicago Press, Chicago, Ill.
9. Pourcho and Bernstein (1975) Am. J. Anat. 143, 371-386.
10. Shulman, A.R. (1970) Optical Data Processing John Wiley and Sons, N.Y.
11. Sidman, R. (1957) "The Structure and concentration of solids in photoreceptor cells studied by refractometry and interference microscopy" J. Biophys. Biochem. Cytol. 3, 15-30.
12. Snyder, A.W. (1969) "Assymptotic expressions for eigenfunctions and eigenvalues of a dielectric or optical waveguide" IEEE Trans. MTT 17, 1130-1138.

13. Snyder, A.W. (1970) "Coupling of modes on a tapered dielectric cylinder" IEEE Trans. MTT 18, 383.

14. Snyder, A.W. (1971) "Mode propagation in a nonuniform cylindrical medium" IEEE Trans MTT 19 402-403.

15. Snyder, A.W. (1972a) "Coupled mode theory for optical fibers" J. Opt. Soc. Am. 62, 1267-1277.

16. Snyder, A.W. (1972b) "Power loss on Optical fibers" Proc. IEEE 60, 757-758.

17. Snyder, A.W. and C. Pask (1973) "Waveguide modes and light absorption in photoreceptors" Vision Res. 13 2605-2608.

APPENDIX 1. PAPERS EITHER PUBLISHED, SUBMITTED FOR PUBLICATION OR IN FINAL STAGE OF DRAFTING:

1.1 Color Vision: A Physical Model for Spectral Discrimination by Retinal Cones
J.A. Medeiros, B. Borwein, J.Wm. McGowan
to be submitted to Vision Research.

1.2 Scanning Electron Microscopy of Normal & Lased Rabbit Retina
Bessie Borwein, Madhu Sanwal, J.A. Medeiros and J.Wm. McGowan
Submitted to Canadian Journal of Ophthalmology.

1.3 Scanning Electron Microscopy of Normal and Lased Rabbit Pigment Epithelium
B. Borwein, M. Sanwal, J.A. Medeiros, and J.Wm.McGowan
to be submitted to Arch. Ophthalmol.

1.4 Studies in Human Retina 1. The so-called normal areas from the retina of an eye enucleated for choroidal melanoma
B. Borwein, M. Sanwal. J.A. Medeiros and J.Wm. McGowan
Rough draft of a paper to be submitted to Investigative Ophthalmology.

1.5 Properties of Electromagnetic Radiation
J.Wm. McGowan
Published, AGARD Lecture Series No. 79, 1975

1.6 Lasers
J.Wm. McGowan
Published, AGARD Lecture Series No. 79, 1975

APPENDIX 2. PRESENTATIONS GIVEN THIS YEAR AND ABSTRACTS SUBMITTED FOR CONFERENCES THIS SUMMER

2.1 September 22, to October 2, 1975. Papers delivered as part of the AGARD Lecture Series 79 on Laser Hazards and Safety in the Military Environment AGARD LS-79

2.1.1 J.Wm. McGowan, Properties of Electromagnetic Radiation

Although the electromagnetic spectrum extends over more than thirty orders of magnitude that portion of it now dominated by the LASER only includes four. It is through this range that all life processes are affected by light, in particular the eye can easily be damaged by it. In this lecture the basic principles dealing with electromagnetic radiation are discussed particularly as they relate to the development of the LASER.

2.1.2 J.Wm. McGowan, Lasers

Principles and properties of the LASER are discussed in some detail together with a description of the various types of LASERS and their applications.

2.2 October 15, 1975, Dept. of Physics, The University of Western Ontario, and September 18, 1975, McMaster University, Hamilton, Ontario

J.A. Medeiros, Colour Vision and Physical Processes in the Human Retina

2.3 November 13, 1975, University of Notre Dame, Radiation Research Laboratory
J.Wm. McGowan, A New Model for Colour Vision

2.4 January 7, 1976, Defence & Civil Institute for Environmental Medicine, Toronto, Ontario

2.4.1 B. Borwein, Laser Eye Experiments

2.4.2 J.A. Medeiros, A New Model for Colour Vision

2.5 April 6, 1976, Ophthalmology Rounds, University Hospital, London, Ontario

B. Borwein, So-called Normal Areas of a Retina from an Eye with Choroidal Melanoma

APPENDIX 2. (cont'd.)

2.6 June 6, 1976, Canadian Ophthalmological Society, Research Session, Quebec City. To be presented by J.A. Medeiros

J.A. Medeiros, B. Borwein, M. Sanwal, J.Wm. McGowan and M.J. Hollenberg
Origin of Preretinal Membranes Following Laser Coagulation of the Retina

Laser-induced retinal lesions of sufficient intensity to rupture the inner limiting membrane were studied at intervals ranging from one hour to six weeks post exposure. The damaged rolled-up fragments of the inner limiting membrane over and around the craters of the lesions are distinctly different from the fine cobweb-like strands which arise and coalesce to form increasingly dense networks across the lesion.

APPENDIX 1.1

This appendix is a draft of a paper on the tapered waveguide model of color vision. A letter on this subject had been submitted to Nature last fall. Correspondence with regard to this submission and the editorial difficulties with its acceptance were included in the third quarterly report (Feb. 6, 1976). Rather than pursue the publication of the short communication we have chosen instead to go directly to a full paper which covers the broad categories of evidence for the proposed model.

APPENDIX 1.1
rough draft

COLOR VISION: A PHYSICAL MODEL FOR SPECTRAL DISCRIMINATION BY THE RETINAL CONES

J.A. Medeiros, B. Borwein, J. Wm. McGowan

Department of Physics and the Centre for Interdisciplinary Studies in Chemical Physics, The University of Western Ontario

Abstract

I. INTRODUCTION

It is generally conceded that there does not yet exist a wholly satisfactory explanation of how the small, intricate and precisely formed receptors of the human retina actually resolve and detect color information.

Most current models assume the basis for color differentiation to be the presence of multiple cone types (usually three), each type having different spectral sensitivity. Serious difficulties with this approach are to be found in the evidence on the details of the structure actually present in the retina and in the performance characteristics of the color vision system. There is no physiological data to support the concept of multiple cone types in the human retina, on the basis of either cone structure or the interconnections among cones. The evidence for the cone photopigments required for the operation of these models is also equivocal. Furthermore, the electrical characteristics of the color vision system are not consistent with multiple cone types.

We will discuss this evidence militating against multiple

cone models in more detail below. The main focus of this paper, however, is a new model in which each cone is pictured as a miniature spectrometer, with full color information potentially available. By a very simple mechanism, based on the physical properties of the cones, the shape and size of the cone and its corresponding optical transmission properties serve to disperse the incident spectra, prism-like, into a readable code. In this proposed model, full color information is detected, and only in the subsequent processing is the content reduced according to a trichromatic scheme. This principle of operation is fundamentally different from multiple-cone models, in which the information content is first reduced to a trichromatic code at the detection level, and subsequent processing must resynthesize the color information.

The proposed model, we submit, offers a more consistent explanation of the diverse data on color vision: it is in accord with the known structural details of the retinal architecture, it simply and plausibly explains the wide spectrum of experimental data on the performance characteristics of the color vision system, and it is amenable to direct experimental verification.

II. DESCRIPTION OF THE MODEL MECHANISM AND ITS ROLE IN COLOR VISION

All the cones within a given region of the retina are very similar in appearance although their size and shape vary systematically through the human retina. No distinct groups or

classes of cones are distinguishable. The cone diameters are only slightly larger than the wavelength of the visible light to which they are sensitive and as a consequence diffraction and interference effects will play an important role in the propagation of light within them. These effects, broadly classified under the topic of dielectric waveguide phenomena, have been investigated in connection with fiber optics (Kapany and Burke, 1972 comprehensively review dielectric wave-guide phenomena) and integrated optical circuits (see, for example, Tamir (1975. Light funneling effects of optical fibers have been advanced as the explanation of the photoreceptor's directional sensitivity, the Stiles Crawford Effect of the First Kind, (di Francia, 1946, O'Brien, 1949). Moreover, transmission of light through the human retinal receptors in characteristic dielectric waveguide modes has been directly and reproducibly observed in excised retina by Enoch (1961, 1967).

A. Spectral discrimination by tapered cones.

If one would like to identify a spectroscopic principle wherein each cone can detect full color information, it is to these physical properties of the receptors to which we must turn. Before describing some of the relevant mathematical details of a simple model for light dispersion by a dielectric waveguide, we first describe some of the qualitative features of the phenomena and how a color discrimination mechanism may be seen to arise.

Light propagates in an optical fiber in particular propagation modes. These modes correspond to particular patterns of radial distribution of the propagated radiation. The number of such modes allowed depends on the physical parameters of the light-guiding structure. It depends on these parameters in the form of the dimensionless quantity V, the waveguide characteristic parameter given by

$$V = \frac{\pi d}{\lambda} (n_1^2 - n_2^2)^{\frac{1}{2}} \tag{1}$$

where d is the guide diameter, λ the free-space wavelength of the incident radiation and n_1 and n_2 are the refractive indices inside and outside the guide, respectively (see Fig. 1). For large fibers, in which V is a large number, many propagation modes are allowed and if V is large enough particular modes cannot be distinguished and the fiber interior can be fully illuminated corresponding to the geometrical optics limit. As V decreases the number of allowed modes decreases as particular modes are attenuated or cut off. For V less than the value 2.405 only one propagation mode, the so-called HE_{11} mode, is permitted. The radiation propagated within the waveguide in this mode also is rapidly attenuated with a further decrease in V.

Noting that V explicitly depends directly on the ratio of the fiber diameter to the wavelength of the incident radiation, then as either d decreases or λ increases V decreases and the guide is more restrictive to the propagation of light. Thus, in a conical fiber whose diameter decreases along the propagation direction of the incident light, the fraction of light remaining at any given point along the cone will depend on its wavelength

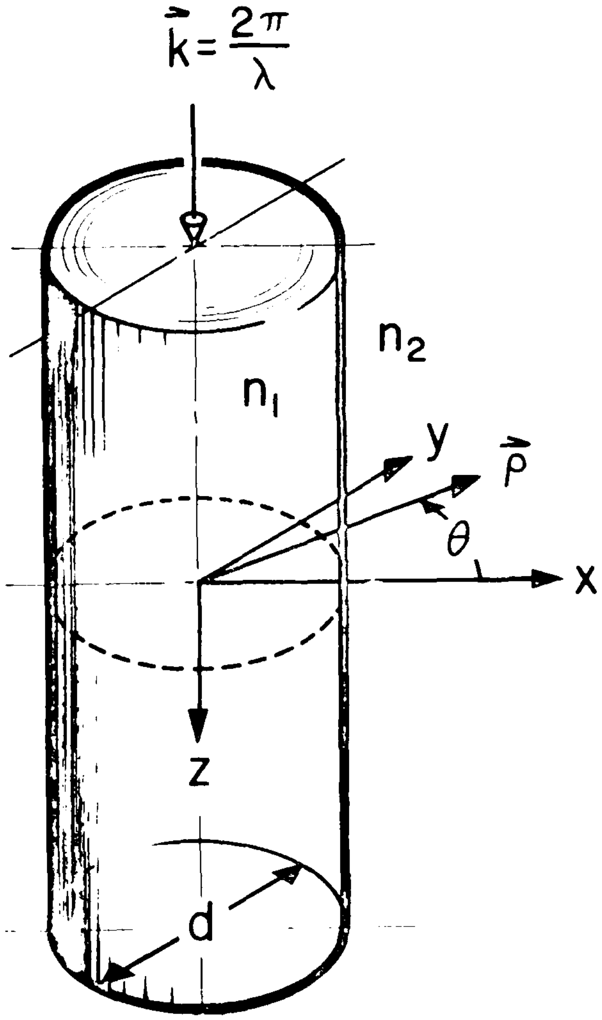

$$V = \frac{\pi d}{\lambda}\left(n_1^2 - n_2^2\right)^{\frac{1}{2}}$$

FIG. 1. DIELECTRIC WAVEGUIDE GEOMETRY. A cylinder of diameter d and refractive index n_1 is embedded in an infinite medium of refractive index of n_2. Light of wavelength λ is incident along the z axis which is coincident with the cylinder axis. The polar coordinates ρ and θ are shown with respect to the rectangular coordinates x and y. The quantities n_1, n_2, d, and λ determine the waveguide characteristic parameter V.

(color). Long wavelength light will be attenuated more rapidly than will shorter wavelength light. As a consequence the color of the light remaining within the cone will be correlated with the axial position.

An easily visualized (although rather crude) analogy of this mechanism is that of using a hollow cone to measure the diameter of spheres of different sizes (Fig. 2a). The position at which a sphere dropped into the cone will jam against the sloping inner wall is correlated with the sphere's diameter, the smallest spheres dropping to the lowest resting points.

Of course this analogy is not exact and must not be taken too literally. There are two main differences between the dispersion of light by a dielectric cone and the capture of a ball in a hollow cone: (1) The cut-off of the propagated light will be "fuzzy", since light of a particular wavelength is attenuated as it penetrates the cone; and (2) the tapered cone model only describes the transmission properties of the cone while the actual pattern of energy deposition within the cone will depend also on the absorbing photopigment it contains (see Fig. 2b). Thus any one photon capture event in the broad entrance end of the cone outer segment will convey little information about the color; it is only the statistical distribution of a large number of capture events that can lead to an inference about the spectral distribution of the incident light. (Note, however, that photon capture events in the narrow distal end of the cone convey much more information, since there is

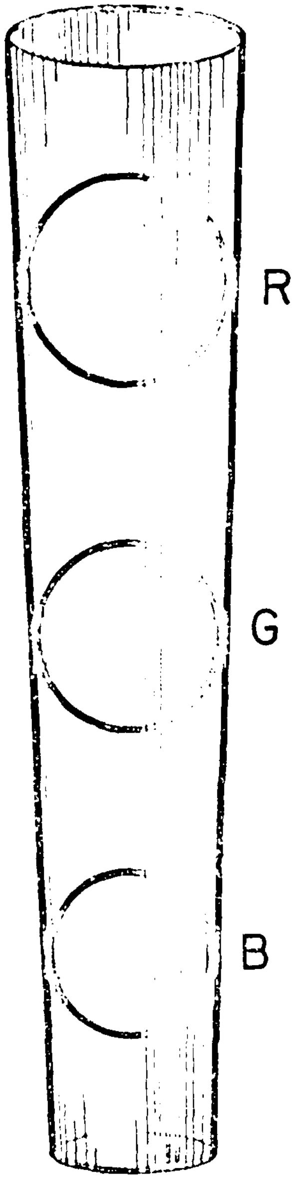

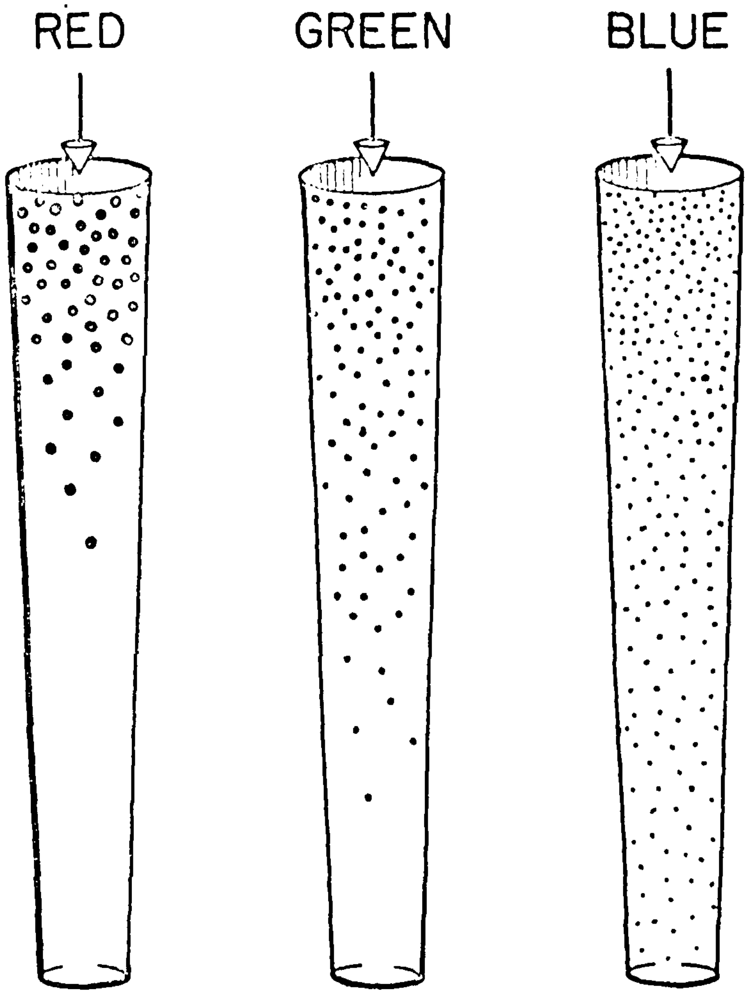

FIG. 2 a. Mechanical analogue of the proposed color discrimination mechanism. The depth within the cone at which a ball comes to rest is correlated with the ball's diameter.

FIG. 2 b. Schematic illustration of the transmission patterns of a dielectric cone for lights of different wavelengths. The cutoff is not discontinuous as in the mechanical analogue. The dots do not represent the position of light absorption within the cone. The actual pattern of photon energy deposition within the cones will depend as well on the nature and distribution of photopigment within the outer segment.

only negligible probability that long wavelengths will reach this region.)

In order that the proposed mechanism be operative, the values of the physical characteristics of the cones must fall within a limited range. A small difference in these parameters can make a large difference in the cone's propagation properties. The size, shape and refractive index of the photoreceptors have not been measured with sufficient precision to critically decide this point. However, we shall see that the best estimates for the human cone parameters are indeed just the ones required for the operation of the model mechanism.

In this connection it is noteworthy that the retinal cone shape and size goes through a smooth variation as one progresses outward from the central retina (Polyak, 1941). The photosensitive outer segments of the human cones in the central retina are long and very slightly tapering cylinders. Progressing outward from the central area the cones become increasingly broader, shorter, and more sharply conical. For color information detected as a position-correlated code, the resolution of the central cones will evidently be better than the more compact peripheral cones; it is to be expected that the corresponding color vision of the central retina will be better than that of the periphery as is, in fact, the pattern actually observed in the human eye (Moreland, 1972). In addition to the shape changes of the cones the retinal cone density is also smaller in the periphery than in the central retina as is the number of bipolars per cone.

the number of bipolars per cone.

Cell counting studies of the retina (Polyak, 1971; Vilter, 1949; Missoten, 1972) reveal that there are three bipolars per cone in the central retina and two per cone in the periphery. This observation is not consistent with multiple cone models of color vision; it does support the view that cones resolve full color information which is reduced to a limited dimensionality only in the process of detection, coding, and transmission of this information through the cone-bipolar link. This corresponds well with the observed approximate trichromaticity of central color vision and the approximate dichromaticity of the peripheral color function.

The obvious advantage of a system where the dimensionality of the spectral information is reduced only at the data processing stage is that it becomes possible for the organism to exercise control via adaptive mechanisms over what information is extracted from that total available, and thus to read only the most relevant information with the maximum accuracy with which its capacity-limited transmission channels are capable.

Before following the logical implication of the model and its connection with the observable features of human color vision we must examine the details of light propagation in small tapered dielectric waveguides.

B. Mathematical Model.

NOTE: This section of the paper is to be a summary of the computational detail presented in section 4 of the Annual Report.

C. Requirements for the human retina to utilize the proposed model

For color information detected as a position-correlated code, the resolution of the central cones will evidently be better than the less compact peripheral cones. It is to be expected that the corresponding color vision of the central retina will be better than that of the periphery, (as is in fact observed for the human eye).

For the cones to detect the available color information through the tapered waveguide scheme, the effect of light absorbed at any given point along the outer segment must be distinguishable from any other. That is, the effect of light absorbed by the outer segment must be local and, moreover the local differences must be detectable. The model would be quite untenable if the cone responded indifferently to the position of light absorbed along its length.

In microelectrode measurements on single photoreceptors Hagins and his coworkers (Penn, Yoshihama, 1970, 1974) have found that the effect of light on the photoreceptor outer segment is indeed local. They transversely illuminated a 12 micron length of a forty micron long rat rod and measured the resulting potential changes to be confined in origin to just that portion illuminated. While the exact nature of the mechanism whereby light absorbed within a photoreceptor is converted into an electrical signal subsequently appearing at the receptor output is still uncertain and is a subject of

intensive research, the picture that is beginning to emerge from the electrophysiological studies is the following:

1. There is steady current of ions flowing between the outer and inner segments of the receptor in the absence of light (dark current).
2. The sources of this current are pores distributed along the surface of the plasma membrane of the outer segment.
3. When light is absorbed at a photoreceptor disk, a transmitter substance (possibly Ca^{++}) is released which migrates to the pores and causes their conductivity to decrease and thus decreases the dark current contribution from the local region of absorbance of the incident light.
4. This decrease in the dark current source in the outer segment eventually appears as a modulation of the current or electrical signal output from receptor.

Given this kind of electrical hook-up for the receptors the potential resolution of a model discriminating color through the kind of position-correlated scheme such as we propose can be no better than the limitations imposed by the spacing of the pores along the receptor length. The more widely spaced are the current sources, the coarser will be the ultimate resolution of the proposed mechanism. The spacing of the pores depends, of course, on their number, and the area over which this number is distributed. The number of such

conductance channels is unknown. Estimates of photoreceptor pore numbers are on the order of 3000 (Yoshikami and Hagins, 1973) to 10^5 (Lebovic, 1976). Assuming 10^4 over the approximately 80 μ^2 area of the assumed foveal cone model gives an interpore spacing on the order of 0.1 μ.

A sensible estimate of the resolution of a cone spectrometer should be the same order of dimension as the cone diameter. The ultimate resolution of the cones will be limited by the amount of axial diffusion of the messenger released at the photoreceptor disks upon the absorption of a photon. The more closely the position of the appearance of the messenger substance at the plasma membrane corresponds to the position of light absorption within the cone, then the more accurate will be the potential information on the photon wavelength. The axial diffusion of the messenger substance will be limited by the photoreceptor disks acting as a baffle, although the exact amount of isolation provided by the disks is not certain. A crude estimate of the spectral resolution obtainable in the proposed scheme is provided by assuming that the entire visible spectrum is read over the cone length. Resolving the 300 nm span (visible wavelengths are roughly 400 to 700 nm) over an outer segment in which the 40 μ length is readable with a 0.5 μ resolution implies that typical resolvable wavelength differences would be 1/80 of 300 nm, $\approx$4 nm. The ultimate resolution, if limited by the 0.1 μ pore spacing would be $\approx$ 0.75 nm. This crude estimate is in surprisingly good agreement with the known ability of the human eye to resolve the two sodium D lines (0.6 nm). The 4 nm estimate is in rough

agreement with the typical spectral discrimination of the normal human eye. Wright and Pitt (1934), for example, experimentally measured this function and - except for variations of a few nm between relative maxima and minima - observed a wave discrimination function which very broadly speaking is three to six nm in the range of 450 to 650 nm and increasing asymptotically at either end of the spectrum.

Thus far we have indicated that the position of light absorption in the cone is potentially readable and that the expected resolution of the model mechanism is in accord with the observations; it must further be shown that the available color information can be coded and read in a meaningful way.

Two possibilities immediately suggest themselves. One very elementary scheme would be a simple grouping of the outer segment length into three different portions, each with its separate output. There is however, no physiological evidence for such a grouping of the outer segments. In addition, such a readout scheme does not exploit the full potential of the available information, reducing it to a trichromatic scheme at the detection level.

Another, more likely mechanism, is the direct conversion of the position-correlated information into a time correlated code. The basis for this conversion can rest on the fact that it takes longer for an electrical signal, once sent, to arrive at a given point when it is coming from a more distant source. We are not here concerned with the time it takes incident light to travel the

length of the cone outer segment, a time on the order of 0.1 picoseconds which is far too small to be resolved by the retinal neuralgia. The relevant delay times are those associated with the finite ionic conduction times for modulations in the photoreceptor dark current to traverse the length of the cone outer segment. These times are not known but are expected to be on the order of tens of milliseconds (see below). The delay times will, in any case, be correlated with the color of the incident light: red light, being primarily absorbed in the near or proximal portion of the cone, will have the shortest associated delay times, blue light, being the only color absorbed at the more distal narrow end of the cone, will be associated with the longest delay times.

In order that the signals from the cones be interpretable as color information there must be some reference established to provide a start time at which the time-dispersed signals may be meaningfully read. This requires that there be some systematic modulation of the cone function. In principle, functions which could be so modulated for this coding include: the light incident on the cone photosensitive segment, the sensitivity of the photopigment, release of the transmitter substance within the cones, or the effect of the transmitter substance at the plasma membrane pores. One of these functions which is actually modulated in the human eye in the manner required for this color vision model is, at the input end, the light distribution incident on the cones. This modulation is available through the small amplitude movement of the eye which

occur repetitively even during fixation. It is known that when this motion is bypassed through optical stabilization of the position of the retinal image, visual perception and especially color vision is rapidly and completely lost until the retinal image motion is restored.

This phenomena generally underscores an important aspect of information processing by the sensory neuralgia. The nervous system works particularly well at detecting changes in input signals; it rapidly adapts to and subsequently ignores constant, ongoing signals; the sensory neuralgia evidently differentiates the input signals in the mathematical sense and are optimized to transmit information as the derivative of the input levels. Information on non-changing signals is suppressed. Thus it is perhaps not surprising that visual perception is lost when the retinal image is artificially held constant (in position and intensity).

There are three components of the eye movements during fixation: a high frequency, small amplitude tremor; larger amplitude, less frequent rapid flicks or saccades; and a general drift between the saccades having the effect of keeping the fixation point within reasonable bounds despite the saccades. The high frequency tremor corresponds to motions of the retinal image of only one or two receptor diameters and has frequency components in the range of something like 100 hz. This motion is probably the retinal analogue of the image resolution enhancement observed when the two ends of a coherent fiber optics bundle are synchronously oscilated (dynamic scanning).

The signal modulation relevant to the proposed model is likely to be accomplished by the larger amplitude saccades. These very rapid flicks correspond to retinal image motion of something like 10 to 15 receptor diameters and thus have the effect of presenting a different portion of the image field to all receptors simultaneously. Moreover, while variable, these saccades occur at typical repetition rates of something like 10 Hz. These two attributes of this motion component are the important ones: amplitude large enough to alter the signal inputs and a period (∿100 msec) that corresponds to the important time constant for a number of visual phenomena. The time scale of roughly 80 to 120 milliseconds is central to phenomena (about which we will have more to say in a discussion of the model's relation to the experimental data) such as: differential chromatic latency, induction of subjective color with achromatic illumination, and brightness addition of a double light pulse. The 10 Hz frequency appears to be a resonant one for many visual functions.

The mechanism we are suggesting is that the output signals from the cones are regularly scanned at a frequency of about $10H_z$ and the signal profile over the 100 msec period is interpreted as information on the spectral distribution of the incident light. This implies that we must look for the delay (latency) of blue light relative to red light to be on the order of 100 msec.

The phenomenon of differential chromatic latency has long been a controversial issue in visual research since

different investigators have reported different results. However this issue may well have been settled by Weingarten (1972). He found that it is of central importance to equate the intensities of the different spectral lights to properly observe the different chromatic latencies; a procedure that has not been uniformly followed by previous investigators. With the hue substitution method Weingarten found that a green wavelength 549 nm had a delay of about 25 msec compared to a red of 621 nm. Despite the disagreement on the results of the different measurements of chromatic latency, one very important result about which there is general agreement is that the chromatic latency is a monotonic function of wavelength; not groups of different response times for different cone classes nor U-shaped like the phototopic luminosity function. Vos and Walraven (1966) and Walraven and Leebeck (1964) found that the relative chromatic phase delay was inversely proportional to the wavelength. This is the result directly predicted by the tapered waveguide color vision model for the time-dispersion method of reading the positionally-correlated color information.

It still remains to decide how this temporal dispersion may be coherently utilized in a color vision system. Corresponding to some rather well-known properties of the eye and the psychophysics of color perception we expect the following kind of shemata. As previously mentioned, there are observed to be three output channels (bipolars) per cone in the central retina and thus we expect to have available three transmission lines

from each cone. One line probably carries intensity information in a black-and-white opponent colors code. The other two channels should carry the color information in the expected opponent color scheme: a red-green (R-G) output, differentiating the cone signals about a wavelength circa 575 nm and a blue-yellow (B-Y) output, differentiating signals about 500 nm.

The two color information channels can operate by differentiating the time sequence of the cone output with respect to their particular balance points (575 and 500 nm). There is substantial reason for deciding on these two wavelengths as the differentiating points for the two color output channels; we will expand on these reasons presently.

We have thus far described a novel spectroscopic principle based on the color dispersion in a near-cutoff tapered, dielectric waveguide. Evidently the architecture of the human retina is consistent with the cones being able to utilize this principle; we have further indicated that the necessary apparatus for detecting and coding the available color information is present in the eye. We now turn to a comparison of the model with the known data on human color vision.

III. COMPARISON WITH THE EXPERIMENTAL DATA

We undertake now in a not necessarily exhaustive fashion, a comparison of models, particularly the one described here with the experimental data on the structure of the retinal architecture and the functioning of the human color vision system. For convenience, we might organize the data

comparison into three broad categories: (A) structural properties of the receptors and retina; (B) static or steady state color vision phenomena; and (C) dynamic color vision phenomena. In the Table 1 a list of some of the phenomena is presented as a sort of score sheet comparing the proposed model and the conventional multiple cone type models.

A. Structure and Architecture of the Receptors and Retina

An obvious advantage of the proposed model is that it directly accounts for the observed physical characteristics of the color receptors, particularly as distinguished from the achromatic rod detectors. The central point upon which the model focuses is the conical shape itself of the cones; the model provides for the first time an explanation of their conical shape and variations in this shape for the different retinal areas. We discussed previously the correlation of this shape and changes therein with the color resolution differences of the retina from the central to peripheral regions.

While the color resolution of small retinal areas is not as good as that of larger areas, the qualitative features of the color discrimination function does not change in going to the smaller image size (Bouman and Walraven, 1972). Moreover color is still resolved with such small spot sizes that only a very few receptors are illuminated (Polyak, 1941) and there does not seem to be a minimum spot size for color resolution. This

TABLE 1.

Partial list of various properties of the human color vision system. Two model explanations are either consistent (YES) or inconsistent (NO) with the phenomena. Cases where the models might or might not be consistent depends on particular assumptions (about photopigments, for example)	MULTIPLE CONE MODELS	TAPERED WAVEGUIDE
A. Structural Properties		
1. Conical shape of the color receptors	NO	YES
2. Variation in cone shape; central and peripheral	NO	YES
3. Uniformity of cones in local regions	NO	YES
4. No change in color vision quality down to very small retinal image size.	NO	YES
5. Disk renewal differences, rods and cones	NO	YES
B. Static Phenomena		
1. Trichromaticity of metameric matches	YES	YES
2. Stiles-Crawford Effect II	NO	YES
3. Liminal Colour Discrimination	*	*
4. Observed photopic sensitivity	*	*
5. Saturation properties of various hues	NO	*
6. Bezold-Brucke Effect	*	*
7. Land Effect	*	YES
8. Colour defective vision	NO	YES
C. Dynamic Phenomena		
1. Prevost-Fechner-Benham Effect; the differential chromatic latencies of the electrical signals of the retina	NO	YES
2. Broca-Sulzer-Pieron Effect Perceptual latencies	NO	YES
3. Brucke-Bartley Effect Intensity variation with intermittent stimuli of different presentation frequency	NO	YES
4. Ditchburn-Ratliff Effect Image movement on the retina	NO	YES

result is at odds with the concept of color discrimination by the differences in signals elicited for different cone types.

Young (1966) utilized a radioautographic technique to observe the flow of radioactively tagged protein into the receptor outer segments. Such studies reveal that the rod receptors undergo continual displacement of their internal disc structure; new discs continually form at the proximal end of the outer segment and displace along the length of the segment, eventually being discarded at the distal extremity. The cones, however, do not apparently follow this scheme. The radioactively labeled protein does not enter and move along the outer segment as a discrete band, as observed in the rods, but rather it diffuses throughout the segment structure. That is, the cone structure seems to remain intact and discs do not undergo displacement along the receptor length. In the terms of reference of the model here proposed, this result is to be expected; if discs were renewed and displaced bodily along the cone segment length, it would not be possible to indefinitely maintain the given cone size and shape.

B. Steady State characteristics of human color vision

A large number of static or steady state aspects of the psychophysics of color vision are known and have been investigated at one time or another. We consider some of these effects and their relation to a model of the color discrimination process. We make no claims that this discussion is comprehensive; the field is far too vast to be so covered in the necessarily

limited space of this paper. A rather general perspective must be taken in this discussion; we observe that the proposed tapered waveguide model qualitatively explains the observations. Detailed quantitative agreement requires a model with specific assumptions about the photopigment contained within the cones. For the purposes of this paper we are more concerned with the appropriateness of the tapered waveguide concept as a central aspect of color vision.

1. Trichromaticity of color vision and cone photopigments

Trichromatic concepts have dominated the study of color vision since the time of Thomas Young's original suggestion. Support for this stance has been assumed to be provided by color-matching experiments in which the eye is used as a comparator to equate the color qualities of two adjacent patches of light. While such experiments show that it usually suffices to vary the intensity of only three appropriately chosen primary colors to effect a match, it does not necessarily follow that the color sense is three-dimensional and specifically that the apparent trichromatic nature is a consequence of three cone classes with different photopigments.

In general one cannot match a particular monochromatic light with any combinations of intensities of any chosen triad of primaries. While the dominant hue can usually be matched, a test patch composed of three primaries cannot match the saturation or purity of a monochromatic reference patch. In

general it is necessary to add one of the primaries to the monochromatic test light in order to desaturate it. The color matches or metamers so obtained are, moreover, variable from subject to subject and even for the same subject the matches are variable from day to day. The variability of the acceptability of such metamers depends on the degree of metamerism; the greater the degree of metamerism, that is the greater the disparity of the actual spectral content of the two colors being matched, then the greater is the instability of the match.

In addition the color reproduction prescriptions provided by such color matching experiments do not translate directly into formulas for producing desired colors in applications such as textiles and painting. In the final analysis, appropriate production of a particular desired color can only be gauged by direct visual inspection of the final product - if the match is satisfactory to the eye then it is a good match - and cannot be predicted on the basis of color matching experiments. These results do not argue favorably for a strict three-dimensionality of color vision.

We have previously discussed the concept that trichromaticity may result for reasons other than the presence of distinct cone groups. In the framework of the proposed model, the approximate trichromaticity of color vision is envisioned as being a consequence of three output channels per cone. That trichromaticity is imposed only after the detection stage allows considerable flexibility in the data manipulation; through adaptive mechanisms the eye is able to select that most relevant

information. Additional support for this view comes from the association of the dichromatic character of peripheral color vision with the presence of only two bipolars (output channels) per cone in the peripheral retina.

Given that no structural or physiological differences corresponding to distinct cone classes have ever been observed in the human retina, it has been argued that the differences must be those at the submicroscopic or molecular level, i.e. in the photopigments only. Although it would be rather surprising for such differences to evolve with no corresponding embryological or physiological differences in the cones, there has in any case been a concerted and longstanding effort to isolate and identify the cone photopigments. While the rod pigment, rhodopsin, has been repeatedly extracted from the retina, it has thus far proven impossible to extract any other photopigment that can be uniquely identified as a cone pigment from the eye of any mammal. It is important to recognize that even if there were definite proof that three cone pigments were present in the retina, it would not, per se, constitute proof that color discrimination is effected by the differential absorption properties of these pigments. While existence of such pigments is a necessary condition for the conventional model of color vision it is not a sufficient condition to prove that it is indeed the only correct explanation. The model we are proposing, for example, while utilizing the physical properties of the cones for spectral discrimination does of course require some kind of photopigment to effect the transduction of light into an

electrical signal and while only one photopigment is necessary the model efficiency would be enhanced by utilization of at least two pigments; that is, other models are possible which may utilize multiple cone photopigments in a secondary role.

The indirect measurement methods of fundus reflection densitometry and single cone microspectrophotometry (MSP) have not resolved the debate on the number and distribution of the cone photopigments. While it is not our purpose to discuss these techniques in detail a number of observations on the results of these measurements may be noted. Reflection densitometry using protanopic observers (Baker and Ruston, 1964) indicates that a primarily long wavelength absorbing pigment may indeed be missing although no such evidence for a missing green pigment in deuteranopes has been obtained. MSP is a very difficult technique and the observations on human cone photopigments (Marks, Dobelle, and McNichol, 1964; Brown and Wald, 1964) are at best equivocal. Consider the following points:

a. The difference spectra on only 11 human cones have thus far been reported.

b. The procedure is techniquely extremely difficult and results for the human eye are particularly complicated by the rapid post-mortem alterations of the retina (Eitiene, 1972).

c. The measurements are not independent of the transmission properties of the photoreceptors.

d. Marks, Dobelle, and McNichol, 1964 reported that their results seemed to indicate the existence of

cones containing both red and green photopigments.

e. The photopigment absorption spectra inferred from the MSP measurements are rather unlikely candidates for trichromatic color vision; the "red" photopigment has its absorption maximum in the yellow and the separation of absorption peaks for the red and green pigments is quite small (on the order of 30 nm).

f. The results are not highly consistent and reproducible; when all the measurements reported by reflection densitometry and MSP are displayed on a single graph (Riggs, 1967) the absorption spectra do not fall into three distinct classes. Such a display reveals an essentially continuous distribution of broadly overlapping absorption spectra with a slight break toward the blue wavelength region.

This situation may be contrasted with the results of MSP measurements on Goldfish cones (Marks, 1965); there the spectral absorption peaks do clearly fall into three distinct groups. It has previously been noted (Walls, 1948) that color vision has developed independently several spearate times in the course of evolution. Goldfish cones are structurally different from human cones and they do not have the appropriate physical

parameters to utilize the tapered waveguide mechanism (at least not in the same way as in the human cones). That the goldfish cones are larger than the primate cones has meant that the MSP measurements have been much easier (and more straightforward) than for the human cones.

The actual pattern of energy deposition of the incident light along the cone length depends not only on the transmission properties of the receptor, but also on the absorption spectrum and location of the photopigments within the cone. While the tapered waveguide model requires only one such pigment for the transduction of light into an electrical signal, the operation of the discrimination mechanism would be enhanced by the presence of more than one photopigment. We might indeed expect that multiple photopigments would be present and play an important secondary role in enhancing the operational efficiency of the model. Consider, for example, one particular possibility for a two-pigment distribution: a maximally long wavelength-absorbing pigment concentrated near the proximal portion of the outer segment and a maximally blue-absorbing pigment concentrated primarily towards the more distal portions of the cone. Such a distribution would maximize the cone detection efficiency of red light, which penetrates the cone to only a limited depth. For blue light, which travels the full length of the segment, such a distribution would minimize the amount of short wavelength light absorbed and thus attenuated in the near regions. This would both enhance the amount of

signal coming from the distal portion of the cone from absorbed short wavelength light as well as decreasing the amount of blue light absorbed in the proximal portions of the cone outer segment. Blue light absorbed in the proximal regions of the cones would convey intensity information, but not contribute usefully to the color resolution.

Plausible candidates for this two-pigment distribution are two rhodopsin-like pigments with peak absorbancies at wavelengths around 575 and 500 nm, respectively. There is good reason for expecting these to be the appropriate choices for the pigments.

Murray (1968), in measuring the difference spectra of sonicated monkey foveal receptors (which attempts to circumvent many of the difficulties of the single cone technique) found evidence for two photopigments with absorption at 576 and 526 nm with approximately ± 20 nm uncertainty.

Rhodopsin with absorbance maximum at ~ 500 nm is already present in the human retina (in the rod receptors, at least) and would be a logical candidate for the short wavelength cone pigment. The R-G and B-Y differentiation of the opponent colors coding are respectively around the 575 and 500 nm points; if two pigments are present, logical points about which to differentiate are, at the absorption peaks of the photopigments. These two wavelengths are central to a number of color vision phenomena. They are the locations of the neutral point in dichromates and are the position of the relative minima in the spectral discrimination curve. The colors in the wavelength

domain between 500 and 575 nm have no complementaries and this region defines a span within which the Stiles-Crawford color change departs from its general pattern.

2. Stiles-Crawford Color Change (Effect of the Second Kind)

It is well-known that as the angle of incidence of light at the retina is increased the apparent intensity decreases (Stiles-Crawford effect of the first kind). This effect is rather well explained on the basis of the transmission properties of a dielectric waveguide or optical fiber (diFrancia, 1946; O'Brien, 1946; Snyder and Pask, 1972). Stiles (1937) reported on a color effect appearing under the same conditions, wherein the apparent color is also a function of the angle of incidence. The effect is primarily that of a shift to longer apparent wavelengths with increase in angle of incidence. Walraven et al (1960) suggested an explanation of this phenomenon on the basis of pigment self-screening effects. However, the pigment densities required to model this effect on the basis of a three-cone model of color vision are much too high (Enoch and Stiles, 1962). In addition, Walraven had to assume a different form of this effect for the blue region. If, instead, one assumes that the physical transmission properties of the cones may serve as the basis of color discrimination, the Stiles-Crawford color change may be explained very simply, very directly and (over most of the spectrum) very accurately. The propagation of light in a dielectric cylinder depends on not only the physical wavelength, but the guide

wavelength, which is a function of both the physical wavelength of the incident light and its direction of incidence. This guide wavelength λ_g is given by the physical wavelength λ and the angle of incidence θ as

$$\lambda_g = \lambda/\cos\theta$$

This is simply the component of the incident physical wavelength in the direction of the guide axis. In a physical analogy, we simply expect that light not incident paraxial to the cones will "jam" sooner within the confines of the cone and not propagate as efficiently as those rays directed along the axis. In figure 3 we make a direct comparison between the original data of Stiles (1937) and the very simple function $\lambda/\cos\theta$. The theoretical curves have all been shifted slightly and uniformly to correspond with the eccentricity of the optical center with respect to the center of the pupil of the test eye reported by Stiles (1937). As is evident, this very simple model, which assumes only that color discrimination depends on the transmission properties of the color receptors, provides a remarkably good fit with the data, except for the region between 575 and 500 nm. In this region secondary effects play an important role. This indicates the need for a more precise calculation (and more experimental data as well) on the details of energy deposition in the cone segment as a function of angle. Such computation requires some specific assumptions about the photopigment identity and density in the cones.

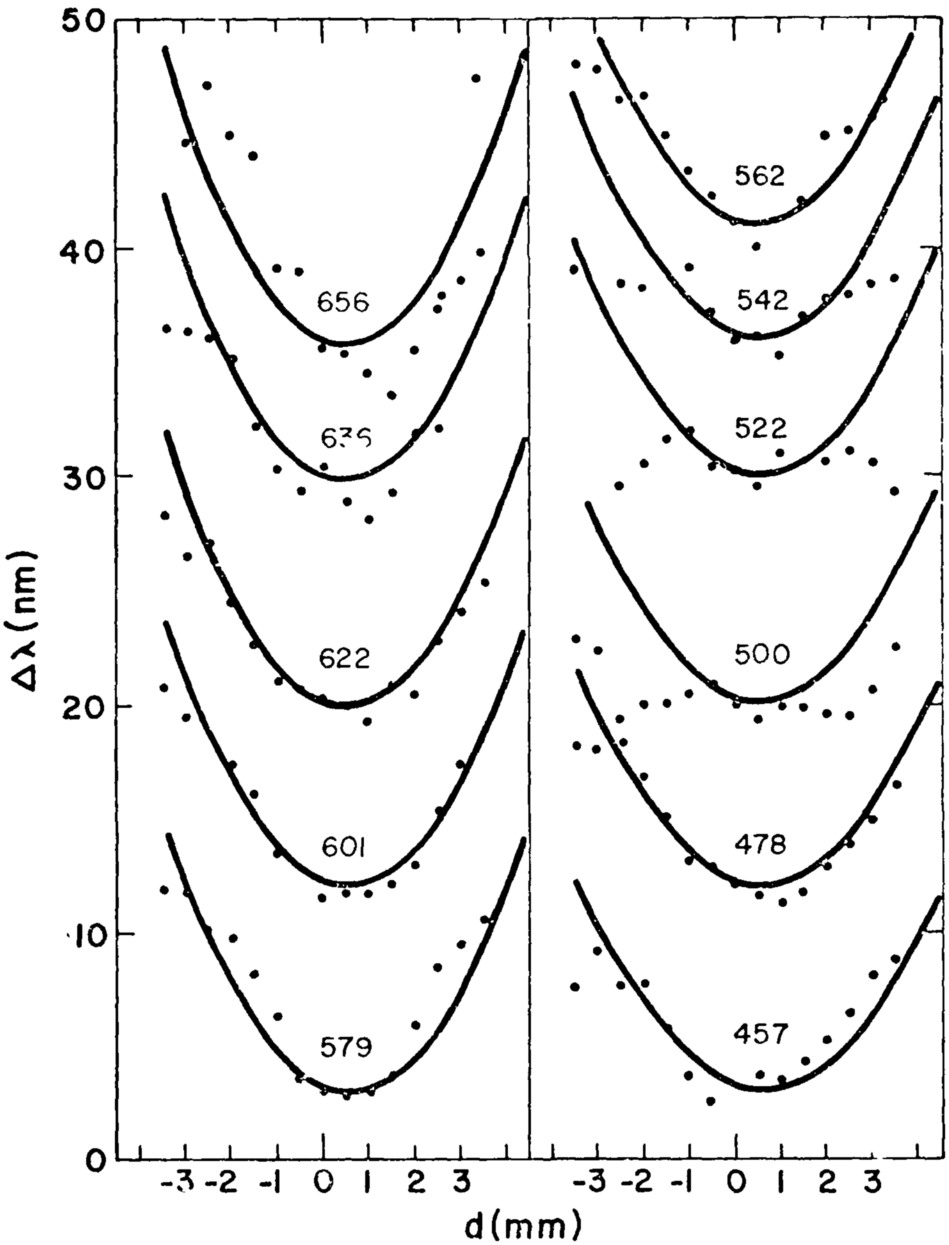

FIG. 3. The Stiles Crawford Color Change. The figure plots the original data (points) of Stiles (1937) and theoretical curves based on the dependence of guide wavelength, λ_g, with angle of incidence. All the theoretical curves have been shifted by about + 0.5 mm to match the eccentricity of the optical center of Stiles' test eye with respect to its pupil center. The fit to the data of this very simple model is good except for the three curves at 542, 522, and 500 nm (although these too are in agreement for pupil displacements less than ± 1.5 mm).

3. Defective Color Vision

Color blindness is not satisfactorily explained by either the fusion or loss mechanisms ordinarily suggested within the trichromatic framework (Balaraman, 1960). The proposed model offers a simple and plausible scheme of accounting for the many aspects of the phenomena.

Our course of deduction has led us to expect the presence of at least two cone photopigments and two color differentiating points on the output channels. The important wavelengths for both of these categories occur at the wavelengths 575 and 500 nm. With this in mind we may look at defects in color vision as defects in the assumed apparatus of the color vision system. The categories of color defective fision are (1) "red-green" color blindness which is the most common form and occurs in two different types, protanopia and deuteranopia. In both cases the dimensionality of color discrimination appears to be reduced from three to two and colors are discriminated only as more yellow or more blue than a central differentiating point at 500 nm (neutral point). (2) "Blue-yellow" color blindness. Much less common than case (1) above is the condition of tritanopia, which is similarly dichromatic with a neutral point ca. 575 nm. (3) Monochromism. Extremely rare is the complete absence of color discrimination, where the spectrum is seen only as shades of black and white. At least two different forms are recognized, rod monochromism and cone monochromism.

In protanopia it is well known that the sensitivity

to long wavelength light is markedly reduced. Moreover, the reflection densitometry measurements (Baker and Rushton, 1964) have made a convincing case that protans probably do, in fact, have a missing red pigment. In the context of the proposed model, the absence of the pigment may well have the effect of crippling the red-green discrimination effected by differentiating signals about the 575 nm point. If there are little or no signals output by the cones corresponding to the proximal portion of the outer segments, now devoid in this condition of the red-sensitive pigment, we would indeed expect the failure of red-green discrimination and the consequent dichromacy.

There is no corresponding evidence that, as expected by the trichromatic theory, a green pigment is missing in deuteranopia. Of course, in the proposed model we look elsewhere for the difficulty. The likely mechanism for deuteranopia is a neural defect wherein the channel performing the differentiation about the 575 nm point is simply inoperative. Conceptually, this is rather similar to the conventional fusion hypothesis ordinarily formulated in the trichromatic theory.

A suggested vehicle for the tritanopic defect is a simple loss of the discriminating point about 500 nm, which may arise from a loss of the blue pigment or (more likely) a neural defect in the differentiation of the time-correlated information about the point corresponding to 500 nm.

Very few studies looking for abnormalities at the microscopic level in the dichromat eye have been reported. To date no differences from the normal appearance have been picked

AD-A131 736 LASER INDUCED DAMAGE IN THE EYE: STUDY OF ENERGY DEPOSITION IN THE RETINA(U) UNIVERSITY OF WESTERN ONTARIO LONDON W J MCGOWAN ET AL. JUN 76 2/2

UNCLASSIFIED DAMD17-76-G-9401 F/G 6/18 NL

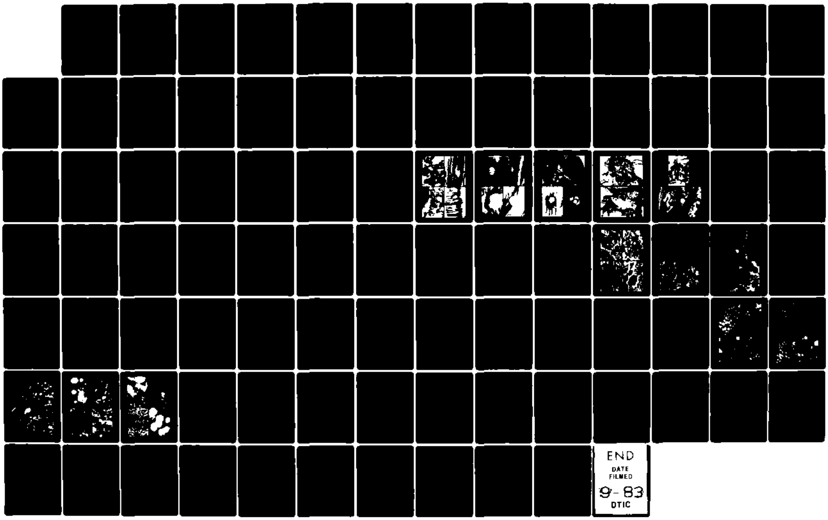

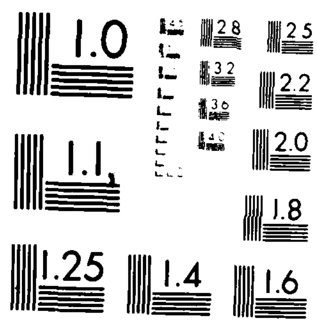

MICROCOPY RESOLUTION TEST CHART
NATIONAL BUREAU OF STANDARDS 1963-A

up. In contrast, the few studies reported on the microscopic examination of the retina in the monochromat eye have revealed striking abnormalities in the retinal architecture.

Microscopic examinations of the monochromat eye have been reported by Larsen (1921), Falls, Walter and Alpern (1965) and Glickstein and Heath (1975). These studies reported in some instances an abnormally low number of cones - though some reported a normal number - but all agreed that the cones were of abnormal shape. The cones were variously reported as "short","abnormally plump," "much wider than normal." If in fact the conical shape per se is the mechanism effecting color discrimination, then quite clearly color vision will not be possible in such cases.

Presumably, the cones' size and shape in the normal retina are just those necessary to effect proper operation over the entire spectral range. If these cones are either too large or too small, (size in the optical sense which depends on both physical diameter and refractive index), color vision characteristics are expected to deviate from the normal.

4. Land Effect

Land (1959) reported observing surprisingly good color reproduction using very limited spectral information. He found that visual scenes could be rendered, for example, using just two wavelength bands (a long wave reference and a short wave reference) with the subjective appearance of the full color range yet present. The two reference wavelengths could be separated by as little as 10 nm and a visual impression

still be that of the scene rendered in the full range of spectral colors, although the colors induced are not fully saturated. The nature of this effect clearly involves higher levels of information processing in the eye-brain system; Walls (1961) discussed the phenomena and concluded that it was not inconsistent with adaptive properties of conventional trichromatic color vision schemes (see Sheppard, 1968).

The effect illustrates that the eye-brain system is able to synthesize and properly assign the full range of colors to a scene in which the information is recorded in a very limited way: the important information is the relative contribution of either long or short wavelengths in each part of the visual scene.

While it is surely remarkable that so little information is required in this process, it is significant that the key information (however compressed) is that of wavelength differences. This scheme is compatible in the rough qualitative fashion(which is our concern here) with the proposed color discrimination mechanism which is optimized to detect wavelength differences.

5. Some Other Static Characteristics

In a rather interesting experiment, Brindley and Rushton (1959), compared the subjective appearance of the color of light incident at the retina in the normal physiological direction to that incident at 180 degrees to this direction by passing light from behind the eyeball through the sclera. They found that there was little apparent difference in the subjective

color impression for the two different directions. It has been commonly assumed that this result rules out color vision being based on waveguide effects. However, as has been stressed by Enoch (1963), the Brindley and Rushton experiment specifically rules out the possibility of selective elements in front of the receptor outer segments mediating color discrimination and it "...does not represent a definitive test of the role of waveguide effects upon vision."

In a tapered waveguide the coupling of light into the guide will be very inefficient for light incident in the "wrong" direction, however, that shorter wavelengths will couple into the cone more efficiently than longer wavelengths will remain unaltered.

Without some very detailed assumpsions about the cone photopigments and the specific workings of the color information processing mechanism it is not possible to make a comparison with such properties as: the photopic spectral sensitivity of the eye, the color discrimination function, and the Stiles π-mechanisms. Our objective in this study is only an examination of the qualitative aspects of the proposed model. A very important test of the model would be just that program of making the appropriate detailed assumptions and looking for the quantitative fit. Unlike the three-pigment, trichromatic model where, in principle, no unique triad can be determined by such a program (even if that model was the correct one) it is not unreasonable to expect that the correct unique set of parameters may be so determinable for the tapered waveguide model.

Indicative of the promise held by this model is the

qualitative aspect of the two color threshold technique of Stiles observed by Brindley (1953). When one attempts to isolate one of the triad of red, green, or blue by exposing the retina to high intensities of the other two colors, the saturation of the "isolated" mechanism was observed to be a highly unsaturated red or pink in the case of long wavelengths, a highly unsaturated blue-green for the middle wavelengths, but a very saturated blue or violet in the short wavelength case. This is clearly the expected result in the proposed model where only in the last named case (blue isolation) is the isolated region not accessible to the red and green lights used to suppress the activity of their respective portions of the cone.

C. Dynamic Properties of Color Vision

Multiple cone models provide little insight into the dynamic properties of human color vision. In contrast, the proposed tapered waveguide model - with the use of assumptions that are essentially forced by the nature of the discrimination mechanism itself - are in accord with response of the color vision system to changes in the incident light signals.

1. Differential chromatic latencies

We have already discussed the conversion of the positionally-correlated color information of a tapered cone into a time dispersion of the cone output signals. The pattern of this time dispersion is dictated by the nature of the color selection mechanism; long-wavelength information is contained in the short-latency electrical output of the cone and short-wavelengths in the long-latency in accord with the data, i.e.

latency is inversely proportional to wavelength (see above).

There are some important observable consequences of the differential chromatic latency which have not hitherto been satisfactorily explained. In one very interesting series of experiments Ives (1917) investigated the response time of the color vision system by displaying to his subjects a bar of light which was moved across their field of view. He compared the perception of such a moving bar for the cases of a yellow constructed two different ways - one a pure spectral yellow and the other of a mixture of green and red combining to form a color matching that of the pure yellow. In the case of the red-green combination motion of the test bar across the field of view resulted in a color separation due to the differential chromatic latencies of the perceptual mechanism. His observers saw the moving pattern spread to a leading red edge, a trailing green edge and the combined yellow remaining at the center. For the case of the pattern formed by the pure spectral yellow, however, no such dispersion was observed and the test pattern remained uniformly yellow. That is, although the eye - to a first approximation - sees the two yellows as matching (a metameric match) the two different lights do not elicit exactly equivalent responses in the retinal receptors. While the colors are metameric to a first approximation, they are inherently distinguishable and some property of the receptors must reflect this.

Ives results clearly contradict the widely held three-receptor model of color vision, but it is just the result

expected in our proposed model, directly reflecting the time dispersion of the positionally-correlated color information (red, green and yellow, all having different associated time constants).

The time coding of color information also plays a direct role in the Benham's top phenomena: the induction of the subjective perception of color using only modulated achromatic illumination (Polizzotto and Peura, 1975; Roelofs and Zeeman, 1958; Sheppard, 1968). For repetitively presented patterns consisting of three components - a neutral reference signal and an on signal composed of two parts one, of shorter duration which is the active component and a longer duration inactive component (where the difference between active and inactive may be of relative brightness, for example) - then color code is: 1) red perception occurs when the active component is presented immediately after the reference signal, 2) green perception for the active component presented at intermediate times, and 3) blue perception for the active component presented after the bulk of the inactive portion (most delay with respect to the reference signal). This is just that code predicted by the proposed model:

2. Eye Movements

The induction of color perception by achromatic stimuli in this procedure is optimized for presentation frequencies of the order of 10 H_z. As previously discussed this appears to be a naturally resonant frequency in visual perception. This is roughly the frequency of the saccadic eye movements which we have suggested is the basis for color

information processing. Use of time coding of color information in the proposed model requires such a mechanism (or something similar) to provide phase or reference information). It is certainly to be expected that the frequency of such reference signals will be central to the dynamic properties of the visual system.

3. Brucke-Bartley Effect

The above aspect is further substantiated by the variation of perceived intensity of intermittent stimuli: the apparent brightness of flashing lights is greatest for the resonant 10 Hz presentation frequency (c.f., Sheppard, 1968).

4. Broca-Sulzer-Pieron Effect

The recognition of a color occurs with greater delay than the production of the electrical signal in the retina (differential chromatic latency). These perceptual latencies were measured by Ferree and Rand (1924). They determined the time for the rise of sensation to maximum for white, red, yellow, green and blue light. They found that the perceptual delay varied systematically with wavelength, with the longest wavelength being the slowest and the fastest rise of sensation occurring for the shortest wavelengths and white light having the longest rise time of all. That is, the most information processing time is required for the longest wavelengths (and even longer for white light).

This phenomenon too is expected in the proposed color vision model and simply reflects a general limitation on any spectrometer constructed on the basis of spectral dispersion along a tapered waveguide. As previously noted signals arising

from light absorbed in the most distal portions of the cones, while delayed relative to signals from the proximal portion of the cone, are uniquely correlated with short wavelength light. The proximal cone signals, while arising first must be associated with further information processing to determine the incident color since all wavelengths pass through this region and, depending on the photopigment present there, all have some probability of producing a signal there. This means that additional information processing time (relative to short wavelength light) is required for the long wavelength signals. This information processing time is long compared to the differential chromatic latencies associated with the delay in propagation time along the length of the cones. As a consequence this gives rise to a reversal of the time course of the color code, that is, the rise time to maximum sensation is a monotonically increasing function of wavelength as opposed to the electrical signals from the cones, which are universally proportional, in agreement with the experimental observations.

IV. EXPERIMENTAL TESTS OF THE MODEL

There are a number of experiments that can critically evaluate the accuracy and efficacy of the proposed model:

(1) Precise measurement of the physical parameters and shape of the retinal cone are needed for verification of the proposed theory. In what has been an intensive and single-minded search for the three cone pigments required by the conventional trichromatic theory there has traditionally been

very little importance attached to these parameters. To date, very little experimental effort has been expended to determine the exact size, shape and refractive index of the foveal cones. The model calculations are consequently based on the best available and rather crude published estimates of these parameters.

(2) Analog experiments can be conducted with tapered optical fibers (or alternatively with microwaves with, for example, appropriately scaled styrofoam cones) to directly confirm the predicted dispersion mechanism. We might also note parenthetically that a spectrometer could be built and operated on just this proposed mechanism. Indeed, if one constructed a tapered fiber with an appropriate photosensitive semi-conducting material, and repetitively pulsed a read-out of photoelectrons one could electronically extract spectral information (once again, technology would emulate nature).

(3) The discriminatory properties of the proposed physical mechanism depend critically on the refractive index difference between the receptor and its surrounding interstitial matrix. Alterations in the refractive index of the medium in which the cones are emerged will profoundly influence their color discrimination. If the refractive index of the inter-photoreceptor space is systematically altered, and the resulting colour vision characteristics of the subject eye are determined, a very sensitive test of the model is possible. In this connection we may note that while the pigment epithelium is a very effective barrier between the plasma and the photoreceptor

layer, the retina is not so isolated from the vitreal side (Kuwabara, 1965). There is thus the possibility of modifying the refractive index in the interphotoreceptor space by introducing appropriate agents through the vitreal side. We might note that the muco-polysaccharide-like substances in the interphotoreceptor space are chemically similar to immunoglobulins and in this connection it is interesting that Raymond (1974) reported observing reversibility of colour blindness in allergenic subjects given IgE hyposensitization treatments. While Raymond gave few details on the color vision characteristics of his subjects this may well be an important line of study to pursue.

(4) The energy deposition pattern of differently coloured lights within the outer segment may possibly be inferred from a destructive testing technique. Exposing the primate retina to high-intensity coherent light will damage the retina and if levels of light are used which are below the gross damage threshold, it is known that the photoreceptor outer segments are the first portions of the retina to show microscopically visible signs of damage (Adams, Beatrice, Bidell, 1972). The model can be tested by varying the output wavelength of a high intensity light source and looking for differences in the resulting damage patterns as a function of the colour. If the standard three-pigment, three-receptor model of colour vision were correct, we would expect to find only a particular portion of the cone population to be damaged at the appropriate

intensity levels as the incident wavelength is varied (distinguishable cone populations). In our proposed model, on the other hand, all cones in a local area will be damaged in rather similar patterns: long wavelength light primarily disrupting the proximal portions of the cone and short wavelength light either damaging only the more distal cone regions or the entire length of the outer segment, depending on the photopigment distribution within the cones.

V. CONCLUSIONS

We have proposed a very simple and straightforward model for color discrimination by the retinal receptors of the human eye. The proposed model depends for its operation on the physical properties of the receptors and enables each cone to individually act as a miniature spectrometer.

The color dispersion of such a spectrometer is clearly demonstrable in principle. The model is consistent with the known structure and physiology of the retina. The apparatus needed to make use of the operating principle of the model is present in the eye and indeed the presence of these attributes there is difficult to explain otherwise.

The model is not contradicted by any known data and even without making any specific assumptions about the details of the cone photopigments it leads to a simple and direct explanation of the wide range of both steady state and dynamic performance characteristics of human color vision. The predictions of the model are subject to direct and critical

experimental test.

The model succeeds remarkably well as a unifying principle and brings together in one simple and connected explanation what has hitherto been a disparate collection of observations. The model, of course, is not complete; indeed it is only a beginning. Complete understanding of color vision awaits understanding of the complete organism: the complex interplay of very sophisticated elements comprising each individual. The model does, however, appear to be an illuminating concept; one which offers some promise towards more complete understanding of color perception.

REFERENCES

1. Alpern, M.; Falls, H.F.; Lee, G.B. (1960) "The Enigma of typical total monochromacy". Am. J. Ophthal. 50, 996-1011.
2. Alpern, M.; Lee, G.B.; Spivey, B.E. (1965) "π_1 Cone Monochromatism". Arch. Ophthal 74, 334-337.
3. Baker, H.D., and Rushton, W.A.H. (1965) "The red-sensitive pigment in normal cones," J. Physiol. 176:56
4. Balaraman, Shakuntala (1962) "Color Vision Research and the Trichromatic Theory: A Historical Review". Psychological Bulletin 59, 434-448.
5. Barer, R. (1957) "Refractometry and Interferometry of living cells". J. Opt. Soc. Am. 47, 545.
6. Biernson, G. (1968) "Evaluation of physiological evidence for trichromatic theory" in H.L. Oestreicher & D.R. Moore, eds. Cybernetic Problems in Bionics. Bionics Symposium 1966, Gordon and Breach, N.Y. (1968), p.p. 407-417.
7. Biernson, G. and A.W. Snyder (1968) "A Model of vision employing optical mode patterns for color discrimination". IEEE Trans. SSC 4, 173-181.
8. Biernson, G. (1968) "A review of models of vision" in Advances in Biomedical Engineering and Medical Physics Vol. 2, S.N. Levine, ed. J. Wiley, N.Y.
9. Bouman, M.A. and Walraven, P.L. "Color Discrimination Data" in Handbook Sensory Physiology, VII/4.
10. Brindley, G.S. (1953) "The effects on colour vision of adaptation to very bright lights", J. Physiol. 122, 332-50.
11. Brindley, G.S. and Rushton, W.A.H. (1959), "The color of monochromatic light when passed into the human retina from behind.", J. Physiol. 147, 204-208.

12. Brown, P.K. and Wald, G. (1964) "Visual pigments in single rods and cones of the human retina", Science 144, 45-52.

13. Clowes, M.B. (1962) "A note on colour discrimination under conditions of retinal image constraint". Optica Acta 9, 65-8.

14. Cohen, A.I. "The fine structure of the extra-foveal receptors of the rhesus monkey", Exp. Eye Res. 1, 128-36.

15. Cohen, A.I. (1963) "The fine structure of the visual receptors of the pigeon". Exp. Eye Res. 2, 88-97.

16. Di Francia, G. Toraldo (1949) "Retina cones as dielectric antennas", J. Opt. Soc. Am. 39, 324.

17. Ditchburn, R.W. (1973), Eye-movements and Visual Perception Clarendon Press, Oxford (421 p.)

18. Dowling, J.E. (1965) "Foveal receptors of the monkey retina: Fine structure", Science 147, 57-9.

19. Enoch, J.M. (1961) "Nature of transmission of energy in the retinal receptors.", J. Opt. Soc. Am. 51, 1122.

20. Enoch, J.M. and Stiles, W.S. (1961) "The colour change of monochromatic light with retinal angle of incidence" Optica Acta 8, 329-58.

21. Enoch, J.M. (1963) "Optical properties of the retinal receptors". J. Opt. Soc. Am. 53, 71.

22. Enoch, J.M. (1967) "The Retina as a Fiber Optics Bundle" in N.S. Kapany Fiber Optics, Academic Press, N.Y. pp. 372-396.

23. Ferree, C.E. and Rand, G. (1924) "Flicker photometry and the lag of visual sensation." Am. J. Psychol. 35, 209-216.

24. Glickstein, M. and Heath, G.G. (1975) "Receptors in the Monochromat Eye", Vision Res. 15, 633-6.

25. Hagins, W.A., Penn, R.D. and Yoshikami, S. (1970) "Dark Current and photocurrent in retinal rods." Biophys. J. 10, 380.

26. Hagins, W.A. and Yoshikami, S. (1974) "A Role for Ca^{2+} in Excitation of Retinal Rods and Cones". Exp. Eye Res. 18, 299-305.

27. Hall, M.O. and Heller, J. (1969) "Mucopolysaccharides of the Retina". Straatsma, Hall, Allen, Crescitelli, eds. The Retina, UCLA Conf., 211-234.

28. Ives, H.E. (1918) "The resolution of mixed colors by differential visual diffusivity". Phil, Mag. 35, 413-421.

29. Judd, D.B. (1945). "Standard response functions for protanopic and deuteronopic vision." J.Opt. Soc. Am. 35, 199-221.

30. Judd, D.B. (1960) "Appraisal of Land's work on Two-Primary Color Projections". J. Opt. Soc. Am. 50, 254-68.

31. Kapany, N.S. and Burke, J.J. (1972) Optical Waveguides Academic Press, N.Y.

32. Kowabara, Toichiro (1965) "Some aspects of Retinal Metabolism revealed by Histochemistry" In Gragmore, Biochem of Retina, Academic Press, 93-98.

33. Land, E.H. (1959). "Color Vision and the Natural Image" Proc. Nat. Acad. Sci. U.S. 45, 115, 636.

34. Liebman, P.A. (1972) "Microspectrophotometry of photoreceptors". Handbook of Sensory Physiology VII, Springer, Berlin, 482-528.

35. Marks, W.B., Dobelle, W.H., MacNichol, E.F., Jr. (1964) "Visual Pigments of Single Primate Cones", Science 143, 1181-1183.

36. Marks, W.B. (1965), "Visual Pigments of Single Goldfish cones", J. Physiol. (Land) 178, 33-

37. Moreland, J.D. Peripheral Colour Vision Anable Serry Physiol VII/4, ch. 20, 517-533.

38. Murray, G.C. (1968) "Visual pigment multiplicity in cones of the primate fovea" Doctoral thesis, Baltimore: John Hopkins U.

39. Myers, Orlob (1962) "Spectral Sensitivity of visual receptor". Nature (Lond.) 193 449-51.

40. O'Brien, B. (1946) "A Theory of the Stiles and Crawford effect." J. Opt. Soc. Amer. 36, 506-509.

41. Polizzorro, L. and Peura, R.A. (1975) "A mathematical approach to explain subjective color perception", Vision Res. 15, 613-616.

42. Polyak, S. (1941) The Retina, Univ. of Chicago Press, Chicago, Ill.

43. Polyak, S. (1957) The Vertebrate Visual System. The Univ. of Chicago Press, Chicago, Ill.

44. Raymond, L.F. (1975) "Physiology of Color Vision and the Pathological changes in Reversible Color Blindness, a Deficiency Disease of the Retina". Ann. Ophthal. 7, 532-534.

45. Riggs, L. (1967) "Electrical evidence on the trichromatic theory". Inves. Ophthal. 6, 6-17.

46. Roelofs, C.O. and Zeeman, W.F.C. (1958) "Benham's Top and the color phenomena resulting from interaction with intermittent light stimuli." Acta. Psychol. 13, 334-356.

47. Sheppard, J.J., Jr. (1968) Human Color Perception, American Elsevier Publishing Company, New York.

48. Sidman, R. (1957) "The Structure and concentration of solids in photoreceptor cells studied by refractometry and interference microscopy" J. Biophys. Biochem. Cytol. 3, 15-30.

49. Snyder, A.W. (1969) "Assymptotic expressions for eigenfunctions and eigenvalues of a dielectric or optical waveguide" IEEE Trans. MTT 17, 1130-1138.

50. Snyder, A.W. (1970) "Coupling of modes on a tapered dielectric cylinder" IEEE Trans. MTt 18, 383.

51. Snyder, A.W. (1971) "Mode Propagation in a nonuniform cylindrical medium" IEEE Trans MTT-19, 402-403.

52. Snyder, A.W. (1972a) "Coupled Mode Theory for Optical Fibers", J. Opt. Soc. Am. 62, 1267-1277.

53. Snyder, A.W. and Pask, C. (1972) "A Theory for changes in spectral sensitivity induced by off axis light." J. Comp. Physiol. 79, 423-427.

54. Snyder, A.W. and Pask, C. (1973) "Absorption in conical optical fibers", J.Opt. Soc. Am. 63, 761-2.

55. Stiles, W.S. (1937) "The luminous efficiency of monochromatic rays entering the eye pupil at different points and a new colour effect." Proc. Roy. Soc. B. 123, 90-118.

56. Vos, I.J. and Walraven, P.L. (1966) Exc. Med. 4, 91

57. Wald, George and Brown, Paul K. (1965) "Human Color Vision and Color Blindness" in Cold Spring Harbor Symposium in Quantitative Biology, 345-361.

58. Walraven, P.L. and Bouman, M.A. (1960) "Relation between directional sensitivity and spectral response curves in human cone vision." J. Opt. Soc. Am. 50, 780-784.

59. Wright, W.D. and Pitt, F.H.G. (1934) "Hue discrimination in normal colour vision." Proc. Phys. Soc. Lond., 46, 459-473.

60. Young, R.W. (1967) "The renewal of receptor cell outer segments" J. Cell Biol. 33, 61-72.

Added in Proof:

61. Adams, D.O.; Beatrice, E.S. and Bedell, R.B. (1972) "Retina: Ultrastructural alterations produced by extremely low levels of coherent radiation." Science 177, 58-60.

62. Feeney, L. (1972) "The Interphotoreceptor Space II. Histochemistry of the matrix" Develop. Biol. 32, 115-128.

63. Leibovic, K.N. (1976) "Photolysis and excitation in vertebrate photoreceptors", Biol. Cybernetics 21, 171-179.

64. Tamir, T. ed. (1975) Integrated Optics, Springer-Verlag, N.Y.

65. Yoshikami, S., Hagins, W.A. (1973) "Control of the dark current in Vertebrate Rods and Cones" in Biochemistry and Physiology of Visual Pigments, 245-255, Springer-Verlag, N.Y.

SCANNING ELECTRON MICROSCOPY OF NORMAL & LASED RABBIT RETINA

Bessie Borwein, Ph.D.

Madhu Sanwal, Ph.D.

J.A. Medeiros, Ph.D.

J.Wm. McGowan, D.Sc.

From the Dept. of Physics and Centre for Chemical Physics
The University of Western Ontario
London, Ontario, N6A 3K7

Presented at:

Supported by grants from:
U.S. Army Medical Research & Development Command

Address for reprints: Dr. Bessie Borwein, Dept. of
Anatomy, The University of Western Ontario,
London, Ontario, N6A 5C1, 679-2688

Bessie Borwein

Scanning electron microscopy of rabbit retina

Summary

This study presents the topography as seen by scanning electron microscopy of the rabbit retina in general and the photoreceptors in particular; and of large laser lesions in the retina.

There are only a few studies of vertebrate retina using scanning electron microscopy[1-8] but none of the rabbit retina, and none of laser lesions in a retina.

This study explores the topography of the rabbit retina in general, and the photoreceptors in particular; and large laser lesions in the retina.

METHODS

Mature New Zealand black rabbits with well pigmented retinas were used. Immediately after lasing, photographs of the fundus were taken with a Topcon fundus camera, and another photograph was taken prior to enucleation; also line-drawing maps were made of the retina with the lesions.

Details of Laser Exposure in Rabbits:-

The laser exposures were carried out with a flashlamp pumped dye laser. The coaxial flashlamp was typically run at 20 KV discharge voltage and rhodamine 6G was employed as the active medium. The laser output wavelengths employed ranged from 570 to 600 nm. (typically 585 nm) The output pulse duration was 0.4 μsec (FWHM). The beam diameter at the rabbit cornea was 5.0 mm. The laser beam divergence was 4 milli radians and the estimated minimum spont size was 75 microns. The retinal energy density of the typical lesion studied in this report was on the order of $10 J/cm^2$.

The rabbits were anesthetized with an intravenous

injection of Nembutol and the pupils dilated with 2% homatrapine hydrobromide.

Details of Tissue Processing:-

Lased eyes were dissected out and washed clear of blood. They were cut open at the ora serrata with a sharp blade and fixed in 2.5% glutaraldehyde + 0.5% paraformaldehyde in 0.1M Sorensen's phosphate buffer. After thirty minutes the eye tissues were sufficiently hardened to be dissected further. The cornea, lens and vitreous were gently removed and the lased areas, located with the aid of maps and fundus photographs, were cut out using new sharp blades. From many trials, it was found that 2 days in the aldehyde fixative and 30 minutes in 1% osmic acid in 0.1 M phosphate buffer gave best results for SEM studies. The tissue was dehydrated in ethyl alcohols and acetone; and critical point dried with CO_2. The specimen was coated with a 20 nm layer of gold using a Technics Sputter coater; examined in a HHS-2R Hitachi Scanning Electron Microscope, and photographed on Kodak plus-X film.

The laser lesions were well above threshold and sufficiently powerful to affect the full thickness of the retina.

Results: -

Since the impact of scanning electron microscopy is visual and in order to avoid repetition and to present the material in the most effective manner, the results are presented photographically with accompanying captions in Figures 1 to 17.

DISCUSSION

Although a good deal is known about the rabbit retina from light and transmission electron microscopy[9-11], confirmation of some information, and the extension of our perceptions and insights is provided by the dramatic impact of the three-dimensional type of view obtained by scanning electron microscopy.

We list some of the more significant observations below.

The rod outer segments are observed to be very long and uniformly cylindrical. The ciliary connectives do not all lie at the same level, so that the outer segments are not all of the same length.

The texture of the inner plexiform layer is so markedly different from all other layers that it can be identified with ease, even as debris in laser lesions.

Müller cell processes are known to surround and envelope the nuclei of the retina[12-15] but here we see how these processes form a distinct nest for each nucleus. The other surprising fact is that even the considerable trauma of a suprathreshold laser insult does not explode the nuclei, but they are extruded whole and discrete from their nests without their connecting fibres.

The sequence of laser lesions shown here is from a barely raised dome covered by intact basal lamina, to small perforations in a small hillock, to large open craters with

much extruded retinal debris over a large swollen mound.

Some of the debris seen at the crater openings can easily be identified as variously: nuclei, blood cells and pieces of inner plexiform layer. However, fine filamentous material is also seen and we do not yet know whether this is vitreal, from the blood, or whether some of it represents healing, or even the beginnings of formation of an epiretinal membrane. This is currently being investigated. Some of the cellophane-like membranous material seen is the vitreal-retinal boundary layer, rolled up after being torn by the laser impact. (Figs. 10,11,13). The "beaded fibres" (Figs.15,16,17) were often seen and we can as yet offer no explanation of their nature. This work is in the process of correlation with transmission electron microscope studies.

Bessie Borwein

Scanning electron microscopy of rabbit retina

Acknowledgments

We thank Dr. M. Montemurro, Chairman, and the entire Anatomy Dept. of The University of Western Ontario for providing facilities required for carrying out this study and Mrs. Artee Karkhanis for her excellent technical assistance.

Bessie Borwein

Scanning electron microscopy of rabbit retina

REFERENCES

1. Cleveland, P.H. and Schneider, C.W.: A Simple Method for preserving ocular tissue for scanning electron microscopy. Vision Res. 9: 1401-1402, 1969.

2. Dickson, D.H. and Hollenberg, M.J.: The fine structure of the pigment epithelium and photoreceptor cells of the newt, Triturus viridescens dorsalis (Rafinesque). J. Morph. 135: 389-432-1971.

3. Hansson, H.A.: Scanning electron microscopy of the rat retina. Z. Zellforsch. 107: 23-44, 1970.

4. Hansson, H.A.: Scanning electron microscopy of the retina in vitamin-A-deficient rats. Virchows Arch. Abt. B. Zellpath. 4:368- 1970.

5. Lewis, E.R., Zeevi, Y.Y. and Werblin, F.S.: Scanning electron microscopy of vertebrate visual receptors. Brain Res. 15: 559-562, 1969.

6. Smith, M.E. and Finke, E.H.: Critical point drying of soft biological material for the scanning electron microscope. Invest. Ophthal. 11: 127-132, 1972.

7. Steinberg, R.H.: Microscopy of the bullfrog's retina and pigment epithelium. Z. Zellforsch. 143: 451-463, 1973.

8. Bekchanov, A.N.: Histological Investigation of the Rabbit Retina. Bull. Expt. Biol. & Med. 69(3): 343-344, 1970.

9. Jan, L.Y. and Revel, J-P.: Hemocyanim-Antibody labeling of rhodopsin in mouse retina for a scanning electron microscope study. J. of Supramolec. Struct. 3: 61-66, 1975

10. Magalhaes, M.M. and Coimbra, A.: The rabbit retina Müller cell. A fine structure and cytochemical study. J. Ultrastr. Res. 39: 310-326, 1972.

11. Prince, J.H. (Ed.): The Rabbit in Eye Research, Charles C. Thomas, Springfield, Illinois, 1964.

12. Borwein, B. and Hollenberg, M.J.: The photoreceptors of the "four-eyed" fish, Anableps anableps L J. Morph. 140: 405-441, 1973.

13. Evans, E.M.: On the ultrastructure of the synaptic regions of visual receptors in certain vertebrates. Z. Zellforsch: 71: 499-516, 1966.

14. Pedler, C.: The fine structure of the radical fibres in the reptile retina. Exp. Eye Res. 2: 296-303, 1963.

15. Uga, S. and Smelser, G.K.: Electron microscopic study of the development of retinal Müllerian cells. Invest. Ophthal. 12: 295-307, 1973.

Bessie Borwein

Scanning electron microscopy of rabbit retina

KEY WORDS: Rabbit retina

Scanning electron microscopy

Laser lesions.

Fig. 1. - Normal rabbit retina. The vitreal surface is uppermost. Some ganglion cell (G) nuclei can be seen and Müller cell processes (MC) are prominent. The ganglion cell and nerve fibre layers are not clearly distinguishable. The inner plexiform layer (IPL) is sponge-like in appearance. The inner nuclear layer (INL) is bounded by the narrow outer plexiform layer which has distinct horizontal processes (HP). The nuclei of the outer nuclear layer (ONL) are smaller and more numerous than those of the INL and at the bottom left-hand of the picture can be seen the photoreceptors. Note that when a nucleus is displaced there is left a discrete nuclear nest (NN) formed from Müller cell processes.

x6,000

Fig. 2. - Normal rabbit rods including their nuclei (N). The inner limiting membrane (ILM) can be seen and also the inner segments (IS), connecting cilium (C) and the long uniformly cylindrical outer segments (OS). Note that the ciliary connective varies in its position in the retina, and the outer segments differ in their lengths.

x12,000

Fig. 3. - Outer nuclear layer to show the "nuclear nests" (NN) that surround the nuclei.

x21,000

Fig. 4. - A 2-day old laser lesion appears as a more or less symmetrical hillock or hump, on the uninterrupted vitreal surface of the retina.

X1,200

Fig. 5. - The vitreal surface of the retina with a 2-day old laser lesion, showing small perforations in the vitreal-retinal boundary layer,at the summit of the hillock.

X2,100

Fig. 6. - A 7-day old laser lesion sectioned through the thickness of the retina. It shows how the retina humps up and folds so that the photoreceptor (PR) layer comes to lie in a central vertical line. The choroid (Ch) and sclera (S) can be seen. The inner limiting membrane (ILM) is very little disturbed.

X1,200

Fig. 7. - A 2-day old lesion with nuclei extruded from well-defined openings on the hillock summit. Cell debris, erythrocytes and some fibrous material are present.

X2,100

Fig. 8. - A piece of retina with a 2-day old laser lesion that appears like the crater of an erupted volcano. There is cellular debris at the crater. Note the cut surface through the thickness of the retina which appears intact and unaffected by the neighbouring laser lesion.

x480

Fig. 9. - Surface view of a large crater of a 7-day old laser lesion with red blood cells, nuclei and debris lying around the edge of the crater.

X2,100

Fig.10. - A 4-day old laser lesion in which the contents of the retina have poured, lava-like, over the slopes of the lesion hillock. Membranous material (M) of the vitreal-retinal border has curled up and lies along the hillock slope.

X1,020

Fig. 11. - A portion of Fig. 10 magnified to show the cellophane-like membranous material (M) which is probably the curled up inner limiting membrane. There are nuclei (N) present, and also sponge-like material resembling the IPL of the normal retina. (See Fig. 1)

X6,000

Fig. 12. - The vitreal surface of the retina with two 7-day lesions, the lower one of which (arrow) has a large crater. Note the wrinkle-pattern of the dried vitreal surface of the retina, and the general depression around the unmarked lesion of the retina.

X210

Fig. 13. - A 7-day old laser lesion (the upper one shown in Fig. 12) magnified to show the crater covered with discrete extruded nuclei, membranous material (M), cell debris and macrophage (Mp).

X2,100

Fig. 14. - A 7-day old laser lesion with a large empty-looking crater and only a few nuclei adhering to the hillock summit. Note the cracks in the vitreal surface at the edge of the crater (arrows).

X2,100

Fig. 15. - The crater of a 2-day old lesion shows a distinct bundle of beaded, fibrous material (F) lying across the centre of the crater, extending from the rim. There are numerous extruded nuclei and considerable cell debris.

X2,100

Fig. 16. - The fibrous material (F) shown in Fig. 15 is magnified here. It consists of loosely packed, approximately parallel, strings or cords of irregular diameter, with occasional beadlike swellings or attachments. Some nuclei (N) can be seen.

X6,000

Fig. 17. - A view looking onto the crater of a 1-day old lesion showing "beaded fibres" (F) lying across extruded material from the retina.

X12,000

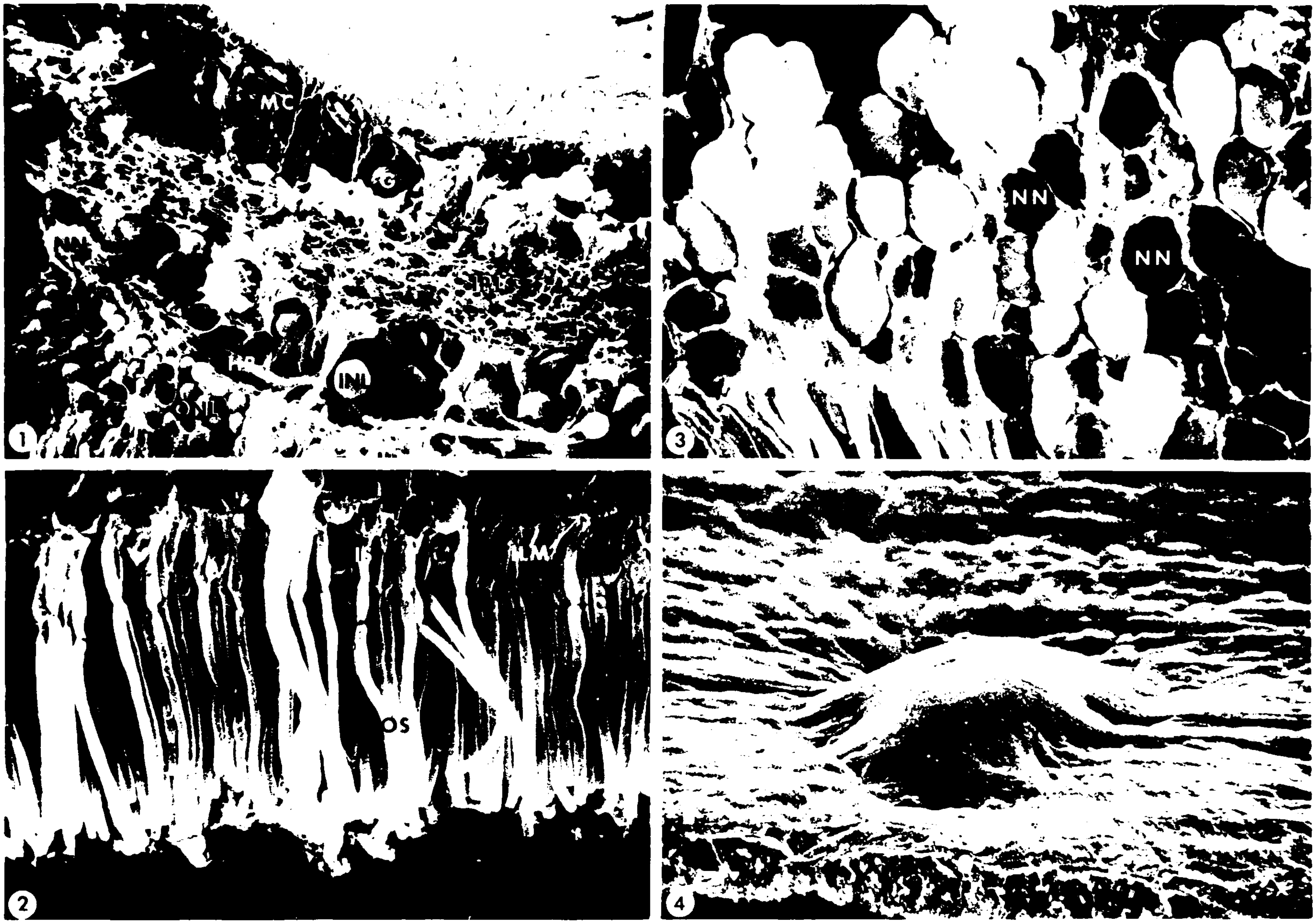

1
MC
G
INL
ONL
2
IS
OS
LM
3
NN
NN
4

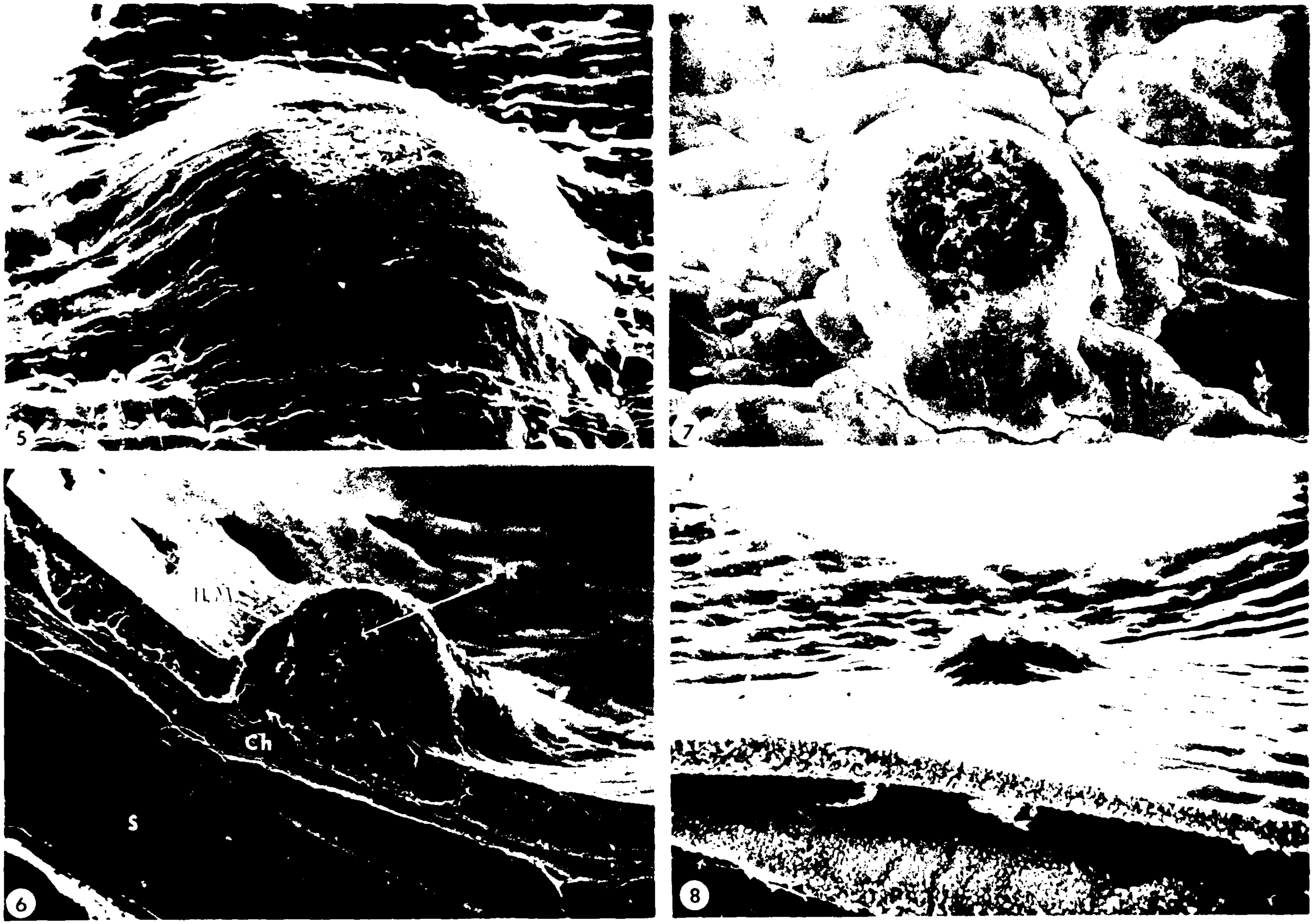
5
7
6
ILM
R
Ch
S
8

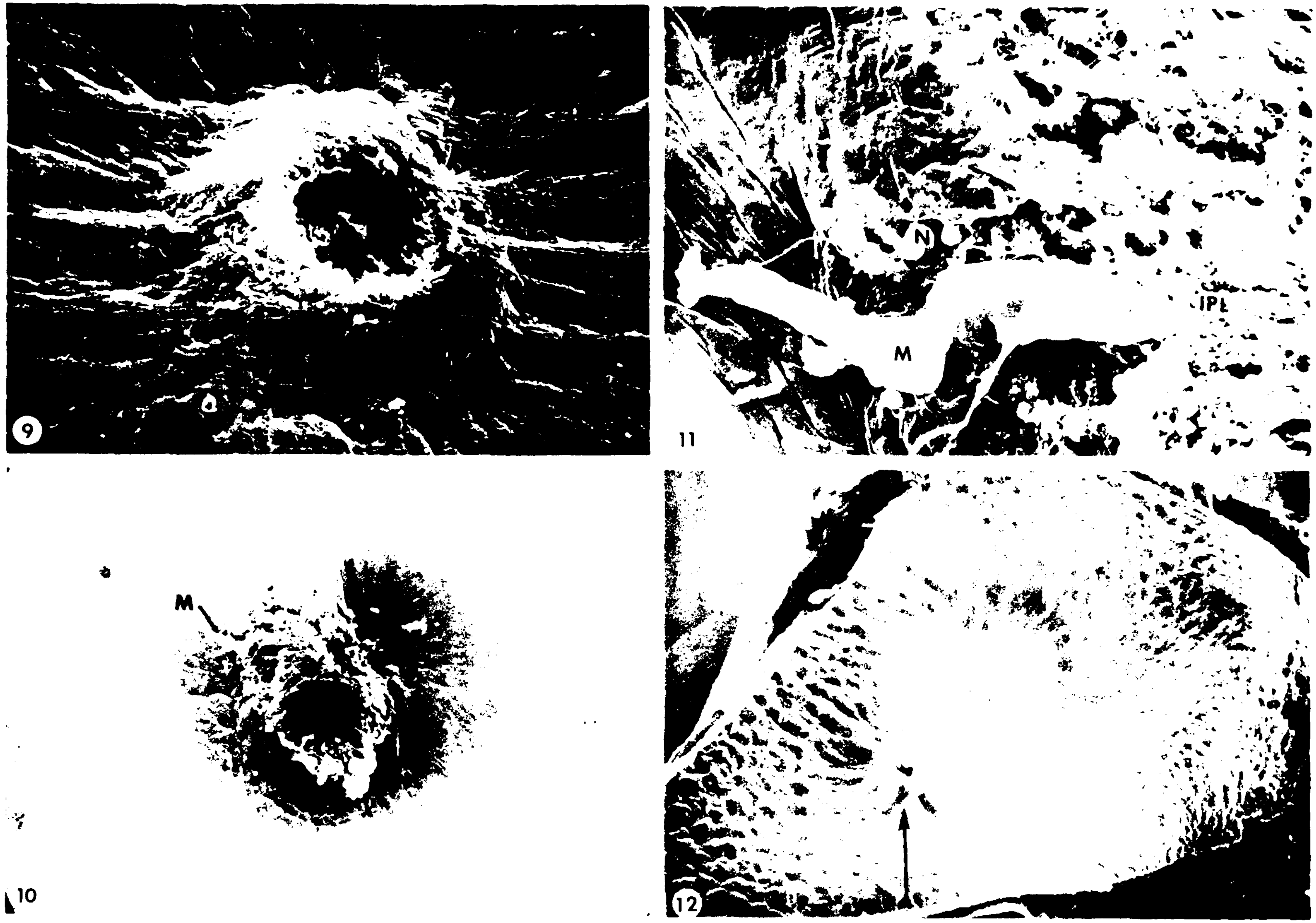
9
11
N
M
IPL
10
M
12

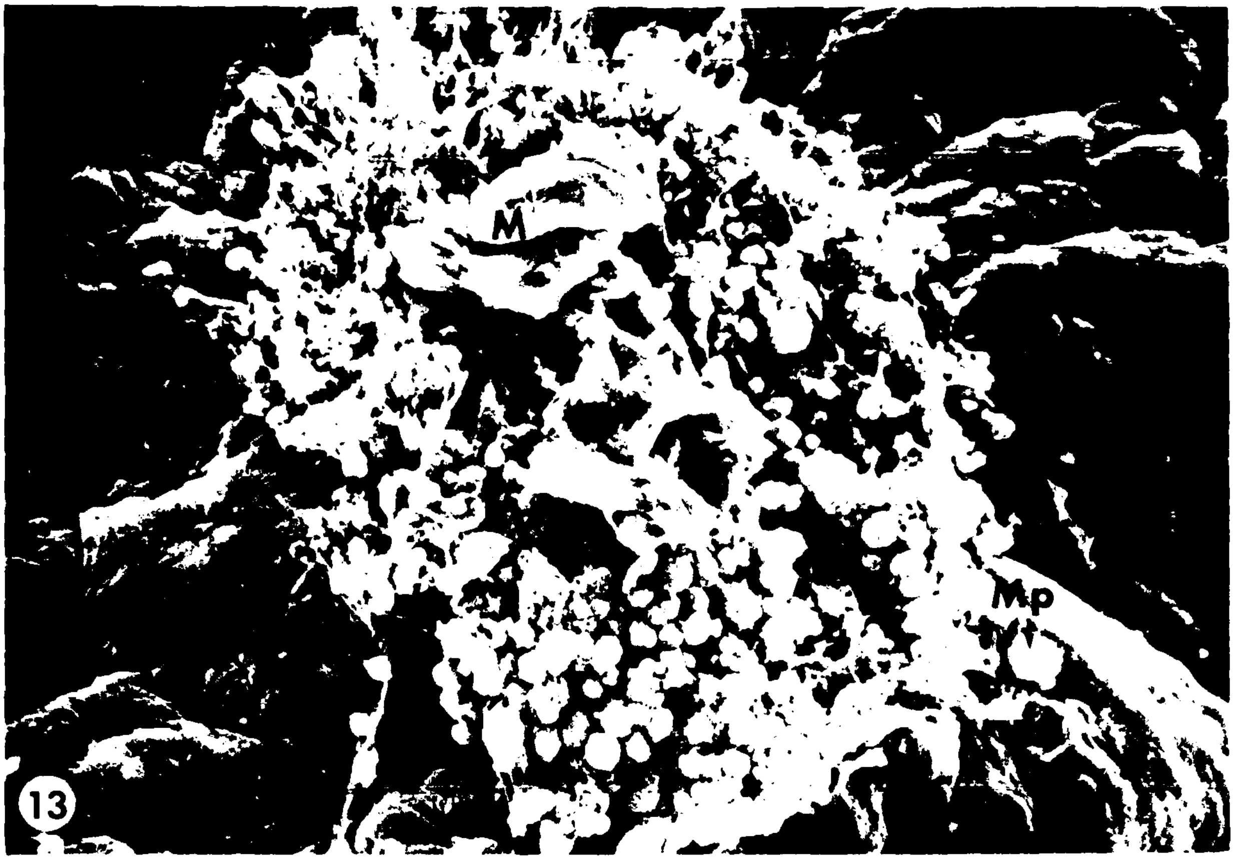
M
Mp
13

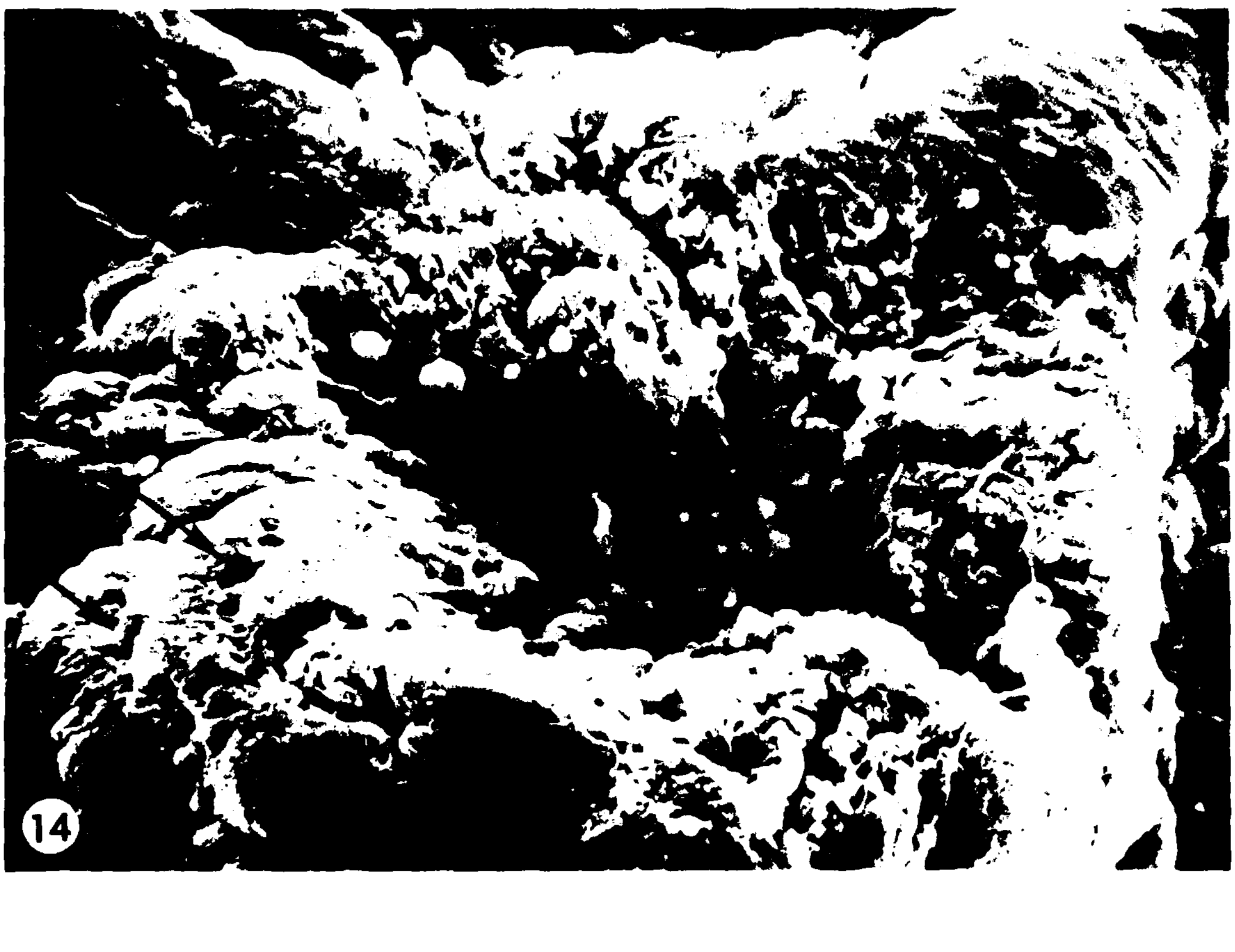
14

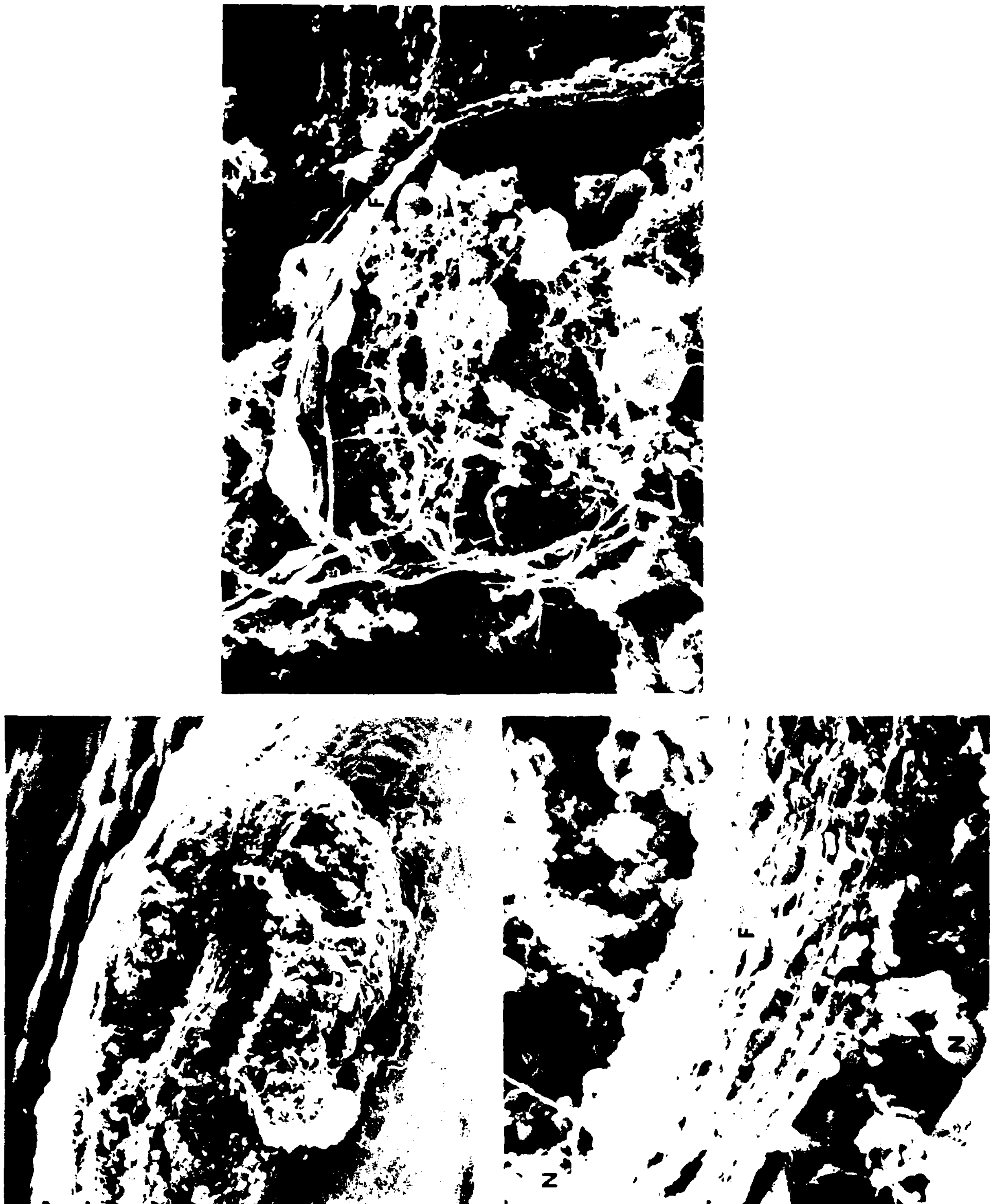

APPENDIX 1.3
draft

SCANNING ELECTRON MICROSCOPY

OF NORMAL & LASED RABBIT PIGMENT EPITHELIUM

B. Borwein, M. Sanwal, J.A. Medeiros, and J.Wm. McGowan

The Department of Physics and Centre for Interdisciplinary Studies in Chemical Physics, The University of Western Ontario

Introduction

There are a few studies of the pigment epithelium of the vertebrate retina by scanning electron microscopy[1-5], but not many. There are none of rabbit retinal pigmented epithelium and none of laser lesions of the pigment epithelium.

This present work reports on the appearance of normal and lased pigment epithelium of the rabbit retina.

Until the advent of SEM , our mental images of structures have been based upon reconstruction from light transmission electron microscopy. These often fail to demonstrate the many facets of surface topography, and the total appearance of large structures.

The dramatic three-dimensional view by SEM obtained extends our perceptions of tissues and cells seen so far only by thin sectioning.

METHODS

Mature New Zealand black rabbits with well pigmented retinas were used. Immediately after lasing, photographs of the fundus were taken with a Topcon fundus camera, and another photograph was taken prior to enucleation; also line-drawing maps were made of the retina with the lesions.

Details of Laser Exposure in Rabbits:

The laser exposures were carried out with a flashlamp pumped dye laser. The coaxial flashlamp was typically run at 20 KV discharge voltage and rhodamine 6G was employed as the active medium. The laser output wavelengths employed ranged from 570 to 600 nm. (typically 585 nm) The output pulse duration was 0.4 sec (FWHM). The beam diameter at the rabbit cornea was 5.0 mm. The laser beam divergence was 4 m Rad and the estimated minimum spent size was 75. The estimated retinal energy density of the typical lesion studied in this report was $10J/cm^2$.

The rabbits were anaesthetised with an intravenous injection of Nembutol and the pupils dilated with 2% homatrapine hydrobromide.

Details of Tissue Processing:

Lased eyes were dissected out and washed clear of blood. They were cut open at the ora serrata with a sharp blade and fixed in 2·5% glutaraldehyde + 0.5% paraformaldehyde in 0.1M Sorensen's phosphate buffer. After thirty minutes the eye tissues were sufficiently hardened to be dissected further.

The cornea, lens and vitreous were gently removed and the lased areas, located with the aid of maps and fundus photographs, were cut out using new sharp blades. From many trials, it was found that 2 days in the aldehyde fixative and 30 minutes in 1% osmic acid in 0.1 M phosphate buffer gave best results from SEM studies. The tissue was dehydrated in ethyl alcohols and acetone; and critical point dried with CO_2. The specimen was coated with a 20 nm layer of gold using a Technics Sputter coater; examined in a HHS-2R Hitachi Scanning Electron Microscope, and photographed on Kodak plus-X film.

The laser lesions were above threshold, and sufficiently powerful to affect the full thickness of the retina.

The posterior fundus was used and only the surface facing the photoreceptors was studied. The lesions were allowed to mature for 2 to 7 days and the eyes were then enucleated.

RESULTS

The pigment epithelial cells are hexagonal in shape, and the cell boundaries are very clearly demarcated. (Figs. 1,2). Microvilli are very abundant, and even when the cells seem relatively denuded of microvilli in the lased cells (Fig. 5) the microvilli can still be seen to be present at much higher magnifications (Fig. 10). Rod outer segments can be seen embedded among the microvillous processes (Fig. 2).

Two kinds of microvilli were observed: the usual long, single, simple microvillous process (Fig. 2) and also broad

sheets of processes with irregular indented margins (Fig. 3).

However, under the visual streak, the pigment epithelial cells are strikingly different, in that the cells are smaller and the long microvilli are absent. The few attached outer segments seem much stockier (Fig. 4) than those of the other areas of the posterior fundus (Fig. 1).

When lased, the pigment epithelial cells seem to retract or lose their microvilli, (Figs. 5,6,7,8,9) but at higher magnifications it is seen that even the apparently denuded cell surface has microvilli (Fig. 10). The difference must thus be one of abundance, density and, perhaps, even length.

The laser lesions are very clearly demarcated and circumscribed (Figs. 6-8), by the relative paucity of their microvilli. In the lased areas, some individual cells are seen each one of which has one hole in it (6,7,8,11).

In some 2-day old lesions, a cap is seen on some pigment epithelial cells (Fig. 9), which seems to lift off and is then shed (Fig. 10), to leave the hole seen in the cells of the 4-day old lesions (Figs. 6,7,8,11).

Associated with the lased areas there are groups of much smaller pigment-epithelial cells (Figs. 5,6,7). In Fig. 5 abundant microvilli can be seen on these small cells. The cells in 2-day old lesions are most denuded of microvilli, and here there appears to be a lifting of the cell apex (Fig. 10). In the 4-day old lesions the microvilli are not quite so sparse, and there are holes in some cells. (Figs. 5,6,7,8). Very few outer segments are seen attaching to the pigment epithelium in the lased areas (Fig. 8).

DISCUSSION

Hogan et al (1971) state that mitoses have not been observed in retinal pigment epithelial cells and that it is generally believed that they are not replaced if they die, but adjacent cells slide laterally to fill the space left by a dead cell. They suggest that the multi-nucleated cells seen at the periphery result from amitotic division. However, Reese (1960) points out that the "pigment epithelium proliferates upon the slightest provocation" and it is known to be very reactive to trauma and to proliferate as a consequence of trauma. Wallow and Tso (1972) found proliferation of the RPE at the periphery of and overlying malignant choroidal melanomas, and so did Font et al (1974) and Fishman et al (1975).

Proliferation of the pigment epithelium has also been observed in response to radiant energy damage (Friedman & Kuwabara, 1968) to inflammation (Frayer, 1966); to detachment (Frayer, 1966; Machemer & Norton, 1968); to xenon photocoagulation (Ishikawa et al, 1973) and to laser irradiation (Marshall & Mellerio, 1970; Bresnick et al, 1970; Powell et al 1971). Within four days of lasing we found clearly demarcated groups of proliferated cells within the lased areas.

The transition between the lased areas showing damage and the normal pigment epithelial cells was abrupt in argon lesions seen by transmission electron microscopy (Marshall et al 1975). In the S.E.M. view of the lesions in this study a dramatic finding is that the laser lesions are very clearly delimited by the surface appearance of the lased pigment epithelial cells, with their relative paucity of microvilli. At

low magnifications it appears that the microvilli have been retracted or destroyed. However, at high magnification, microvilli are seen to be present, but they are sparser and shorter and almost completely absent on parts of the cell surface.

We were unable to locate holes in the cells away from the lased areas. The holes seem to be a result of laser insult, being found in some cells in all lased areas, and it seems that a cell 'cap' may be shed to leave the hole (Fig. 10).

Fig. 1 - Normal pigment epithelial cells facing the photoreceptors, from an unlased area of the posterior fundus, Showing the hexagonal cell outlines. The microvilli are abundant, and long rod outer segments (ROS) are attached to some of the cells, embedded among the microvilli.

X5,400

Fig. 2 - Normal pigment epithelial cells, with their multitudinous microvilli. The individual cells can be clearly distinguished. Portions of rod outer segments (ROS) adhere to the microvilli.

X12,000

Fig. 3 - Normal pigment epithelial cells from an area near a 7-day old lesion. The processes are of two kinds: long, single microvilli (MV), and broad, rampart-like processes (BP).

X24,000

Fig. 4 - Normal pigment epithelial cells in the region of the visual streak. These are different from the pigment epithelial cells of the posterior fundus in that the cells are smaller and the long microvilli are absent here. Some squatter outer segments are seen (OS)

X6,000

Fig. 5 - Pigment epithelial cells at the margin of a 4-day old lesion. The cell outlines are clearly demarcated, and the microvilli are prominent. There are present a large number of very small cells with abundant microvilli.

X5,000

Fig. 6 - A 4-day old lesion is easily distinguishable on the pigment epithelial surface. There are many red blood cells lying on the lesion surface among other cellular debris. The pigment epithelial cells in the lesion are denuded of microvilli. A few holes can be seen (arrows), and also zones of very small proliferating pigment epithelial cells (arrow heads).

X1,200

Fig. 7 - A 4-day old laser lesion seen at the pigment epithelium surface. The more-or-less circular lesion area is distinguished and circumscribed by the absence of microvilli on the cell surfaces. Some erythocytes and cell debris can be seen at the lesion centre. There are groups of smaller cells (arrow heads),and there is one hole per cell in some of the cells (arrow).

X1,200

Fig. 8 - The edge of a 4-day old laser lesion showing clearly the abrupt transition from denuded pigment epithelial cells in the laser lesion to those with abundant microvilli of the unaffected cells.

There are no attached outer segments in the lesion area, in contrast to the many rod outer segments seen in the normal cells. Note the holes in some of the lased cells (arrowheads).

X2,100

Fig. 9 - Pigment epithelial cells in a 2-day old lesion showing caps forming on the cells. No holes are present.

X1,200

Fig. 10 - Pigment epithelium cells in a 2-day old laser lesion. The microvilli are almost completely absent and some cells appear to have a cap-like part (c) in the process of being shed. This is possibly the manner of formation of the hole seen in the 4-day lesions.

Some outer segments (OS) can be seen.

X12,000

Fig. 11 - A pigment epithelial cell is a 4-day old lesion showing a hole surrounded by microvilli. This cell is a mganified view of the cell marked Fig. 7. Note the microvilli, which appear so sparse and flat in Fig. 7, and the red blood cells (RBC).

X24,000

REFERENCES

1. Breipohl, W., et al.: Scanning electron microscopy of the retinal pigment epithelium in chick embryos and chicks, Z. Zellforsch. 146: 543-552, 1973.

2. Hansson, H.A.: Ultrastructure of the surface of the epithelial cells in the rat retina. Z. Zellforsch. 105: 242-251, 1970.

3. Steinberg, R.H.: Scanning electron microscopy of the bullfrog's retina and pigment epithelium, Z. Zellforsch. 143: 451-463, 1973.

4. Sakuragawa, M. and Kuwabara, T.: The pigment epithelium of the monkey. Topographic study of scanning and transmission electron microscopy. Arch. Ophthal. 94: 285-292, 1976.

5. Dickson, D.M. and Hollenberg, M.J.: Scanning electron microscopy of the photoreceptor cells and pigment epithelium of the adult newt, Triturus virvidescens dorsalis (Rafinesque). J. Morph. 135: 389-432, 1971.

6. Hogan, M.J., Alvarado, J.A., and Weddell, J.E.: Histology of the Human Eye, W.B. Saunders Co., Philadelphia, 1971, p. 405.

7. Wallow, I.H.L., and Tso, M.O.M.: Proliferation of the retinal pigment epithelium over malignant choroidal tumors: a light and electron microscopic study. Am. J. Ophthal. 73: 914- , 1972.

8. Font, R.L., Zimmerman, L.E. and Armaly, M.F.: The nature of the orange pigment over a choroidal melanoma. Archiv. Ophthal. 91: 359-362, 1974.

9. Fishman, G.A., Apple, D.J. and Goldberg, M.F.: Retinal and pigment epithelial alterations over choroidal malignant melanomas. Annals. Ophthal. 7: 487-492, 1975.

10. Friedman, E. and Kuwabara, T. The retinal pigment epithelium IV. The damaging effects of radiant energy. Arch. Ophthal. 80: 265-279, 1968.

11. Frayer, W., Reactivity of the retinal pigment epithelium: an experimental and histophathological study. Tr. Am. Ophthal. Soc. 64: 586-643, 1966.

12. Marshall, J., Hamilton, A.M. and Bird, A.C.: Histophathology of ruby and argon laser lesions in monkey and human retina. A comparative study. Brit. J. Ophthal. 59: 610-630, 1975.

13. Reese, A.B.: The role of the pigment epithelium in ocular pathology. Am. J. Ophthal. 50: 1066-1084, 1960.

14. Machemer, R. and Norton, E.: Experimental retinal detachment in the owl monkey II. Histology of retina and pigment epithelium. Am. J. Ophthal. 66: 396-410, 1968.

15. Ishikawa, Y., Uga, S. and Ikui, H. The cell division of the pigment epithelium in the repairing retina after photocoagulation. J. Electronmicroscopy, 22: 273-275, 1973.

16. Marshall, J. and Mellerio, J.: Laser irradiation of retinal tissue. Brit. Med. Bull. 26: 156-160, 1970.

17. Powell, J.O., Bresnick, G.H., Yanoff, M., Frisch, G.D. and Chester, J.E. Ocular effects of argon laser radiation. II. Histophathology of choirioretinal lesions. Am. J. Ophthal. 71: 1267-1276, 1971

18. Bresnick, G.H., Frisch, G.D., Powell, J.O., Landers, M.B., Holst, G.C. and Dallas, A.G.: Ocular effects of argon laser radiation. I. Retinal damage threshold studies. Invest. Ophthal. 9: 901-910, 1970.

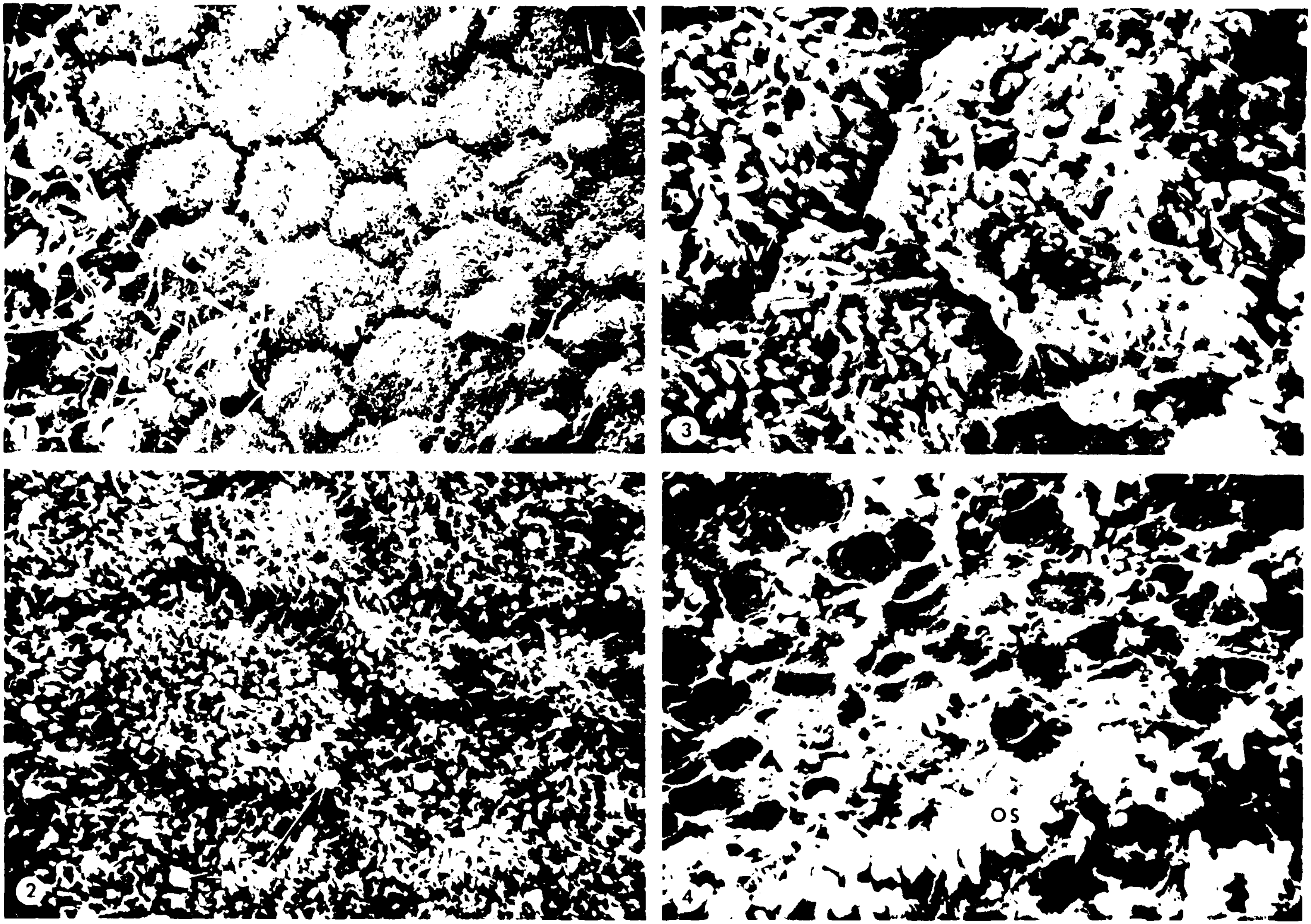

1
3
2
4
OS

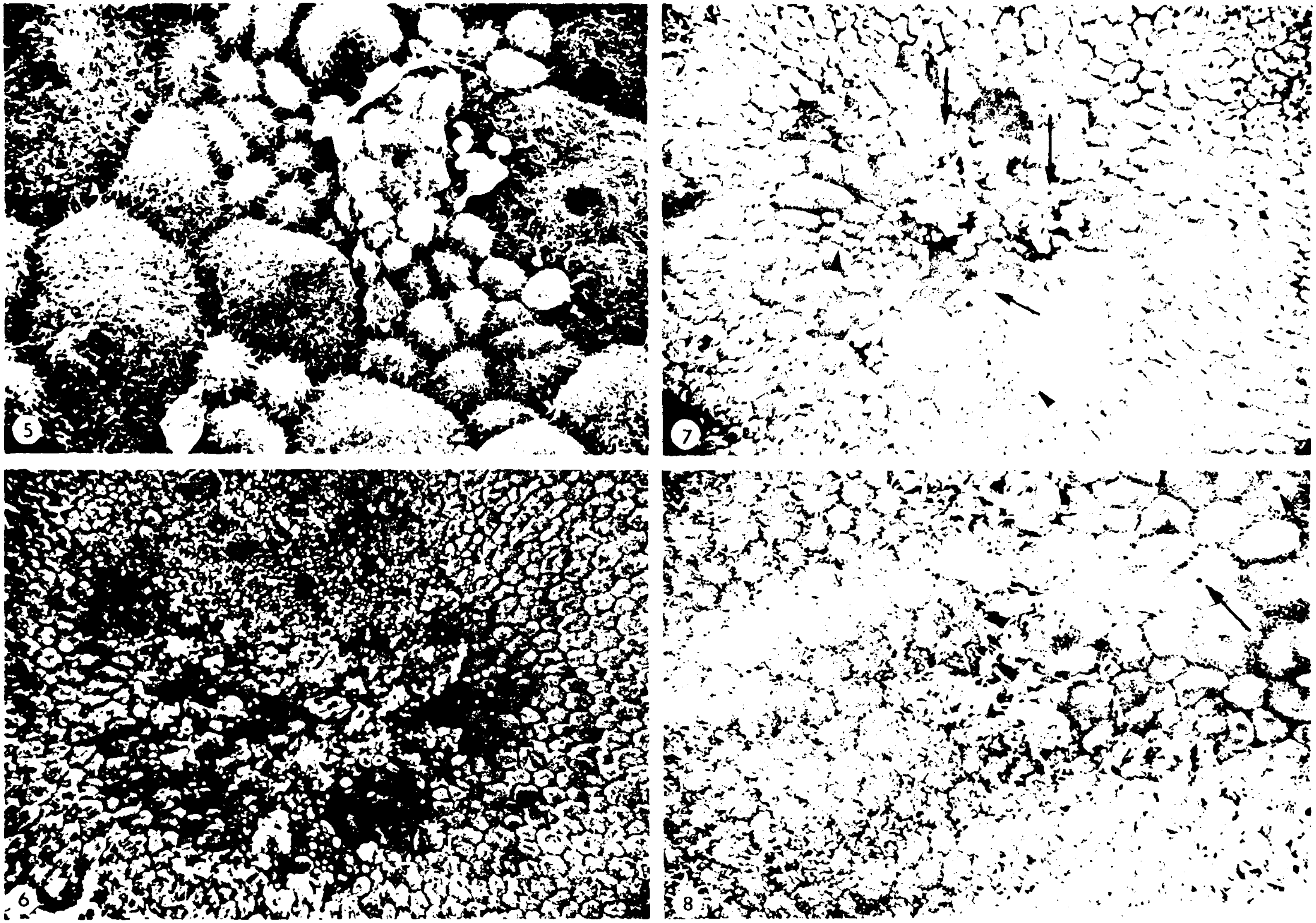
5
7
6
8

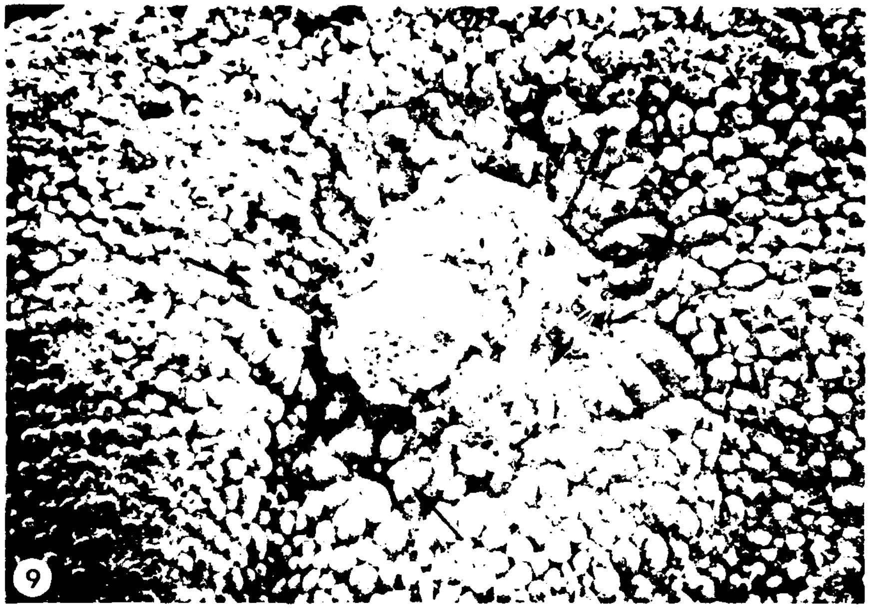
9


C
C
C
OS
10

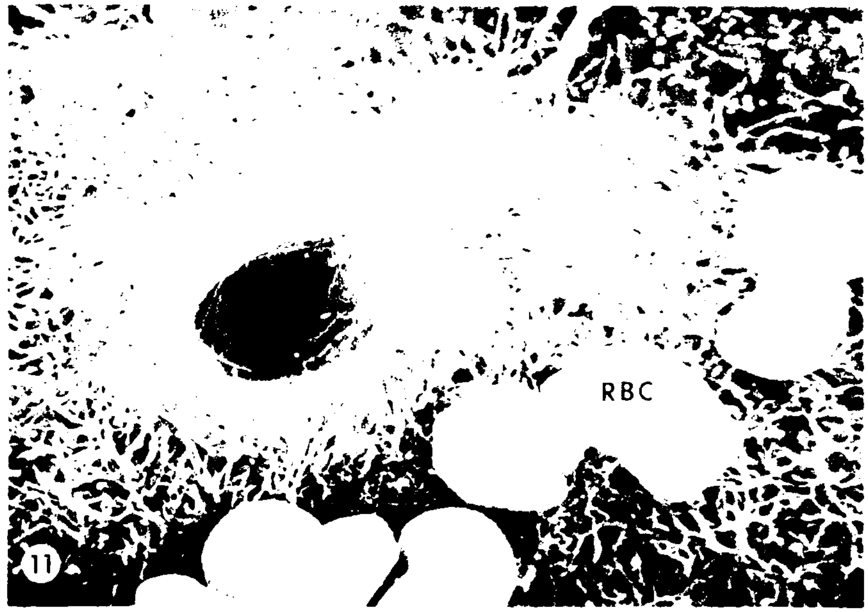
RBC
11

APPENDIX 1.4
ROUGH DRAFT

DRAFT of paper entitled "STUDIES IN HUMAN RETINA 1. The so-called normal areas from the retina of an eye enucleated for choroidal melanoma" by B. Borwein, et al in preparation for submission to Investigative Ophthal.

ABSTRACT

A retina from an eye enucleated for choroidal melanoma from a 47-year old woman was examined by electron microscopy. In previous studies using retinas from human eyes enucleated for choroidal melanoma there has been an implicit or explicit assumption that the areas not immediately bordering the melanoma are normal.

Normal portions of the retina were seen in this study, but this paper reports on the abnormalities that were present in areas distant from the melanoma.

These abnormalities include blood cells within the pigment epithelium, and immediately below it; holes in the photoreceptor layer; pigment bodies and phagosomes within the inner retinal layers; rod outer segments clumping and fusing together in groups; small foci of pyknotic photoreceptor nuclei; and cystic pigment epithelium with and without proliferation and/or degenerating nuclei.

In the great majority of sections examined, the outer segment discs were normally arrayed.

Many studies of human retina and choroid have used tissue from eyes enucleated for choroidal melanomas (1,2,3,4,5,

6,7,8,9). Cohen (11) states clearly that he used eyes "removed for reasons not directly involving the visual function (e.g. maxillary carcinoma)". Frequently the cause for enucleation is not given and the only statement made is that the eyes were obtained from human patients following surgical removal (10,11); or the kind of tumour is not specified (10). None of these papers describe the method of enucleation, which may possibly affect the degree of ischemia to which the retina is subjected.

The primary aim of our study was to investigate threshold laser lesions, too small to be visible ophthalmologically, in human retinas. In the course of this work we found that there were areas in the posterior fundus remote from both the melanoma and the laser lesion areas that were abnormal, and nearby were found zones showing typically normal structures. This paper reports the abnormal findings.

MATERIALS & METHODS:

A 47 year old white woman with normal 6/6 vision donated her left eye which was enucleated by the snare method, for a choroidal melanoma, infero-temporal to, and near, the macula. The tumour was 10 x 5 x 3 mm, mainly of epithelioid cells and with a shallow serous retinal separation. The overlying pigment epithelium had focal areas of proliferation. There was no yellow pigmentation associated with the neoplasm. The tumour was found in the course of a routine examination and the patient did not report any visual symptoms.

Three to four hours before enucleation, argon laser lesions were made in the posterior fundus around the disc and

macula, ranging from 50 - 1000μ spot size.

Following enucleation, the pathologist cut out the area of the eye with the melanoma, and within half an hour after surgery the retina was put into fixative. The delay was due to unforeseen hospital procedures.

The fixative used was phosophate buffered 2.5% glutaraldehyde and 0.5% paraformaldehyde (0.1M, ph7.4) for four hours and the material was post-fixed in 1% buffered osmium tetroxide for two hours. The tissue was further dissected in fixative and the laser lesion areas were cut out with a sharp blade. All the tissues were processed through alcohols to Epon 812.

One micron sections were cut and specific areas selected for ultrathin sectioning. These were stained with 1% toluidine blue. Thin (60nm) sections were stained with uranyl acetate and laed citrate. The sections were examined in an AEI 800 electron microscope.

The areas of the retina surveyed were nasal to the disc; and paramacular.

OBSERVATIONS

The great majority of the nuclei of the outer nuclear layer were normal and well-fixed (Fig.1) but in three separated areas, focal pyknosis of both rod and cone nuclei was seen (Fig. 2) in cells with normal outer segments. In a paramacular zone, the pyknosis (Fig. 3) was associated with irregular "holes" in the photoreceptor layer, extending from the pigment epithelium (which was degenerating, but continuous, to as far as the external limiting membrane (Fig. 11).

Bruch's membrane was intact and uninterrupted in all sections surveyed, even when blood cells were present within or below the pigment epithelium. Its appearance was normal for the age group, even when overlying abnormal pigment epithelium. The variations seen were slight. These were variations in the amount and denseness of collagen; the abundance of coated vesicles; and the number of tubular structures in the central zone (Fig. 4). Drusen were never seen. The elastica did not stain prominently. The endothelium of the choriocapillaris was much fenestrated and showed wedge-like thickenings at intervals, some of which indented and even penetrated into Bruch's membrane and sometimes seemed to interrupt the endothelial basal lamina Membrane-bounded electron-dense bodies with a lighter periphery were occasionally seen (Fig. 4).

In many areas the pigment epithelium appeared classically normal (Fig. 5), and although recently-ingested phagosomes were seen (Fig. 6), they were never abundant. Occasionally, electron-dense large pigment-like bodies were found to be phagasomes when seen in very undeveloped photographs.

Abnormal pigment epithelium varied from slightly cystic in the apical areas mainly, to cystic throughout. (Figs. 4,6-8). Even within one block, in near neighboring sections, the number and sizes of the vacuolar cystic spaces varied. The basal infoldings were largely normal (Figs. 4,7). When more severely affected the pigment epithelium lost its polarity, and large and often irregularly shaped pigmented bodies (Fig. 4) were crowded into the basal portion (Fig. 8)

and the microvilli were retracted. Some nuclei became misshapen and there was nuclear proliferation (Figs. 7-9) and pyknosis (Figs. 8, 9, 11). The basement membrane of the pigment epithelium was of uniform thickness and intact (Figs. 4,7-9).

In some areas blood cells, mainly erythrocytes with a few neutrophils, were found within the pigment epithelium. The pigment epithelium was vacuolated and cystic-looking, but the outer segments and inner segments were normal (Fig. 10). Where there were "holes" in the photoreceptor layer associated with areas with blood in the pigment epithelium and below it, the photoreceptors around the "hole" were distant from the pigment epithelium, sparser, and some were clumped together in groups (Figs. 11). These "holes" were found in the photoreceptor layer only and some of them extended as far as the external limiting membrane.

Pigmented bodies were seen within the inner retinal layers. They were mainly in the ganglion cell layer (Fig. 12), but extended into the inner plexiform layer, and were sparsest, in small isolated groups, in the inner nuclear layer (Fig. 13). This was observed in only one zone, superior and nasal to the disc, and near to a laser lesion, but not within the lased area. The pigment bodies varied in size but bore a remarkable resemblance to those of the pigment epithelium. The cytoplasm around the pigment bodies was cystic; there were misshapen and pyknotic nuclei and some were shrunken (Figs. 12-14). In places the cytoplasm looked washed out, there were swollen

mitochondria (Fig. 12) and varied dense bodies (Figs. 12,14). The cytoplasm looked generally disorganized. Structures strongly reminiscent of phagosomes formed from recently-ingested outer segments were seen in these areas (Figs. 12-15). When photographs were underdeveloped, a few more phagosomes could be identified.

In a paramacular area, outer segments were clumped together in groups. Some were disorganized and disintegrating; others were normal (Fig. 16). Here some of the inner segments were swollen and contained swollen mitochondria. In another zone which was near to, but not within, nor immediately bordering on a laser lesion, there were normal looking outersegments clumped together in groups (Fig. 17). At higher magnifications, from both these areas, these rod outer segments were seen to be fusing together in groups of from two to four by the confluence of their plasma membranes (Figs. 18, 19).

The calycal processes were small and sparse and were not seen regularly in cross sections of outer segments close to the inner segments, as expected.

The blood vessels of the retina seemed normal for the age-group, and the "swiss cheese" effect was not excessively developed (Fig. 20).

DISCUSSION:- ROUGH DRAFT

What emerges from this study is that normal and abnormal tissues were found within this one retina, sometimes juxtaposed, in areas distant from the melanoma and from the laser lesions.

Whether the choroidal melanoma was responsible for some of the abnormalities seen is not certain, but it may be connected with the migration of pigment epithelial cells into the inner retinal layers, probably through the holes seen in the photoreceptor layer. Some phagosomes were seen in the inner retinal layers and by underdeveloping photographs with pigmented bodies a few of these pigmented bodies could be identified as phagosomes.

In several studies of chloroquine poisoning, pigment is reported within the retina. Smith & Benson (1971) saw pigment epithelial cells in the inner retina and these included lamellar inclusion bodies, in cats; and Francois & Maudgal (1967) saw this in rabbits; and Abraham (1970), in a TEM study, saw pigment bodies in the inner-retinal layers in albino rats. Bernstein (1964) reported migration of pigment in the form of very large clumps into the inner nuclear layer in a 38 year-old woman treated with chloroquine for two years for lupus, but Wetterholm & Winter (1964) saw very large cells laden with pigment granules in the outer nuclear and outer plexiform layers in a similar case.

In retinitis pigmentosa, pigment granules accumulate around the blood vessels and in the inner retinal layers (Yanoff & Fine, 1975),(Reese 1960).

The pigment epithelium is well known to be very active to trauma, to "proliferate at the slightest provocation" and to migrate into the retina if there are breaks in the E.L.M. The pigment epithelium overlying a choroidal melanoma may proliferate, desquamate and migrate so that it will be seen not only over the tumor but elsewhere, too (Reese 1960).

We do not know what specific trauma caused the cystic reaction in the pigment epithelium. It could be lasing of the eye; or the fact that there were lesions near the macula (Frisch, Schwaluk & Adams) or the effects of the choroidal melanoma.

Wherever there was blood in the pigment epithelium and holes present in the photoreceptor layer the pigment epithelium was cystic, to a greater or lesser degree.

In many forms of trauma the melanin granules withdraw from the optical villi and the general polarity of the cell is lost (refs.), as we see here.

The clumping and fusing of the outer segments in groups of 2 - 4 has not been previously reported but organelles in general are known to coalesce under trauma (ref.).

There are holes seen in the photoreceptor layer but it is noteworthy that the pigment epithelium is neither torn nor detached. The presence of blood cells may be due to surgical trauma but no similar reports were found in the literature of other melanoma retinas (refs.). No tears were seen in

Bruch's membrane but there must have been some to enable the blood to pass from the choriocapillaris; or else the blood would have to have come from inner retinal vessels which seem more unlikely.

In subthreshold laser lesions the pigment epithelium shows (Adams, et al) condensation nd thickening of microvilli, loss of pigment granules, condensation of smooth endoplasmic reticulum and increase in lysosomes. There was associated disorganization in the outer segments, shrinkage, separation from each other, retraction from the pigment epithelium and disarray.

Why are the calycal processes not prominent? Others illustrate them in human retinas (Hogan et al). It is possible that they withdraw or are destroyed in response to trauma.

No matter what observations were seen in the pigment epithelium and the other retinal layers, Bruch's membrane remained normal in appearance.

REFS:

1. FINE, B.S. Limiting membranes of the sensory retina and pigment epithelium. Arch. Ophthal. 66: 847-860, 1961

2. HOGAN, M.J. and J. Alvarado Studies on the human macula IV. Aging changes in Bruch's membrane Arch. Ophthal. 77: 410-420, 1967

3. GARRON, L.K. The ultrastructure of the retinal pigment epithelium with observations on the choriocapillaris and Bruch's membrane Trans. Am. Ophthal. Soc. 61: 545-588, 1963

4. MIKI, H., M.B. Bellhorn, and P. Henkind, Specialization of the retinochoroidal juncture. Invest. Ophthal. 14: 701-706, 1975

5. SPITZNAS, M. & M.J. Hogan, Outer segments of photoreceptors and the retinal pigment epithelium. Arch. Ophthal. 84: 810-819, 1970

6. BAIRATI, A., N. Orzalesi, The ultrastructure of the pigment epithelium and the photoreceptor-pigment epithelium junct ion in the human retina. J. Ultrastr. Res. 9: 484-496, 1963.

7. LERCHE, W. Licht-und elektronenmikroskopische Beobachtungen über die Einwirkung von Argonlaser stralen auf das Pigmentepithel der anliegenden menschlichen Retina. Albr. v. Graefes Arch. klin. exp. Ophthal. 187: 215-228 1973.

8. LERCHE, W. Elektronenmikroskopische Untersuchungen über Struktur veranderungen im Pigmentepithel der menschlichen Retina Albv. v. Graefes Arch. klin. exp. Ophthal. 189, 323-338, 1974.

9. FEENEY, L.J. J.A. Grieshaber and M.J. Hogan, Studies on Human Ocular Pigment, 535-548, In: Rohen, J.W., The Structure of the Eye II Symposium Stuttgart, 1965, F.K. Schattauer - Verlag.

10. DOWLING, J.E. and B.B. Boycott - Neural Connections of the Primate Retina p. 55-68. In Rohen, J.W. The Structure of the Eye II Symposium. Stuttgart 1965. F.K. Schattauer-Verlag.

11. YAMADA, E. Some structural features of the fovea centralis in human retina. Arch. Ophthal. 82: 151-159, 1969.

HOGAN, M.J., J.A. Alvarado and J.E. Weddell, chapter 8 Choroid Histology of the Human Eye, 320-392 Pluta London, Toronto, W.B. Saunders Co., 1971

KROLL, A.J. Experimental central retinal artery occlusion Arch. Ophthal. 70: 453-469, 1968.

SHAKIB, M. Ashton, N. 1966 Part II Ultrastructural changes in focal retinal ischaemia. Brit. J. Ophthal 50: 325-384, 1966.

WEBSTER, H F. & A. Ames 3rd. Reversible and irreversible changes in the fine structure of various tissue during oxygen and glucose deprivation J. Cell. Biol. 26: 885-909, 1965.

SMITH, R.S. & Benson, E.L. Acute toxic effects of chloroguire on the cat retina; ultrastructural changes Invest. Ophthal. 10(4) 237-246, 1971 (migrating PE. lamellar bodies GC)

ROBISON, W.G., T. Kuwabara & D.G. Cogan - Lysosomes & melania granules of the retinal pigment epithelium in a mouse model of the Chediak-Mipashi Syndrome. Invest. Ophthal. 14(4) 312-317 1975.

SPITZNAS, M.: Morphogensis and Nature of the pigment granules in the adult human retinal pigment epithelium (melania) Z. Ze sch 122: 378-388, 1971.

FRAYER, W.C. Reactivity of the Retinal Pigment Epithelium: an experimental and histophathologic study. Trans. Am. Ophthal. Soc. 64: 586-643, 1966.

HOGAN, M.J. Role of the retinal pigment epithelium in macular disease Trans. Am. Acad Ophthal. Otolarg. 76: 64-80, 1972.

MACHEMER, R. Experimental retinal detachment in the owl monkey II. Histology of retina and pigment epithelium Am. J. Ophthal. 66: 396-410, 1968.

TSO, M.O.M. and E. Friedmen, The retinal pigment epithelium. I. Comparative Histology. Arch. Ophthal. 78: 641-649, 1967.

TSO, M.O.M., I.H.L. Wallow & J.O. Powell Differential susceptibility of rod and cone cells to argon laser Arch. Ophthal. 89: 228-234, 1973.

FRIEDMAN, E. and T. Kuwabara The Retinal Pigment Epithelium IV. The damaging effects gradiant energy Arch. Ophthal. 80: 265-279, 1968.

HAM, W.T. Mueller, M.A., Goldman, A.I., Newnam, B.E., Holland, L.M. Kuwabara, Y. Ocular hazard from picosecond pulses of Nd:YAG laser radiation. Science 185: 362-363, 1974.

GLEISER, C.A., Dukes, T.W., Lawwill, T., Read, W.K., Bay, W.W. and R.S. Brown, Ocular Changes in swine associated with chloroquire toxicity Am. J. Ophthal. 67-399-405, 1969.

REESE, A.B., The role of the pigment epithelium in ocular pathology Am. J. Ophthal. 50: 1066-1084, 1960

KROLL, A.J. and R. Machemer III E. microscopy of retina and pigment epithelium, Am. J. Ophthal. 66:410-427 , 1968

FRANCOIS, J. and Maudgal, M.C. Experimentally induced chloroquire retinopathy in rabbits. Am. J. Ophthal. 64: 886-893 1967

BERNSTEIN, H.N. and Ginsberg, J. Archives Ophthal 71: 238-245, 1964. The pathology of chloroquire retinopathy

WETTERHOLM, D.H. and F.C. Winter Histopathology of chloroquire retinal toxicity. Arch. Ophthal. 71: 82-87 1964.

ABRAHAM, R., R.J. Hendy, Irreversible Rysosomal damage induced by chloroquire in the retinas of pigmented and albino rats Exp. & Mol. Path. 12: 185-200, 1970.

ADAMS, D.O., E.S. Beatrice and R. Bruce Bedell Retina: Ultrastructural alterations produced by extremely low levels of coherent radiation. Science 177: 58-60, 1972

YANOFF, M and FINE, B., Ocular Pathology, 1975, Harper & Row p. 438.

FRISCH, Schwaluk and Adams, Nature, 248: 433-435, 1974.

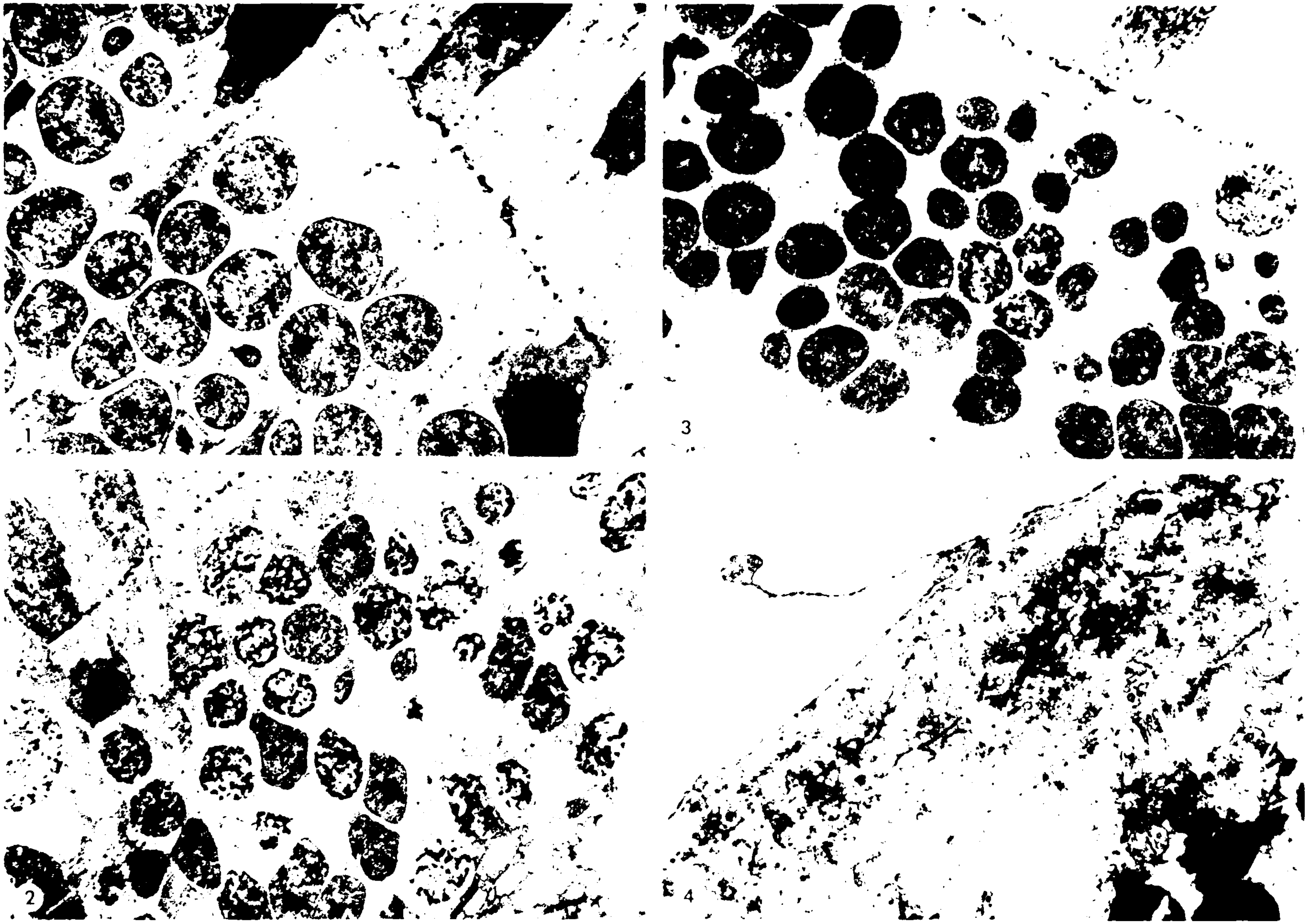

1
3
2
4

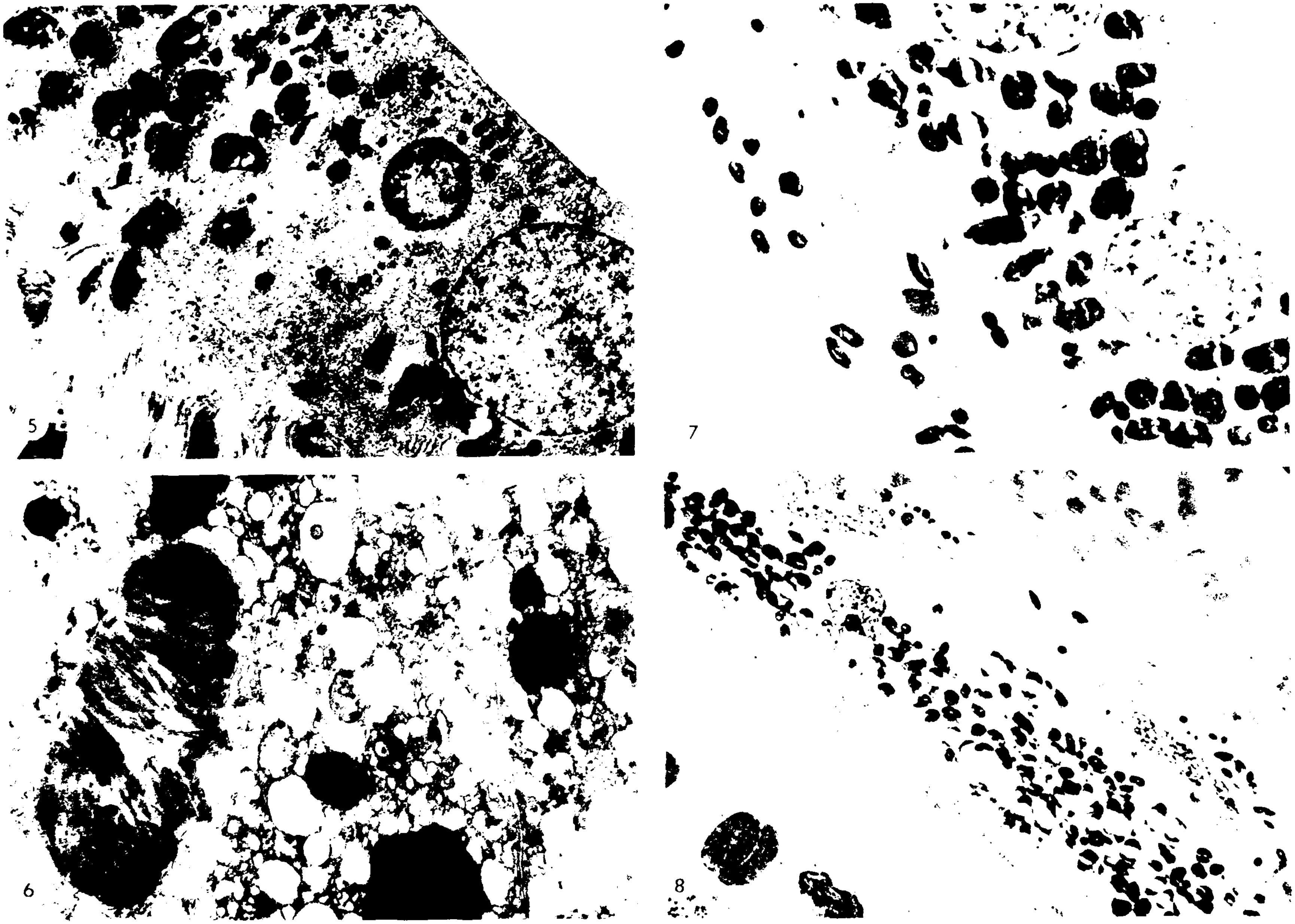
5
7
6
8

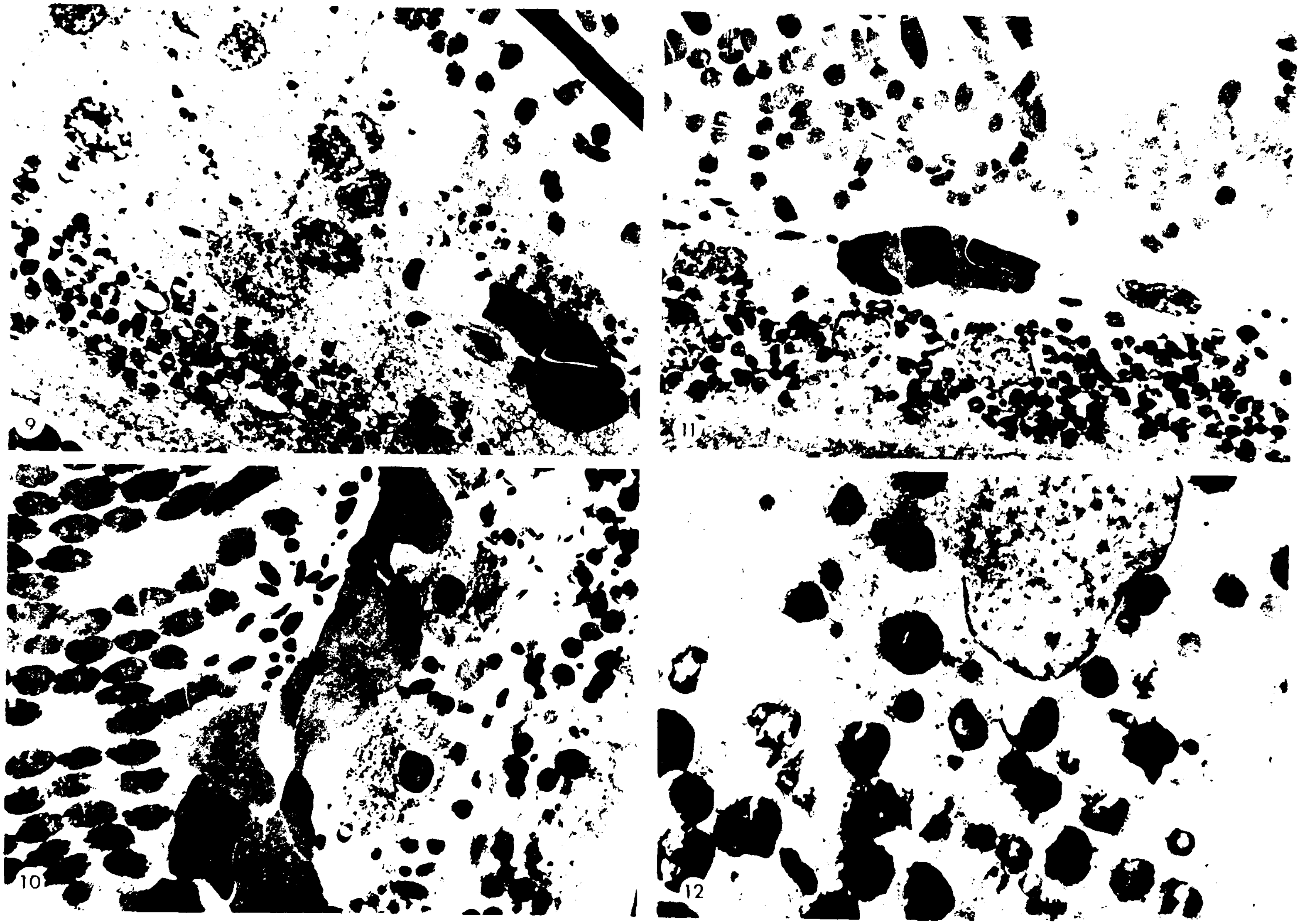
9
11
10
12

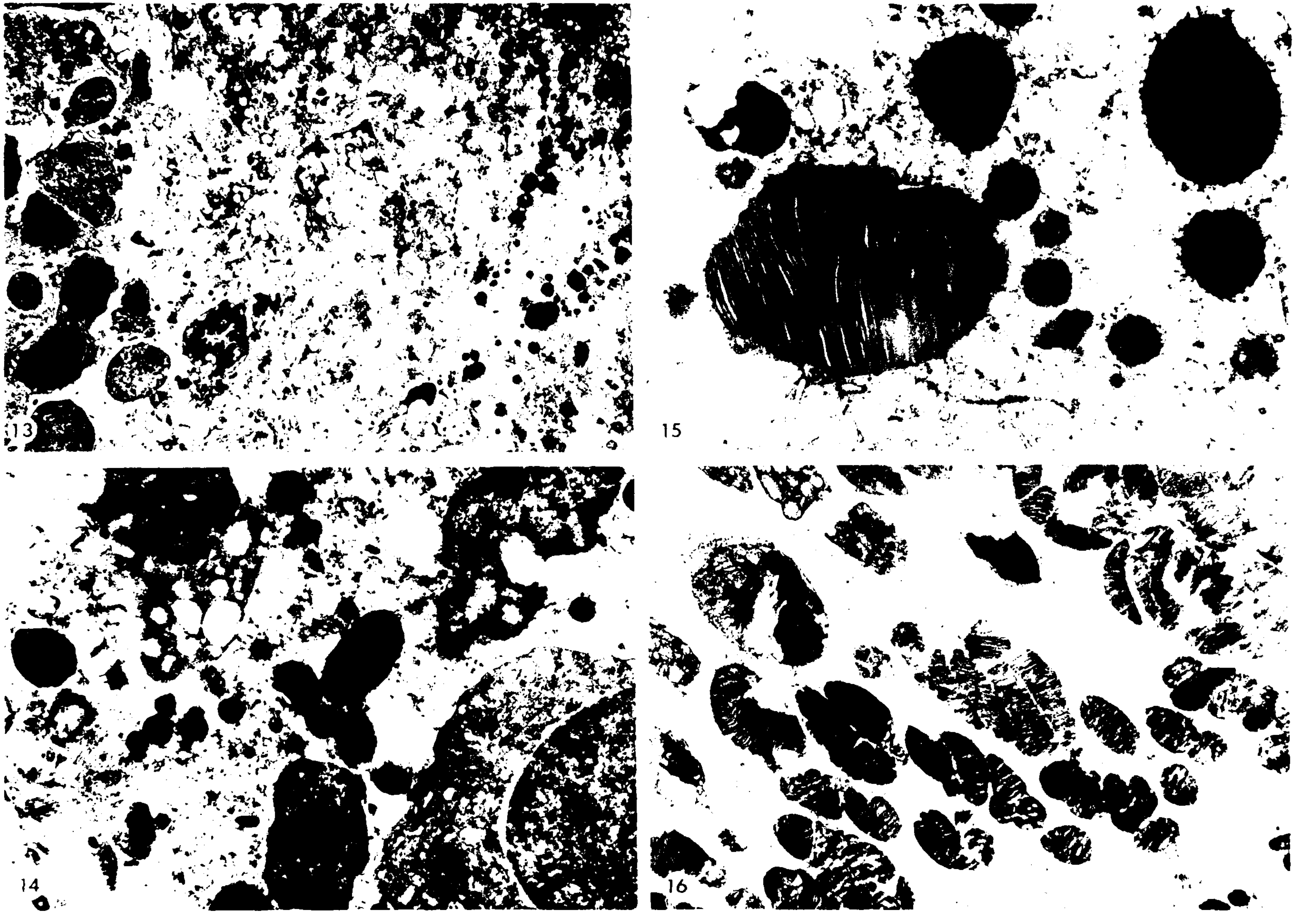

13 14 15 16

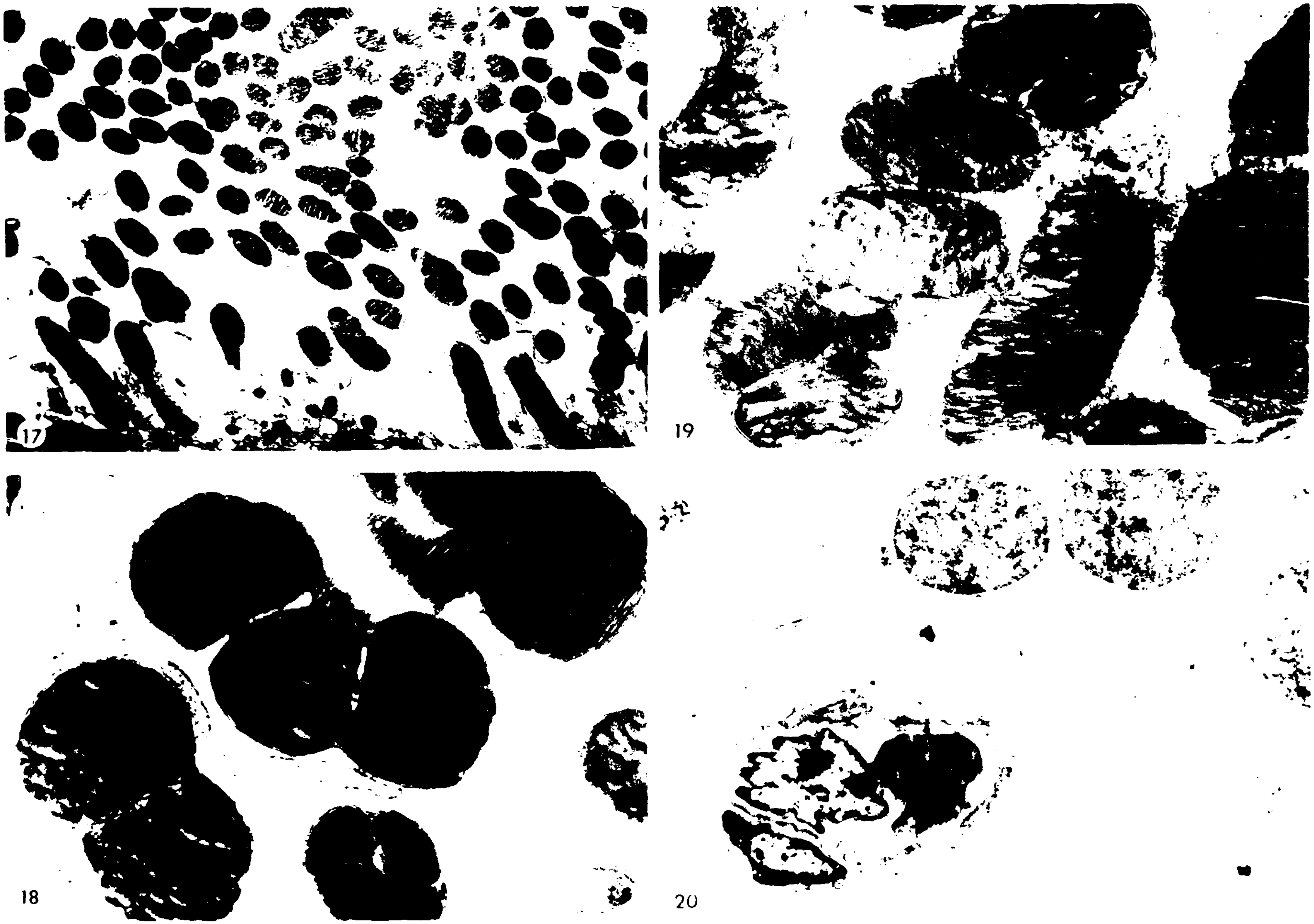
17
19
18
20

PROPERTIES OF ELECTROMAGNETIC RADIATION

APPENDIX 1.5

J.Wm. McGOWAN
Physics Department
and
Centre for Interdisciplinary Studies
in Chemical Physics
The University of Western Ontario
London, Canada N6A 3K7

SUMMARY

Although the electromagnetic spectrum extends over more than thirty orders of magnitude that portion of it now dominated by the LASER only includes four. It is through this range that all life processes are affected by light, in particular the eye can easily be damaged by it. In this lecture the basic principles dealing with electromagnetic radiation are discussed particularly as they relate to the development of the LASER.

1. INTERACTION OF ELECTROMAGNETIC RADIATION WITH LIVING SYSTEMS.

From the beginning of time the interaction of electromagnetic radiation - light - with atoms, small molecules, and eventually large biologically significant molecules, has led to life on this planet as we know it today. Until this last century there had evolved an equilibrium between the flux of radiation from extraterrestrial and from natural sources on the earth and with living systems. Now the ingenuity of man has led to the development of sources of radiation which range from the lower frequencies, through radio, radar, infrared, visible, to x-ray which have significant effects upon life processes. Particularly dangerous is the new light source, the LASER, which through the region of the electromagnetic spectrum which includes visible radiation cannot only directly [illegible] biologically significant molecules when the energy contained in the radiation is sufficient to dissociate or ionize them, it can [illegible] transfer enough heat energy to biological systems (most vulnerable is the eye) to literally cause them to boil. If sufficient energy is deposited in the system in a very short time a mechanical shock can develop which literally shatters the system much as the impact of a bullet on a window shatters the pane.

In this first lecture, I will discuss the entire electromagnetic spectrum with particular attention given to that part of it that we can see, the visible region, as well as to that part which embraces the far red or infrared, the heat portion of the spectrum, and the far violet, or ultraviolet - the region that we normally associate with suntanning and skin cancer.

Although electromagnetic radiation of all frequencies falls upon the earth, the biosphere in which we live is shielded on the violet end of the spectrum from ultra-violet radiation by an ozone layer of the atmosphere which exists between 22 and [illegible] kilometers above the earth surface. Such shielding is now perhaps in jeopardy as a result of the pollutants dumped there by supersonic transports and freon from spray cans. Similarly we are not boiled in our own juices, because of the absorption of far infrared radiation by the water vapour in our atmosphere.

Most vertebrates see radiation with wavelengths between 380 and 700 nanometers (1 nm=10^{-9}m=1 millimicron, 10 Å) while the flux of radiation in which they live lies between 340 and 1100 nanometers (nm). Some insects are sensitive to and can see all of this radiation. However, we normally do not consider that man can see in the ultraviolet and infrared, because of the absorption of these radiations in the cornea and eye fluids. However, if the radiation is intense enough, not all of the radiation is absorbed before it reaches the retina. As a result, he can perceive radiation with wavelengths shorter than 300 nm and in excess of 1000 nm. This includes all of that portion of the electromagnetic spectrum where photosynthesis and photobiology take place.

It is not surprising that the powerful new light source, the LASER, has been developed through this portion of the electromagnetic spectrum, since the atomic and molecular processes which make possible LASER action are the same processes involving rotational, vibrational and electronic excitation of atoms, molecules and ions, as are involved in life processes.

As we consider the radiation from various parts of the electromagnetic spectrum and the power available from different sources, it is important that all of us from many fields establish a common reference point - since it is unfortunate that each field encourages a specific set of units that best fits the community. Many of these are hybred and thus even more confusing.

Let me suggest that the MKS (meter, kilogram, second) system be used. To facilitate this, consider the definition and equivalencies for a few things:

Wavelength λ of light in nanometers (nm), 10^{-9} meters is equal to 1 millimicron (mμ)
or 10 Angstrum (Å)

Energy E in joules is equal to 10^{7} ergs.

Energy E in electron volts (eV) is equal to 1.6×10^{-19} joules
23.06 kcal/mole.

Power J in watts is equal to joule/second.

2. ELECTROMAGNETIC WAVES

Wave motion in a string, or the ocean, or a soundwave in air is generated by a moving (vibrating) object. Similarly, an electromagnetic wave, like any other wave motion, is developed by periodic motion, this time of an electrically charged particle, e.g., an electron. An electric field naturally exists

around an electron. As it moves and its velocity rapidly changes, an oscillating electromagnetic field is generated, and an electromagnetic wave is produced which has both an electric and magnetic component transverse to the direction of propagation of the wave. In Fig. 1, I show schematically an electromagnetic wave propagating in the z direction with the velocity of light. The wave is plane polarized where both the electric and magnetic vectors oscillate normal to one another and in phase. The plane of polarization of the wave is characterized by the plane in which the E vector lies.

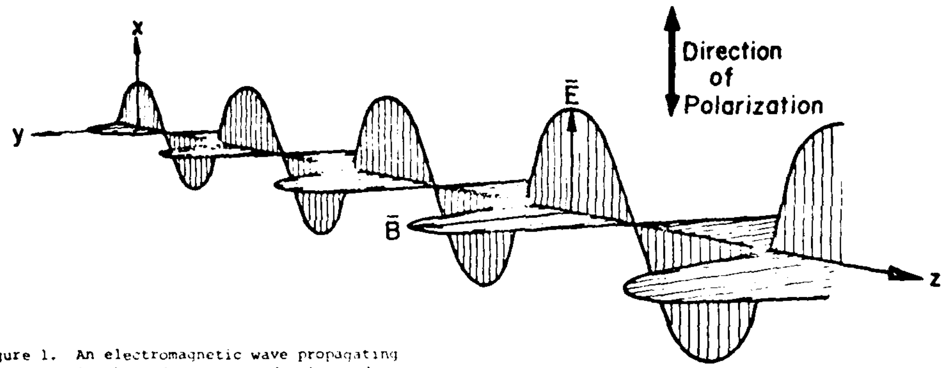

Figure 1. An electromagnetic wave propagating in the z direction and polarized in the x-direction.

The spectrum of electromagnetic radiation is very extensive, reaching from extremely long waves, which have wavelengths that are thousands of kilometers long to very high energy cosmic rays with wavelengths much smaller than the diameter of a nucleus, 10^{-14}m. The notion of a classical oscillation of charge as an electromagnetic wave generator breaks down as the wavelength of the emitted radiation approaches the size of the atom, 10^{-10}m. For radiation which includes the visible part of the spectrum we have to consider an atomic or quantum oscillator governed by very special rules. Indeed LASERS are based upon the quantum picture of nature where waves are particles, that is, photons, and photons are waves. For the moment let it suffice to say that within the quantum picture the energy of the photon (a quantum of energy) is directly proportional to the frequency ν of the oscillating charge

$$E = h\nu$$

where the constant of proportionality h is Planck's constant, 6.6×10^{-34} joule sec.

The relationship between the velocity of propagation of an electromagnetic wave in vacuum, c, and the frequency of the oscillation ν (Hertz, Hz or cycles/sec) and the wavelength of the propagated wave λ (meters) is a simple one,

$$c = \lambda\nu.$$

The velocity of light c has magnitude of 3×10^8 m/sec. Although all other waves require propagation within a medium, electromagnetic waves propagate within a vacuum with a constant velocity throughout the entire electromagnetic spectrum. However, if the EM wave passes through a medium its velocity is changed. The ratio of the velocity of the electromagnetic wave in vacuum and that within the medium, v, is commonly known as the index of refraction of the medium

$$n = \frac{c}{v}.$$

The major part of the EM spectrum is shown schematically in Fig. 2, where we have listed the wavelength in meters, frequency in Hz (cycles per second) and energy of each photon in electron volts (eV), a unit *primarily* used by the physics community to describe the energy of one electron which has passed through a potential difference of one volt ($1\ eV = 1.6 \times 10^{-19}$ coulomb). One cannot help but be impressed with the enormity of the spectrum which stretches over more than [illegible] orders of magnitude. Through this entire range the same simple laws organized by Maxwell in the late 1800's describe the entire electromagnetic spectrum. Notice that out of the entire spectrum the visible portion which largely governs life processes and visual communication is very narrow indeed.

3. EMISSION AND ABSORPTION OF RADIATION BY QUANTUM OSCILLATORS

By the turn of the century the stage was set for Planck and Einstein to recognize the importance of the quantum oscillator. In order to describe the distribution of EM radiation that was given off by hot bodies, Planck had to propose that the radiation that was emitted came in bundles of energy, quanta, instead of coming as continuous waves. Man finally recognized the dual particle-wave nature of matter. For a particular hot body in which radiation and absorption is in complete equilibrium, that is for a black-body radiator, Planck showed that for an infinite number of quantum oscillators each with a different frequency ν, the energy density of the radiation between ν and $\nu + d\nu$ is U_ν which for a system in thermal equilibrium at an absolute temperature T K is given by Planck's law:

$$U_\nu \, d\nu = \frac{8\pi h\nu^3}{c^3} \frac{d\nu}{[\exp(h\nu/kT)-1]} .$$

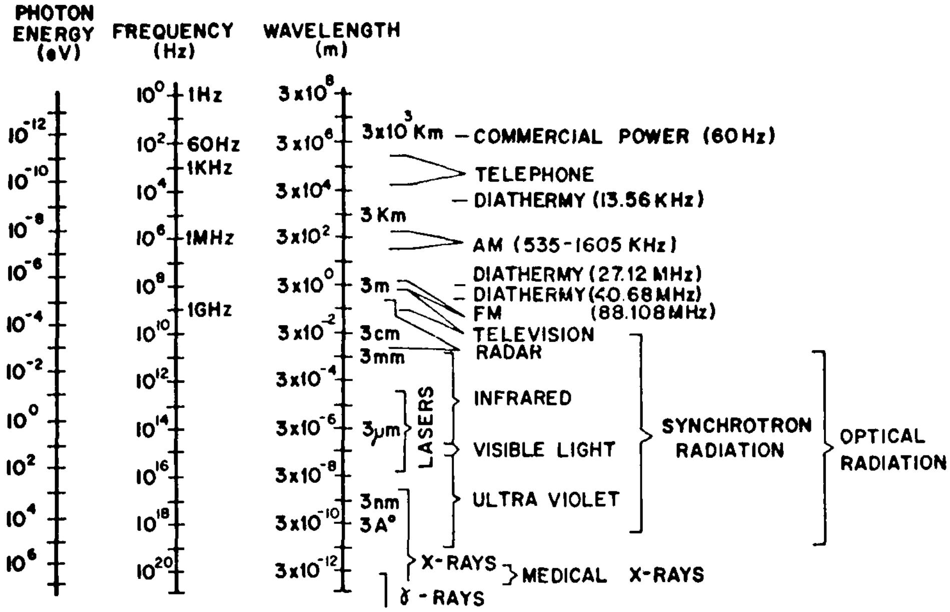

Figure 2. Electromagnetic spectrum showing the various Spectral Regions.

Here $k = 1.38 \times 10^{-23}$ joules/$^\circ$K is Boltzmann's equilibrium constant. The expression states that there are $\frac{8\pi\nu^2}{c^3}$ degrees of freedom in the system of oscillators with an average energy $h\nu[\exp(h\nu/kT)-1]$ per degree of freedom at temperature T.

If one considers a hole cut in the wall of the blackbody cavity, the radiant power emitted normal to the emitting surface per unit area of the emitting surface per wavelength often called the spectral radiant emittence of the blackbody can be expressed equally well in terms of a wavelength interval between λ and λ-$d\lambda$

$$W(\lambda,T)\,d\lambda = \frac{C\,d\lambda}{\lambda^5\,[\exp(hc/\lambda kT)-1]} \quad \text{watts/m /nm.}$$

if the wavelength λ is given in nanometers (nm) and C = 3.74×10^{25} watts nm^4 m^2. It follows then that one can define the spectral brightness of a source as the spectral radiant emittence normal to the emitting surface contained in a small cone or solid angle [illegible] steradians around the normal. This quantity is plotted in Fig. 3 for the blackbody radiator with a temperature which varies from [illegible]$^\circ$K through to 10 million degrees K, a range which was unrealistic to consider at the time of Planck, but which now includes the temperature of the corona of the sun, approximately [illegible] K, the temperature for nuclear fusion about $10^{8\,\circ}$K and the equivalent temperature of a high energy synchrotron radiation source (radiation from highly relativistic electrons) approximately [illegible] million K. I mention this latter source since synchrotron radiation sources which emit a very intense continuum from the infrared through to the x-ray region are rapidly developing as research tools in many parts of the world.

From the Planck radiation formula it follows that the wavelength associated with the distribution maximum λ_m times temperature is a constant,

$$\lambda_m T = 2.9 \times 10^6 \ \text{nm}^\circ\text{K}.$$

which is the well known Wien's displacement law. This relation was identified empirically before Planck's work. In a similar way, one can derive the Stefan-Boltzmann law for the total power radiated by a blackbody through the surface of the area emitter summed over all wavelengths

$$W_t = \int_0^\infty W(\lambda,T)\,d\lambda = \sigma T^4$$

Most radiation emitters, with the exception of the LASER, are not as intense as blackbody radiators, therefore the blackbody curves represent the upper limits of power emitted from a surface. Many solids and some gas discharges radiate like an idealized blackbody. In fact, the spectral distribution emitted by incandescent lamps, and high density arcs and stars can be calculated to a good approximation from Planck's formula. As a reference point, a blackbody at a temperature of 5200°K has its radiation peak at

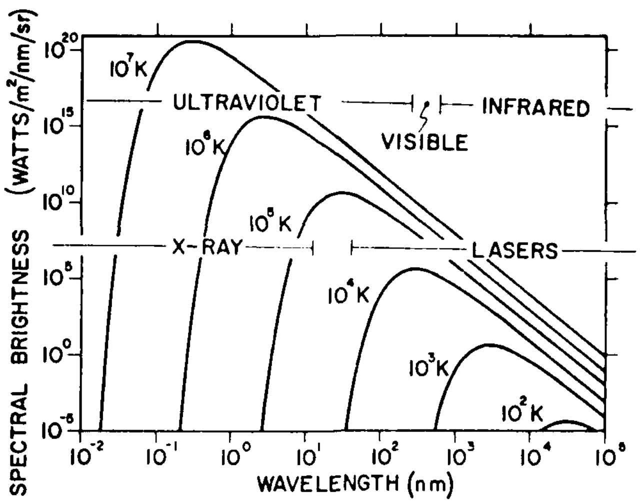

Figure 3. Spectral brightness for the blackbody radiator as a function of temperature.

558 nm near the centre of the visible spectrum, where the human eye is most sensitive. Yet only 40 percent of the radiation falls within the visible part of the spectrum, six percent in the ultraviolet and the rest in the infrared.

There is yet another quantum process which was important in establishing the particle nature of light - the photoelectric effect. It was observed that electrons were removed from a metal surface only when the energy of the photon was equal to or greater than the binding energy ϕ of the electron in the metal,

$$KE\ (electron) = h\nu - \phi\ .$$

Any excess energy went into the kinetic energy KE of the outgoing electron. It is only since the advent of LASERS that it is realistic to consider what happens when many photons of insufficient energy to release an electron arrive at the same time. Now multiphoton excitation and ionization processes (that is, non-linear processes) are commonplace.

Once the concept of the quantum oscillator was recognized it followed directly that atoms with negative electrons moving around positively charged cores did not continuously emit light, instead light was spontaneously emitted only when the electron made a quantum jump from a higher level of the atom E_2 to a lower one E_1 (refer Fig. 4a). If $h\nu$ equal to the energy interval shines upon state 1, the light can be absorbed (Fig. 4b) thus exciting the system, the frequency of the light is given by

$$\nu_{21} = (E_2 - E_1)/h$$

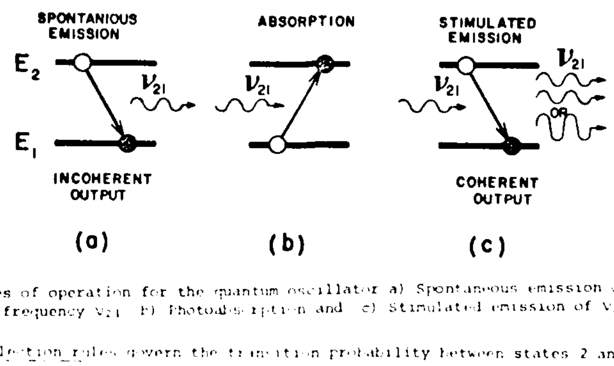

Figure 4. Three modes of operation for the quantum oscillator a) Spontaneous emission of a photon of frequency ν_{21} b) Photoabsorption and c) Stimulated emission of ν_{21}.

Rules known as selection rules govern the transition probability between states 2 and 1. The time on the average it takes t_{21} for a transition to occur is the radiative lifetime of the excited system. In the case of molecules one must not only consider the electronic transitions but transitions from one state of vibration of the molecule to another, and a state of rotation of the molecule to another. The principal terms describing the energy level of the system including electronic vibrational and rotational energy are

$$E_{nvJ} = E_n + E_{v_n} + E_{J_{nv}}$$

where n is the electronic level, v_n a particular vibrational level within the electronic state and J_{nv} the rotational sub-level.

It is important to keep in mind the relative magnitude of the intervals which exist between energy levels. Normally pure electronic transitions give rise to electromagnetic radiation which appears in the near infrared, visible and ultraviolet portion of the spectrum. This corresponds to energies between a fraction of an electron volt to tens of eV. Pure vibrational transitions however occur in the red to infrared region, while rotational transitions are dominantly in the infrared. It is these transitions which are the basis of radiation from LASERS.

When an atomic system is forced to make a transition from E_2 to E_1 (Fig. 4) by light of frequency ν_{21}, the light that is emitted tends to [illegible] in the same direction as that of the stimulating light [illegible] that the intensity of the emitted radiation [illegible] that of the stimulating light. It is just this process of stimulated emission which makes possible the formation of optical radiation which is intense, monochromatic, and [illegible] rather than being randomly [illegible] in time as is the case when a number of quantum oscillators [illegible] in their own time. [illegible] radiation sources have long existed in the power, radio, television and radar portions of the EM spectrum but only with the advent of the LASER has it been possible in the optical part of the spectrum as well.

4. LASER PROCESSES

Consider the usual relation which describes the attenuation of a beam of radiation passing through an absorptive medium. This is the familiar exponential relationship (Beer's Law)

$$I(x) = I_o \exp(-\alpha x)$$

where $I(x)$ is the intensity at a distance x of a light beam originally of intensity I_o after passing through the optical medium of optical thickness αx. α is the absorption coefficient, which can be written in terms of the Einstein coefficient for the absorption of light, B_{12}, and the stimulated emission of light, B_{21}, simply

$$\alpha = N_1B_{12} - N_2B_{21}$$

where N_1 and N_2 are the number densities of atoms in the lower state 1 and the excited state 2. Since the probability of absorbing the radiation or stimulating its emission are equal, $B_{12} = B_{21} = B$, it follows that

$$\alpha = B(N_1 - N_2).$$

Anyone from 1917 onward could have readily observed that α can be made negative if N_2 is greater than N_1 thereby causing $I(x)$ to grow larger than I_o the original intensity as x increases. This possibility is called negative absorption or amplification. In other words amplification of the radiation [illegible] when the number density of particles in the higher lying excited state 2 exceeds that in state 1. This situation constitutes population inversion. Although the [illegible] was extensively studied [illegible] and 30's the invention of the MASER, [illegible] light source and light amplifier did not occur until the late [illegible].

There are many ways of establishing a population inversion in gases, liquids and solids. This will be discussed in lecture [illegible] along with more detail [illegible] LASERS. [illegible] let it suffice to say that for laser [illegible] and that this medium must be [illegible] which is 10 - 40 per cent transparent. [illegible] through the medium in order to [illegible] will be amplified (Fig. 5) [illegible] inverted state. If the gain per pass of the radiation is greater than [illegible] then the system will be made to lase.

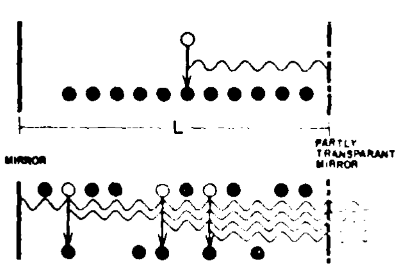

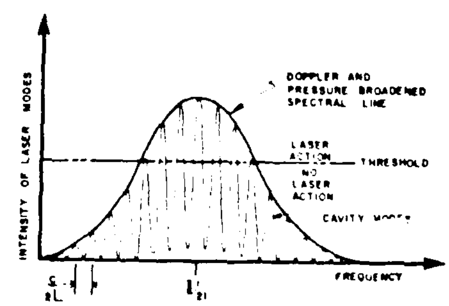

Figure 5. Shown in a) is the optical cavity with the medium slightly excited. In b) there is a marked population inversion. Some levels are stimulated to emit.

Figure 6. Spectral line centered at ν_{21} showing seven normal cavity modes with intensities which exceed the threshold for laser oscillation.

Since normally each atom prefers to be in its lowest energy state, an external source of energy is required to maintain an inverted system. [illegible] that this external energy [illegible] disturb the Boltzmann (thermal) equilibrium [illegible] called pumping. As long as pumping continues the [illegible] the atoms will rapidly return to an equilibrium between states through the process of [illegible] and

stimulated emission, and lasing action will cease.

We have seen that the frequency of the laser light is limited to a narrow band centred around ν_{21} associated with the spectral width of the transition 21. This width includes the width due to the natural decay of the excited state, the motion of the radiating atoms and pressure broadening. However, within this broad band of frequencies the LASER radiation is *even more restricted* by the properties of the optical cavity. Atoms which oscillate in phase with one another in the cavity are said to be in normal modes. The frequencies of the normal modes of the free oscillations are harmonics of the fundamental frequency ν_{21}, Fig. 6. Within the optical resonating cavity of length L, standing waves similar to those in a string occur only for wavelengths which are an integral number of one-half the emitted wavelength λ, so that

$$L = m\,\lambda/2 \qquad m = 1,2....$$

From the simple relationship between the velocity of light, wavelength and frequency discussed above, the frequency interval between adjacent modal lines is

$$\Delta\nu = c/2L$$

If for example for red light where ν_{21} is approximately 5×10^{14} Hz (as for He-Ne red laser light) and an optical cavity of length 1 meter, then the number of modes that exist in this case is 3×10^{6}. In other words the radiation which had a line width associated with the atomic transition plus doppler shifting plus pressure broadening is now divided into nearly three million parts only some of which will show LASER action because they meet the necessary [illegible]. The spectral width of each of these lines associated with the normal modes of oscillation of the cavity is at least a million times narrower than the original spectral line. It is reasonable then to imagine that in the case of 5×10^{14} Hz radiation with a normal line width of 10^{9} Hz, [illegible] the line width associated with the excitation of a single mode can in principle if not easily in practice be [illegible] Hz, thus the spectral [illegible] the amount of power available per unit area of emitter within [illegible] at a given wavelength or frequency is extremely large, in fact larger than any other source.

Normally we also consider the spatially distributed modal pattern from a cylindrical or a rectangular cavity. This pattern is quite complex [illegible] transverse electromagnetic modes TEM_{mn} the details of which are beyond the scope of this lecture. In the designation of modes m and n are integral values where for circular mirrors n denotes the order of angular variation and m the order of radial variation. TEM_{00} is usually the dominant mode in most cavities.

5. PROPERTIES OF LIGHT SOURCES

The special properties of the radiation produced from laser action will become clear as we compare the LASER as a light source with other sources of electromagnetic radiation:

a. Point sources and extended sources - Although all light sources have finite dimensions it is useful idealization to consider a source as a point, even though there is no true point in nature. For example, an atom has its extension and stars which appear to us as points in reality are very large. The light from a point source differs from that of an extended source in that it propagates radially from its origin. Close to the source most of the rays intercepting the small surface area A strongly diverge, however as that same surface area is moved off at a large distance, divergence is minimized and the light can be considered collimated.

An extended source by contrast can be considered as made up of a large number of point sources. Close to this source, the light rays passing through the test area A have a larger divergence than those from a point; however, as A is moved off to a very large distance, often referred to as infinity, the light behaves like it comes from a point source. Unlike most other extended light sources the LASER because of the organized nature of its radiation can be considered as a point source, even though in reality it is not.

b. Monochromaticity or Temporal Coherence - A few years ago one would have called the light from a mercury arc lamp monochromatic. However, when this light is viewed through a spectroscope one finds it made up of approximately five lines with the dominant line in the blue. Since the advent of the LASER the spectral width of the blue line is reduced by more than a million so that the light for the first time can truly be considered monochromatic.

c. Spectral Coherence of Light - Light from a point source has a very special quality, spatial coherence. If light could be emitted from a point source, anywhere on a sphere surrounding the source, the electromagnetic wave would show the same maximum or minimum in its intensity. This light is coherent. As one backs away from the point to infinity, the light reaching the observer remains in phase or in step.

In the case of LASER the very process of stimulated emission which produces the amplification of the light leads to the emission of radiation in which all the waves moving in the direction are in step or in phase, quite similar to the situation one observes from a point source at infinity. The coherence of laser light then is one of its most important properties.

The coherence of LASER light is best [illegible] interference and diffraction effects. They involve the constructive and destructive interference [illegible] of the electromagnetic waves. Interference effects can most clearly be demonstrated with monochromatic coherent light from a LASER. In fact, interference photography, holography, is only [illegible] with the LASER as a light source.

Consider the case of diffraction from a narrow slit of width d. In Fig. 7, I show monochromatic coherent light coming from the left, illuminating the slit, [illegible] some distance away, is the diffraction pattern. The position of the maxima where there is constructive interference of the waves is given by the

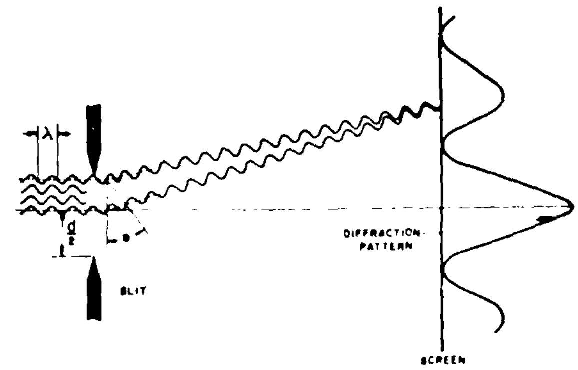

Figure 7. Single slit diffraction pattern

simple formula

$$n\lambda = (d/2)\sin\theta$$

where n (known as the order) is the number of full wavelengths that a wave coming from a point source in the middle of the slit [illegible] that at the [illegible] destructively interferes with one from the upper or lower edge. [illegible] is the angle between the [illegible] of the [illegible] rays and the point of observation on the screen. [illegible] one can readily see that if the light were not coherent at the slit (that is, the waves were out of phase), and many wavelengths were involved, no diffraction pattern would be [illegible] at the screen.

d. Polarization of light - Electromagnetic radiation may be polarized in a number of ways. In the case of radiowaves which are produced by the [illegible] of electrons up and down an antenna the wave is by nature polarized. In [illegible] this would be [illegible] the direction of the [illegible]. Normally light which is generated by very many atomic oscillators [illegible] independently is not polarized. However, it can be made so by reflection, as for example reflection of sunlight at an angle near [illegible] from the surface of a lake; or the back scattering of sunlight from the molecules of the air. [illegible] scattering is known as Rayleigh scattering. With [illegible] experience we find that polarized sunglasses eliminate the enormous glare associated with such processes.

The radiation normally [illegible] from a [illegible] LASER is also polarized, not because of some basic atomic process but because the exit windows of the LASER [illegible] that the beam axis is approximately [illegible] with respect to the normal to the exit windows. At Brewster's angle only radiation which is polarized will build up within the laser cavity. As a result the light which is emitted is highly polarized.

6. GENERAL DEFINITIONS AND COMPARISON BETWEEN LASERS AND OTHER SOURCES

LASERS vary considerably in output power from a few thousandths of a watt as in the case of the very useful (red) helium-neon [illegible] to [illegible] in the case of [illegible] pulsed carbon dioxide-gas (infrared) lasers. [illegible] are capable of operating [illegible] while other types of LASERS are operated in a pulsed mode. In the [illegible] which follows, we will compare a helium-neon cw gas laser with a power of one milliwatt with other light sources.

a. Divergence and diffraction limit - Because of diffraction any beam of light emitted from a source with a small [illegible] diverges with a minimum half-angle of divergence θ given by the ratio of the wavelength to the diameter of the beam, [illegible] directly from the single slit diffraction equation discussed in the previous section. A beam of light having this divergence is said to be collimated [illegible]. Because of the monochromaticity and coherence of LASER light its divergence [illegible] limit. On the other hand light from other extended sources, because the light is neither monochromatic nor coherent, has a divergence that is considerably larger. One of the best [illegible] in the now classic picture of the partially eclipsed earth as seen [illegible] where two low power argon ion laser beams (in the green) can be seen emanating from [illegible] in the western part of the United States while none of the light from the major centres in the west can be seen at all.

The approximately [illegible] from a helium-neon LASER with the output diameter of 2 mm has a half-angle divergence of approximately [illegible]. Consequently, one can consider the beam [illegible] behind the exit mirror of the oscillating cavity. The [illegible] energy [illegible] within the [illegible] while the brightness of the extended [illegible] in the direction of the beam it is zero at other angles, which are outside the cone [illegible].

b. Radiant power, radiant emittance and intensity - A point of coherent source is measured by its radiant power, the measure of energy emitted per unit time in all directions. Radiant emittance is the radiant power emitted normal to the emitting surface per unit area of the emitting surface. The intensity is the radiant power per unit solid angle.

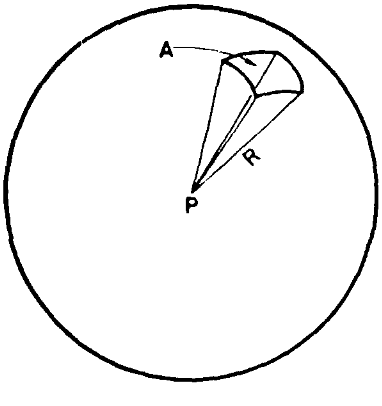

Figure 8. Sphere showing the elements defining solid angle.

Consider a sphere of radius R around a point source which has some closed area on the surface, as shown in *Fig. 8*. *The area* on the surface divided by the radius R^2 of the sphere is the definition of the solid angle ($\Omega = A/R^2$) measured in steradians (Sr). Since the entire surface area of the sphere is $4\pi R^2$ it is clear from the definition that 4π steradians represent the maximum solid angle around a point source. If we consider a fixed area like the size of the cornea of the eye, as one moves away from source the intensity of the light which enters the eye decreases as $1/R^2$ since the solid angle subtended from the point source changes as $1/R^2$. This is what is normally called the inverse square law which governs many of the basic physical principles of nature.

It can be easily demonstrated that for the LASER, the solid angle into which the power is emitted from a point source is equal to $\pi\theta^2$. Since for our He-Ne LASER θ is equal to 3×10^{-4} radians, and if the power is 1 milliwatt, it follows that

$$\text{Intensity} = \frac{10^{-3}}{\pi (3 \times 10^{-4})^2} \cong 4 \times 10^3 \text{ watts/Sr.}$$

c. Brightness - The brightness of an extended source is the radiant emittence/unit solid angle or the intensity/unit area of the emitter. Both intensity and brightness fall off as cos θ the angle with respect to the normal to the emitting surface. If in the case of the 1 milliwatt LASER the radius of the beam is 1 mm or 0.001 meters,

$$\text{Brightness (LASER)} = \frac{4 \times 10^3 \text{ watts/Sr}}{4\pi\ (0.001)^2 m^2} \cong 3 \times 10^8 \text{ watts/m}^2\text{/Sr}$$

By comparison, for various other light sources:

Brightness (Tungsten filament @ 3300°K) = 7 x 10 [illegible] watts/m²/Sr

(High power carbon arc) = 3×10^6 watts/m²/Sr

(Sun) = 2×10^7 watts/m²/Sr

(0.25 MW Synchrotron radiation source) ≈ 1×10^8 watts/m²/Sr

Thus, the smallest of lasers, is brighter than all known light sources, in fact it is two orders of magnitude brighter than the sun, the source of all life on this planet.

d. Spectral Brightness - We have already spoken of spectral brightness as it relates to a blackbody radiator. Once again it is defined as the brightness of a source per unit wavelength or frequency.

There is no comparison between the amount of power in the form of light which can be delivered from an He-Ne 1 milliwatt LASER and a 10^4 watt carbon arc radiating in the same spectral slice of the [illegible] spectrum. Although 10 million times more total optical power is delivered from the arc, the amount of power in a small spectral band is much larger for the helium-neon LASER. For the arc lamp the power is distributed over approximately an interval of 500 nanometers, therefore, we have [illegible] watts/nm. However, in the case of the helium-neon LASER, which as we pointed out before [illegible] frequency width as narrow as [illegible] hertz by the choice of a single mode (1 Hz at the wavelength of the helium-neon laser [illegible] nm corresponds approximately to a spectral line width of 1 x [illegible] nm), the power per unit wavelength is equal to [illegible] or [illegible] watts/nm. In other words the amount of light available in a narrow spectral band is much larger from a laser than from any other light source.

e. Illumination at a distance - Although it is possible to photograph the light from the argon-ion LASER on the moon, is it realistic to imagine that lasers can be used to light the surface of the moon? Let's look at this problem. A distant surface subtends a very small solid angle at the source. Therefore one wants a source that emits a great deal of light into a small solid angle, and that is just what a LASER does. Let us compare the amount of light which the 1 milliwatt LASER can bring to a distant surface, A, with the amount coming from the same surface from a Tungsten filament at 100 W incandescent lamp. Since the lamp radiates 100 watts into the entire sphere of area $4\pi R^2$ the power reaching the area A on the sphere is given by

Power = Intensity x Solid Angle

$$\text{Power (Tungsten Bulb)} = \frac{100\ (\text{Watts})}{4\pi\ (\text{Sr})} \times \frac{A}{R^2}\ (\text{Sr})$$

$$= 8\ A/R^2 \text{ watts}$$

distributed over the entire visible spectral range. From above,

$$\text{Power (He-Ne Laser)} = 4 \times 10^3 \text{ watts/Sr} \times \frac{A}{R^2}\ (\text{Sr})$$

$$= 4 \times 10^3\ A/R^2 \text{ watts.}$$

in a single spectral line. It follows then that the ratio of the powers reaching a small area A is

$$\frac{\text{Power}_A\text{(He-Ne Laser)}}{\text{Power}_A\text{(Tungsten Bulb)}} \approx 500$$

When one remembers that LASERS have been developed that are a thousand-million-million times more intense than our helium-neon laser one recognizes the enormous potential for the transfer of energy and information available through the LASER.

In Section 3 we showed that the brightness of even the smallest helium-neon LASER is in excess of that of the sun. Does this mean that the LASER placed as far away as the sun could do a better job than the sun in illuminating the earth? Of course not! The power of each is its brightness times the solid angle subtended times the area of the emitting surface. Under these circumstances one sees that

$$\frac{\text{Power (Sun)}}{\text{Power (Laser)}} = \frac{2 \times 10^7 \text{ watts/m}^2\text{/Sr} \times \pi(10^{11})^2 \times A/R^2 \text{ (Sr)}}{3 \times 10^8 \text{ watts/m}^2\text{/Sr} \times \pi(10^{-3})^2 \times A/R^2 \text{ (Sr)}} \approx \frac{6 \times 10^{25} \text{ A/R}^2 \text{ watts}}{9 \times 10^2 \text{ A/R}^2 \text{ watts}}$$

$$\approx 7 \times 10^{22}$$

Even though the sun is a source of lower brightness than the LASER its very large area more than makes up for it.

f. Concentration of power into a small area - Though it won't be proven here, radiant power density at a point on some area which is being illuminated by a source depends only upon the brightness of the source. In this case the size of the source is immaterial. Furthermore, the power per unit irradiated area has a value which is the same order of magnitude as the brightness. Since the laser has the greatest brightness of all light sources, it follows that the laser is capable of producing a greater power density than any other sources.

As one might expect the smallest area into which radiation in a parallel or nearly parallel beam can be focused by a lens is limited by diffraction to an area of approximately λ^2 where λ is the wavelength of the radiation. The highest power density produced by 1 milliwatt LASER is thus given by a power output divided by λ^2 or

$$\text{Power Density He-Ne (LASER)} = \frac{1 \times 10^{-3} \text{ watts}}{(600 \times 10^{-9} \text{ m})^2} \approx 3 \times 10^9 \text{ watts/m}^2$$

Note that the value for the power density is within an order of magnitude of the brightness of the LASER. Remember again that this particular LASER is one of the lowest power LASERS. Therefore, as one might expect the effectiveness of more intense LASERS like a 6000 watt CO_2 cw LASER for the machining of metals, welding and other such purposes, is extremely good. Another impressive example is a picture of approximately ten burns in one hemoglobin cell caused by the light of a ruby LASER focused onto the cell. Microsurgery using LASERS is now a reality.

Although LASERS are far better than any other man-made sources for many purposes, they are not the solution to all problems. Other light sources are far superior to the LASER for many purposes such as general illumination. The applications of LASERS will be discussed in the next lecture.

7. GENERAL REFERENCES

Allen, L., Essentials of Lasers, Pergamon Press: Oxford, 1969.

Goldman, L. and R.J. Rockwell, Jr., Lasers in Medicine, Gordon and Breach, Science Publishers, Inc.: N.Y., 1971.

Halliday, D. and R. Resnick, Physics, John Wiley and Sons, Inc.: N.Y., 1962.

Laser and Optical Hazards Course Manual, U.S. Army Environmental Hygiene Agency: Aberdeen Proving Ground, Md., 1975.

Laser Technology and Applications, edited by S.L. Marshall, McGraw-Hill Book Company: N.Y., 1968.

Lasers and Light: Readings from Scientific American, introduction by Arthur L. Schawlow, W.H. Freeman and Co.: San Francisco, 1969.

Lengyel, B.A., Lasers, Wiley-Interscience: N.Y., 1971.

8. ACKNOWLEDGMENTS

I gratefully acknowledge the assistance of my associates P.K. John and J.A. Medeiros, Physics Department, The University of Western Ontario, who assisted me with the literature and reading of the manuscripts and the help of D.H. Sliney, U.S. Army Environment Hygiene Agency who brought the Laser and Optical Course Manual to my attention and the support of the Canadian Defence Research Board and U.S. Army Medical Research and Development Command who with the Richard and Jean Ivey Fund and the Veeco Foundation are supporting our research.

APPENDIX 1.6

LASERS

J.Wm. McGOWAN
Physics Department
and
Centre for Interdisciplinary Studies
in Chemical Physics
The University of Western Ontario
London, Canada N6A 3K7

SUMMARY

Principles and properties of the LASER are dis[illegible] in some detail together with a description of the various types of LASERS and their applications.

1. MORE ABOUT LASER PROPERTIES

The acronym LASER stands for Light Amplification by Stimulated Emission of Radiation.

Several years after [illegible] and the Americans Gordon, Zeiger and Townes[2] had shown that [illegible] wave frequencies could be accomplished with the ammonia molecule [illegible] proposed that such amplification could occur in the infrared and [illegible].

In order to maintain amplification [illegible] the system to be sufficiently excited so as to have a net round trip [illegible] cavity at least equal to unity. However for oscillation to build up [illegible], the net round trip gain must be greater than unity. This leads to the [illegible] inversion necessary for laser action. The relationship describing this [illegible]. If we assume that the shape of the radiation line is [illegible] it follows that

$$N_2\frac{g_2}{g_1} - N_1 \geq \frac{8\pi [illegible]}{\lambda^{[illegible]} [illegible]}$$

where N_c is the critical population [illegible] density necessary to maintain laser oscillation. In the expression N_2 and N_1 are the populations [illegible] states 2 and 1 while g_2 and g_1 are the degeneracies associated with each of these states, [illegible] the half width of the broadened spectral line, while [illegible] is its natural half-life and [illegible] characteristic of the cavity construction. One sees immediately that as the energy interval between levels increases, that is, as the wavelength decreases, the necessary critical population inversion density increases rapidly. Similarly as the lifetime of the radiative state increases [illegible] critical population inversion density. However, there is advantage in using states for the upper laser level with very long lifetimes, since atoms decaying from still higher levels may be trapped in the [illegible] level, thus increasing the density of excited atoms.

Many materials can now be made to lase, not only in the infrared, but the visible and near ultraviolet regions of the electromagnetic spectrum as well. There appear to be serious limitations to developing a far UV or x-ray LASER but [illegible] x-ray lasers may yet be developed.

Using the above mentioned criterion for minimum inversion [illegible] necessary for laser oscillation, for a ruby system which will be discussed in greater detail later one can estimate that the ruby rod [illegible] in length can be made to amplify radiation [illegible] the upper level exceeds that of the ground level by as little as [illegible]. Since the concentration [illegible] in pink ruby is [illegible] atoms cm^{-3}, states 1 and 2 each contain approximately [illegible] atoms cm^{-3}, and the population difference must be approximately [illegible] x $10^{[illegible]}$ atoms cm^{-3}.

The formulation described above was developed in [illegible] with a model two-level laser system. However, most solid state LASERS like the [illegible] ruby [illegible] are three, while most others are four level LASERS like neodymium doped systems. As a result the [illegible] may [illegible]. Exact analysis of a system requires that [illegible] with the total number of excited atoms [illegible] states under stationary conditions can be derived. If [illegible] the system [illegible] the power of optical pumping radiation [illegible]. It follows then that one can calculate the equivalent minimum [illegible] temperature [illegible] adequate illumination in the spectral energy interval where [illegible] for the ruby [illegible] the necessary blackbody temperature of the [illegible]. In reality it must be higher because of [illegible].

The primary method [illegible] for laser [illegible] the intense flash lamp [illegible] which normally is mounted along with the laser [illegible] all the optical energy on the [illegible] produced in gas discharges through [illegible] ance excitation, energy transfer [illegible] brought about through the chemical [illegible] through electron excitation [illegible] fields across the [illegible] with an external beam of electrons. [illegible] ultraviolet can be produced with the [illegible] very high energy, high current electron beam.

2. MODES OF OPERATION

Many LASERS, particularly low powered LASERS can be made to operate in a continuous wave mode where power is continuously added to the system to maintain the [illegible] at the same time [illegible] is extracted from it. As more power is extracted from the system the [illegible] will tend to oscillate. The natural pulsation reflects the repeated breakdown

natural pulsation reflects the repeated breakdown of the minimum inversion criterion for laser oscillation caused by the depletion of the excited state due to laser action, or focusing effects on the light beams due to the change in the optical properties of the medium during operation. These regular pulsations of the LASER are disturbing for some applications, especially communication where the timing and the control of the intensity envelope are particularly important.

Often LASERS are intentionally ... [illegible] ... This is brought about by pulsing of the optical radiation ... [illegible] ... The length of the light pulse from the laser ... [illegible] ... system begins ... [illegible] ... properties of the ... [illegible]

Since the LASER is an oscillator ... [illegible] ... amplifier with a feedback ... [illegible] ... the threshold condition of oscillation ... [illegible] ... greater than the sum of the losses. The loss rate of the system ... [illegible] ... cribed by the ... [illegible] ... creases the ... [illegible] ... necessary for the oscillation ... [illegible] ... increases. ... [illegible] ... technique ... [illegible] ... cillation ... [illegible] ... in the LASER ... [illegible] ... spoiling. ... [illegible] ... single giant pulse ... [illegible] ... Q-switching ... [illegible] ... the lifetime of the ... [illegible] ... hence the time ... [illegible] ... high Q can be ... [illegible] ... development of the greatest population inversion in the material.

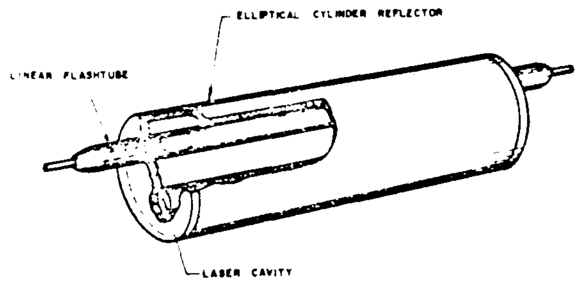

Figure 1. One of many laser configurations. The laser cavity is ... [illegible] ... by mirrors at each end, one of which is semi-transparent.

In general the principle of Q-switching ... [illegible] ... of inserting a switch ... [illegible] ... This switch ... [illegible] ... in such a way that it separates ... [illegible] ... from the laser action. ... [illegible] ... cavity can then be ... [illegible] ... one single giant pulse ... [illegible] ... during pumping, the total ... [illegible] ... during the Q-switching ... [illegible] ... that of the normal ... [illegible] ... the pulse is ... [illegible] ... endously ... [illegible] ... of Terawatts ... [illegible] ... release greater than ... [illegible]

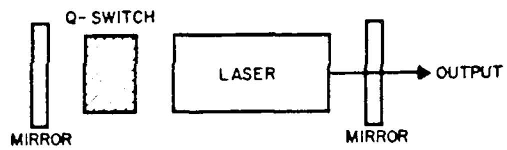

McClung and ... [illegible] ... produce ... [illegible] ... an optically ... [illegible] ... use of the ... [illegible] ... light and ... [illegible] ... of the light ... [illegible]

Figure 2. Schematic representation of a Q-switched laser system. In some systems the switch and mirror are combined.

Mechanical ... [illegible] ... The idea of employing a rotating chopper wheel to ... [illegible] ... medium and one of the mirrors was first used by Collins ... [illegible] ... from the time the ... [illegible] ... active medium until the medium is fully excited. Faster ... [illegible] ... rotating one of the mirrors, or by replacing one of the mirrors with a ... [illegible]

A much simpler ... [illegible] ... a dye solution which bleaches within ns when the impinging intensity ... [illegible] ... completely transparent. The dye must have two energy levels ... [illegible] ... to that of the laser ... [illegible] ... is absorbed ... [illegible] ... the lower level are ... [illegible] ... When saturation ... [illegible] ... the dye ... [illegible] ... cavity ... [illegible] ... dyes ... [illegible] ... filter or CRANE ... [illegible] ... sensitive ... [illegible] ... the shutter.

3. FREQUENCY ... [illegible]

From its very nature ... [illegible] ... stimulates the emission of the radiation associated with the transition between the ... [illegible] ... in the resonant ... [illegible] ... Although one frequency ... [illegible] ... the frequency of the radiation ... [illegible] ... and its associated optical system.

a. Modes of oscillation ... [illegible] ... spectral band width of the emitted radiation ... [illegible] ... number of ... [illegible] ... exist in the ... [illegible] ... will be caused to oscillate ... [illegible] ... however, associated with each spectral line ... [illegible] ... the laser can be tuned. In the early LASERS, ... [illegible] ... was 1 Hz.

b. Stimulated Raman Emission[9] - When for example ruby laser light at 694 nm (6943Å) from a million watt pulsed LASER [illegible] liquids such as nitrobenzene, or in fact any solid, liquid or gas within or even [illegible] the laser cavity, this results in a number of spectral lines that are shifted down in frequency from the original line by [illegible] corresponding to the electronic, vibrational or rotational levels of the molecules within the material which is being irradiated. This is known as Raman Effect. When the light intensity is very high as in a laser cavity, the energy available as Raman scattered light [illegible] the stimulated Raman effect. For example, if in a focused light [illegible] vibrational or rotational levels of the molecules in the medium are stimulated [illegible] the refractive index of the material oscillates strongly at one of these frequencies. [illegible] the characteristic frequencies of the molecules are [illegible] frequency they are added to it as well. These shifted [illegible] each line of which is a source of light at a different frequency.

The large variety of [illegible] the Raman effect provide hundreds of new coherent sources of light from the ultraviolet [illegible] efficiency has been obtained in converting laser light [illegible] nonlinear processes, such as Raman scattering.

c. Frequency doubling, tripling [illegible] other nonlinear processes in certain asymmetric crystals such as [illegible] the conversion of up to a few percent of [illegible] frequency [illegible] known as frequency [illegible] converting the infrared radiation into visible light. [illegible] nonlinear [illegible] lead to higher harmonics as well, thus expanding laser [illegible] the ultraviolet.

4. SUMMARY OF LASER PROPERTIES

i. Although in reality an extended source, the LASER is effectively a point source.

ii. Because the laser cavity [illegible] to oscillate in one mode, the source is very monochromatic. In many materials the spectral width [illegible] more than six orders of magnitude [illegible] than the Doppler [illegible] the source is unequalled.

iii. Laser light is spatially coherent similar to what we would expect from point source at infinity.

iv. In most gas and liquid LASERS [illegible] for solid state LASERS, the light that is emitted [illegible]

v. Laser light [illegible] with a divergence angle as small as the diffraction limit for the wavelength emitted.

vi. The [illegible] any other source, particularly when one considers the [illegible]

5. TYPES OF LASERS

In the following [illegible] I will try to describe the various types of LASERS, indicate the basic [illegible] their basic parameters. The first five are solid state LASERS [illegible] LASERS. In Table 1 I give a summary of the most powerful [illegible]

a. Ruby LASER [illegible] The [illegible] solid state ruby laser [illegible] by weight Cr_2O_3 in it [illegible] crystal is known as sapphire [illegible] the physical [illegible] laser crystals. [illegible] diagram for the chromium [illegible] in the LASER. [illegible] laser lines [illegible] cause of transition [illegible] greater than that [illegible]

In all solid state lasers there [illegible] problem associated with [illegible] the laser material, [illegible] be introduced into the system [illegible] the inversion. [illegible] absorption bands [illegible] the blue, and [illegible] the green, the [illegible] mercury lamp [illegible] light absorbed [illegible] ruby. However, the efficiency [illegible] other solid state LASERS can be [illegible] with the addition of other ions with [illegible] ated in the host lattice [illegible] transfer for the excitation to the [illegible] as happens in the case of the [illegible] laser which will be discussed shortly.

Table 1
High intensity lasers

Laser Medium	Wave-length	Efficiency ($\%$)	Peak power (W)	Pulse duration	Laboratory
Nd: glass	1.06 µm	0.2	$7\times10^{1?}$	1.5 ns	Battelle, Columbus, USA
			4×10^{12}	230 ps	Lawrence Livermore, USA
			10^{12}	1 ns	KMS Fusion Inc. USA
			2×10^{12}	500 ps	Univ. Rochester USA
			5×10^{11}	2 ns	Lebedev, Moscow, USSR
CO_2	10.6 µm	3-5	5×10^{11}	1 ns	Los Alamos, USA
Iodine	1.31 µm	0.5	$10^{1?}$	700 ps	Max-Planck-Inst Garching, Germany
Hydrogen Fluoride	2.7 µm	180 (electrical) 5 (chemical)	10^{11}	35 ns	Los Alamos and Sandia, USA
Dye	605 nm	$<10^{-?}$	3×10^{9}	3 ps	Imperial College London
Xenon	173 nm	>2	4×10^{9}	20 ns	Los Alamos and Maxwell Labs Inc. USA

The optical quality of the ruby is a critical factor in laser operation. Not only are scattering centres detrimental but so are all variations in optical path from one end to the other. The mode structure, divergence, and the pattern of the radiation generated are largely determined by optical path variations. One of the disturbing observations about the radiation emitted by the ruby rod with parallel

uniform end surfaces is that it does not emit coherent radiation uniformly over the surface. Small, very bright spots - hot spots - appear at the end faces which vary in size and intensity. These reflect the quality of the rod.

It should be noted that although the three-level ruby system is still among the most popular LASERS, it is perhaps one of the most inefficient because the terminal level is the ground state requiring that slightly more than half of the atoms be in an excited state for the system to work. By contrast, most of the solid state LASERS are four-level systems, which normally have efficiencies that are much greater than that for ruby.

b. Neodymium Crystal Lasers[11] - A neodymium LASER is characteristic of all the rare earth ion lasing systems that have now been studied. [illegible] all of the rare earth ion systems which include both the spectral ions [illegible] are important, and have been observed operating in a number of host crystals and glasses. By varying the ion and the host material one can vary the wavelength of the LASER over an extensive range. A [illegible] listing of these is given in reference[1]. The list of rare earth atoms that have been used include all fifteen members of the LANTHANIDE series ranging from La through Lu.

The big advantage of the four-level system (Fig. 4) over the three-level system is that energy from a photo flashlamp is absorbed in a very [illegible] level, transferred [illegible] non-radiatively to the third level, followed by a laser transition between the third and second level. The system finally comes to equilibrium again in the ground level. The requirements with regard to inversion are much less stringent than in the three-level system.

The most frequently used host crystals for neodymium include $CaWO_4$, $SrWO_4$, $SrMoO_4$, $CaNbO_3$ and $Y_3Al_5O_{12}$ (YAG) with neodymium concentrations of the order of [illegible]. Of these yttrium aluminum garnet (YAG) operating at room temperature at 1.06 [illegible] is the most commonly used. In other crystals the neodymium lines appear at wavelengths between [illegible] and 1.3 [illegible]. The substitution of the other rare earth ions leads to a multiplicity of other levels in the same general region.

Although the neodymium crystal LASER can be run at room temperature it is much more effectively pumped if the laser rod is at 77°K, since at room temperature the terminal laser level is partially filled, whereas at liquid nitrogen temperature it is not.

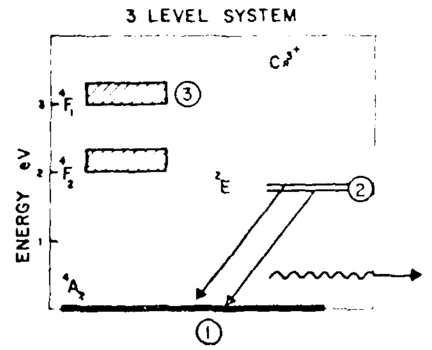

Figure 3. Energy level diagram for the three level ruby system.

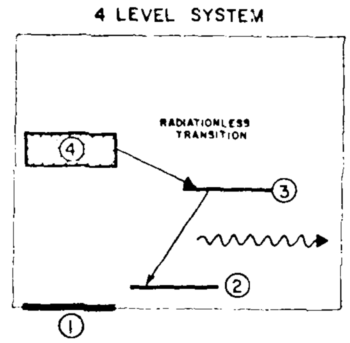

Figure 4. Schematic energy level diagram for the four level system.

c. Neodymium Glass Lasers[11] - The neodymium crystal LASER is a useful tool for the research laboratory however where high power is needed [illegible] ions embedded in glass [illegible] crown glass being the most favorable medium [illegible] the potential of the ruby LASER. Neodymium glass laser rods that are two to three m in length and three to four cm in diameter are [illegible]. Such LASERS can deliver more than 5000 joules in a single pulse. As with the ruby and crystal LASERS, the glass LASER is excited by means of a xenon flash tube. Furthermore, any of the rare earth ions may be embedded in glass giving laser action over a wide range of wavelengths.

The main advantages of glass as a laser host, are flexibility of size and shape of the rods and the excellent optical quality. There is also a flexibility in some of the physical properties, in particular the refractive index, which may be varied from approximately [illegible] by selection of the glass. It is possible to adjust the temperature coefficient of the index of refraction so as to produce thermally stable optical cavities. However, the major disadvantage of glass is the low thermal conductivity which imposes limitations on continuous operation or high repetition rates.

Although times shorter than 1 nsec can be obtained in the giant pulse laser systems by Q-switching, it is possible by developing oscillations within the giant pulse to produce pulses with half-widths of the order of picoseconds. The highest peak power achieved thus far by solid state LASERS are obtained within the giant pulse [illegible] with these ultra-short pulse techniques. These methods are particularly important for specialized uses such as laser fusion.

d. Semi-Conductor LASERS[11,12] - Of the solid state LASERS the semi-conductor LASERS are the most efficient, and are by far the easiest to modulate, but they operate effectively only at very low temperatures. Unlike most other LASERS where electrical energy is converted first into photons or into electrons that bombard the system, in semi-conductors it is possible to convert electrical energy directly into coherent light. Such conversion takes place in the diode injection LASER in which excitation is the immediate result of work done by an imposed electric field on the charge carriers in the material.

A schematic energy level diagram for a PN junction diode is shown in Fig.5. Semi-conductor LASERS depend on radiative recombination of electrons and holes in semi-conductors for their operation. Only certain semi conductors, those such as GaAs with a direct gap between conduction and valance bands are suitable.

Semi-conductor LASERS differ from other solid state LASERS in most of the physical and geometric characteristics. They are two to three orders of magnitude smaller in size than the typical crystal or gas LASER. The largest dimension of a common semi-conductor LASER is at most 1 mm. The relevant physical properties of semi-conductors and their variation with external parameters such as pressure and temperature that make them good candidates for tunability of energy.

Gallium arsenide occupies the same role among semi-conductors that ruby occupies among solid crystals. It is the first and the most used semi-conductor laser material. The band gap in GaAs varies with temperature and in purity content and pressure. At [illegible] the band gap of the pure crystal is [illegible]. At [illegible] it is only around 1.41eV. Electroluminescence is obtained from heavily doped GaAs diodes [illegible] with a spectral distribution that has a peak between [illegible] and [illegible] nm. This corresponds to a photon energy between 1.4[illegible] and 1.48eV. Several hundred watts of peak power may be obtained from a GaAs diode in pulsed operation at 77°K whereas only 15 watts has been reported at room temperatures.

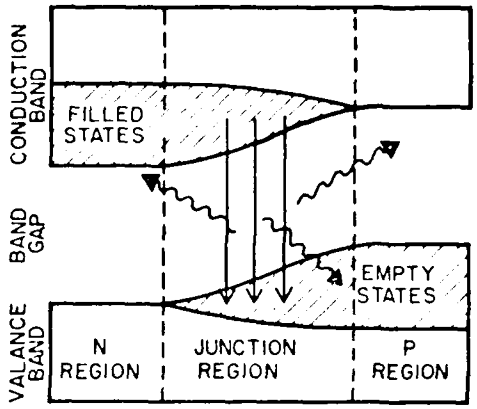

Figure 5. Schematic level diagram for PN junction laser excited with an electric field.

The light emitted from the diode is usually plane polarized but the polarization varies from one diode to another. An effective emitting area is maybe as small as [illegible] μm. As a result the divergence of the beam is about 10°, much broader than beams radiated from crystal lasers. High power diode LASERS not only emit in the near infrared region around [illegible] nm but also in the blue region 4[illegible] nm, twice the frequency of the infrared radiation. The blue emission is the result of harmonic generation or frequency doubling within the diode itself.

A large number of other injection laser systems have been developed with wavelengths which vary through much of the spectral region. Furthermore, one of the advantages of using semi-conductors is that the wavelength can be shifted over a considerable range by alloying. Semi-conductor lasers can also be optically pumped, or pumped by high-energy electron beams, or by electric field breakdown within the system.

e. Organic Dye LASERS[13] - Although the organic chelate LASERS are built with rare earth ions and non-organic niodeodymium-selenium oxychloride LASERS exist, most important of the liquid LASERS is the organic dye LASER. Such LASERS have emerged as the most versatile laser systems now available. Both pulsed and continuous operation are possible. With [illegible] locking of the waves within the resonant cavity pulses as short as one picosecond have been obtained. The emission from organic dyes is extremely broad-band. Consequently, as a research tool its use is virtually unlimited, since with the proper choice of organic dyes it is completely tunable over a range that runs from the infrared through to the ultraviolet. In a recent article[14], a list of more than fifty organic dyes which can be used in the dye LASER have been given. Since that time many chemical companies have been active in developing new dyes.

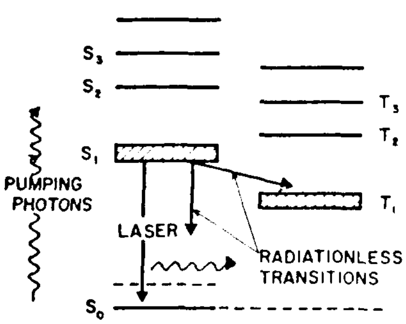

Figure 6. Schematic level diagram for the organic dye LASER.

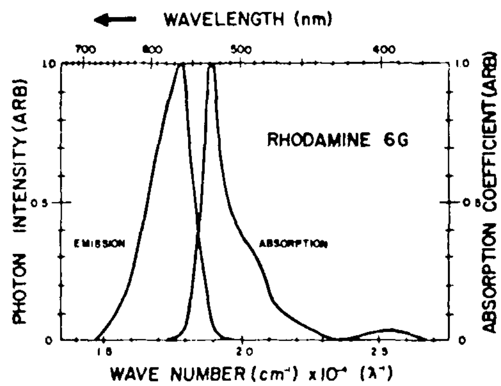

Figure 7. Absorption and emission curves for rhodamine 6G.

The operating principles are the same as any LASER (Fig.6). When optically pumped, dye molecules are raised to the lowest excited singlet state S_1 either directly or via cascades from higher singlet states which relax quickly to S_1. Lasing involves the return to the ground state S_0 by stimulated emission of a photon. In practice the process is very complex. The light emission has competition from several other processes, mainly the non-radiative conversion of S_1 to the state S_0 and from inter-system crossing to the triplet T manifold. In particular the accumulation of dye molecules in the triplet state T_1 can be detrimental to laser action if these triplet molecules absorb the light from the singlet system,[11] thus diminishing amplification within the cavity. Shown in Fig.7 is the characteristic absorption of one of

the popular dyes, rhodamine 6G, as well as its emission spectrum. If the laser cavity is not tuned to a particular frequency the system will oscillate over a broad band. For example the characteristic colour of the rhodamine 6G emission is in the orange.

Typical dyes are dissolvable in alcohol or water. In order that the efficiency remains high it is necessary that they be cooled. As a result they are either circulated through the optical cavity or fired in a liquid jet stream through the optical cavity. For stability and reproducibility the use of the jet is becoming more popular. Excitation of the organic dyes is accomplished by optical pumping using either solid state LASERS, nitrogen or argon discharge LASERS, or extremely fast flashlamps. Normally the gain achievable by using dye solutions is extremely high.

Initially dye LASERS were found to operate only with very short pulses. However, a careful study of the quenching mechanisms have made it possible for the system to be run cw.

f. *Helium-Neon*[15] *and other Nobel gas LASERS* - All of the gaseous Lasers which follow depend upon a variety of atomic and molecular collision processes which include electron impact excitation, electron impact excitation through resonant processes, electron impact deexcitation (superelastic collisions), photo-excitation as in the solid state case, energy transfer from an excited atom or molecule to another, charge transfer between an ion and an atom or molecule leading to excited products, etc. In the helium-neon LASER which is among the most used LASERS available today population inversion results from electron impact excitation of the helium metastable states followed by energy transfer to upper radiative states of the neon atom

$$e + He \rightarrow He^{*} + e'$$

$$He^{*} + Ne \rightarrow He + Ne^{*}$$

$$Ne^{*} \rightarrow Ne^{**} + h\nu_1,\ h\nu_2 \text{ or } h\nu_3.$$

The schematic energy level diagram is shown in Fig.8. As indicated in the final equation, and as shown in the diagram, the helium-neon LASER operates in three distinct spectral ranges: in the red at 632.8 nm, in the near infrared at around 1150 nm and further in the infrared at 3390 nm.

He-Ne LASERS were first discovered in 1960 by Javan et al[16]. Although there are three dominant lines, as many as thirty neon transitions can be caused to oscillate, most under very special conditions. As one can see in the diagram, the 632.8 nm transition is in competition with the 3390 infrared transition. In order to cause the system to oscillate primarily in the visible it is necessary to suppress the infrared line. This is done in a number of simple and often very sophisticated ways in the commercial LASERS. Because of its simplicity and significant power in the visible the He-Ne LASER is used primarily for instructional purposes and in the laboratory. Furthermore, it is the primary laser tool used for alignment and is a source of coherent radiation in holography. Its power output ranges from less than a milliwatt to powers well in excess of a Kwatt. Under normal circumstances the He-Ne LASER is run in a continuous mode, although it can be operated at higher power in a pulsed configuration.

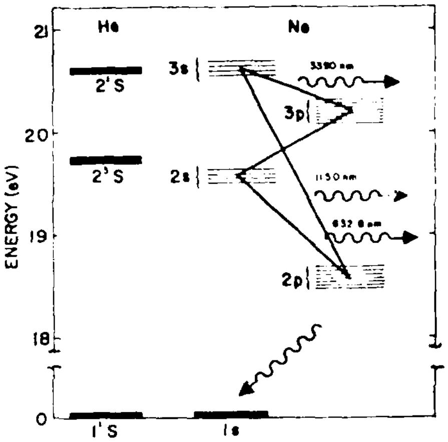

Figure 8. Level diagram for He showing first two metastable states, which transfer energy to the Ne levels which subsequently lase.

Although the He-Ne LASER is the principal nobel gas LASER it should be noted that gas discharges in helium, neon, argon, krypton and xenon can produce atomic radiation that can be the basis of a LASER. Not only are the pure gases used, but often it is found that mixtures produce enhancement of some of the laser lines. As a rule the output power of the nobel gas LASER is low. Under normal conditions they work in the cw mode. In all cases the laser configuration is the same as the helium-neon case. It becomes more difficult to achieve stimulated emission at short wavelengths because of the required pumping power increases as the 3rd power of the frequency. The large emission band widths reduce the net gain of a given population inversion. These difficulties are further aggravated by the absence of effective sources capable of rapidly pumping the nobel gas to higher energy levels.

Until recently stimulated emission at shorter wavelengths has been through the excitation of gases by high powered ns pulse discharges. Now high energy-high current electron beam pumping has resulted in some of the shortest laser wavelengths observed to date approaching 100 nm. Recent progress in electron beam pumping of vacuum UV LASERS is an outgrowth of work on condensed nobel gases by Basov and his co-workers[17] at the Lebedev Physical Institute. In this paper the Russian group demonstrated stimulation of 176.0 nm radiation in liquid xenon which resulted from the diatomic molecule of xenon making a transition to its repulsive ground state in a fashion similar to that shown in Fig.9. The final state of the xenon excited dimer came about through a sequence of events such as:

$$e(\text{high energy}) + Xe \rightarrow Xe^{+} + 2e$$

$$Xe^{+} + 2Xe \rightarrow Xe_2^{+} + Xe$$

This occurs in $\sim 10^{-10}$ sec at 10 atm.pressure. Ionization was then followed by three-body recombination

$$Xe_2^{+} + Xe + e \rightarrow Xe_2^{*} + Xe$$

the final transition from the excited xenon dimer to the repulsive ground state represents the laser transition which occurs in a time approximately 10^{-12} sec.

g. Ion Lasers[18] - In principle, ion LASERS are similar to other gas discharge LASERS, however they

operate in the near infrared, the visible, and the near ultraviolet. Ion LASERS operate with considerable dissipation of power but their peak energy output is usually orders of magnitude higher than those of atomic gas LASERS. They are not an efficient LASER, since in the discharge it is necessary to excite a level of an ion, thus requiring considerable amount of energy, most of which ultimately ends up as heat. The output of the LASER is dependent upon the square of the current. The first electron ionizes the atom while the second excites it. Although many ions have been excited through discharges the most popular ion LASER is the 488 nm Ar^+. The argon ion LASER has become very popular, primarily for therapeutic work in ophthalmology. Besides argon ions, neon, krypton, xenon, oxygen, mercury, iodine, iron, chlorine, bromine, boron, carbon, sulphur, silicon, manganese, copper, zinc, germanium, arsenic, cadmium, indium, tin and lead ions have also been used in ion LASERS as the active medium. The cadmium ion LASER is now becoming very popular.

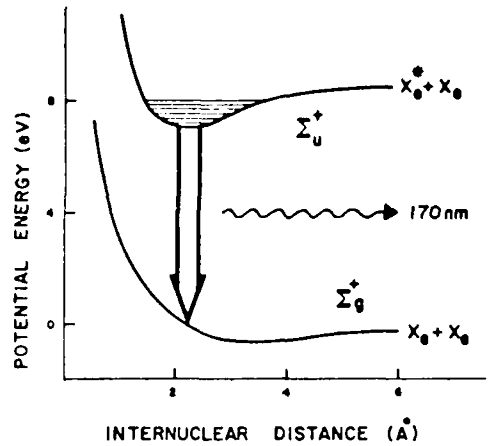

Figure 9. Level diagram for lowest two levels of the high pressure Xe gas laser.

It has been suggested[19] that charge transfer might be an effective method of producing excitation of radiation in the visible and UV. In fact, for cadmium, zinc and tin, this has been suggested of one of the primary pumping mechanisms. Quite recently it has been demonstrated by a group at the University of Texas[20] that charge transfer of He_2^+ with N_2 leads subsequently to radiation of the nitrogen ion at 427 nm with an efficiency approaching 2%.

h. Molecular Lasers[21] (Not including Chemical Lasers) - The most significant advances in laser technology have come within the last five years in this area. It is probably fair to say that all molecular gases can be made to lase in one mode of operation or another. As pointed out in Lecture 1, within a molecule there are combinations of electronic, vibrational and rotational transitions. Most of the molecular LASERS that have been made operative have involved the vibrational-rotational transitions. However, a substantial number of transitions have been observed in the infrared, the near infrared, visible and ultraviolet, associated with electronic transitions of a number of diatomic and triatomic systems. The most useful electronic transitions thus far used have been in nitrogen, particularly associated with what are known historically as the first positive, and second positive systems. In the first positive system which involves the transition between $B^3\Pi_g$ and $A^3\Sigma_u^+$ electronic states, [illegible] watt peak power output has now been measured through the wavelength range [illegible] and [illegible] nm. The transitions associated with the second positive system of N_2 ($C^3\Pi_u - B^3\Pi_g$) lie in the near ultraviolet. More than [illegible] laser lines of this system have been observed between the various vibrational-rotational branches. Other groups of lines have been observed at [illegible] nm and [illegible] nm. Pulse powers in excess of [illegible] kW are routinely obtained. Other electronic transitions have been observed in the infrared. Besides nitrogen, H_2 and D_2 have been caused to lase associated with an electronic transition.

The most significant work in the past five years has been associated with vibrational and rotational excitation of N_2 and CO_2 as well as mixtures of these gases with He and sometimes minute impurities. All of these systems have been caused to effectively lase with high powered output in the standard gas discharge laser tube. However, the biggest advances have occurred in several areas, particularly associated with the high pressure gas discharge systems[22]. It is only these systems which I will consider, since they are the basis of many of present and future industrial and military uses of LASERS.

The high pressure systems include the TEA LASER (Transverse Excited Atmospheric LASER), the E beam and Blumlein excited LASER and the electric discharge [illegible] LASER. Before examining any of the technical details let us consider the basic physics of the processes involved. In N_2 the lowest vibrational level of the molecule in its ground electronic state is excited through the formation of giant N_2^- resonances in the vicinity between [illegible] and [illegible] eV. It is the resonance excitation that is primarily responsible for the large probability of forming N_2 (v [illegible]). In mixtures of N_2 and CO_2, CO_2 in the first asymmetric vibrational mode is excited by resonant vibrational energy transfer from the v [illegible] level of N_2. This is demonstrated in Fig. 10. The [illegible] LASER transition then results between the first asymmetric vibrational mode and the symmetric vibrational mode, while the terminal level is subsequently destroyed through cascade to the ground vibrational level. The vibrational levels of N_2 are metastable and therefore represent a reservoir of stored energy for selective and effective excitation of CO_2.

A pulsed transverse excited atmospheric LASER in CO_2 was first reported by Beaulieu[23] in 1970. More recently various methods of preionization involving either electrons, heavy particles or ultraviolet radiation are now used in conjunction with the TEA type LASER to obtain large volumes of gas discharge and thus more energy. Preionization results in large quantities of charged particles in the gas volume prior to the initiation of the discharge. These charges aid in the production of a large volume glow discharge of high spatial uniformity. In a recent development the onset of the electrical discharge is controlled until the optimum degree of ionization exists within the discharge volume. The [illegible] system developed by Richardson, et al[24] has given output pulse energies of [illegible] in the multi-gigawatt range and with an overall energy extraction efficiency approaching [illegible].

The production of stable uniform discharges at high pressure has also been accomplished using electron beam (E-Beam) preionization. This technique involves the use of a high energy (0.1 to 1.5 MeV) electron beam to ionize the gas. An applied electric field accelerates the resulting charges and provides electrical excitation of the laser molecules. The discharge is not self-sustaining without the electron beam. In a recently developed system described by [illegible][25] [illegible] a uniform [illegible] discharge was produced in a 40 litre CO_2-N_2-He gas at 1 atm. The output [illegible] and a pulse length [illegible].

Increased operating pressure has led to greatly improved performance by increasing pulse energy peak power and maximum permissible repetition rate. At very high pressures much greater than one atmosphere the discrete vibrational rotational lines broaden and merge into a continuous emission band. Such a LASER will now be tunable over a broad spectral range or mode locked to produce picosecond (10^{-12} sec) pulses. Already, as reported by the [illegible], CO_2-N_2-He LASERS have been operated at pressures in excess of [illegible] atm. [illegible] systems in excess of [illegible] watts have now been developed in [illegible] pressure flowing systems[illegible]. [illegible] of the significant advances in the study of the dynamic laser system has been the complete analysis and predictability of the system using the [illegible] section data available[illegible]. The dependence of power output on the temperature, pressure, gas flow, [illegible] and impurity has been [illegible], has led to a predictable increase in efficiency.

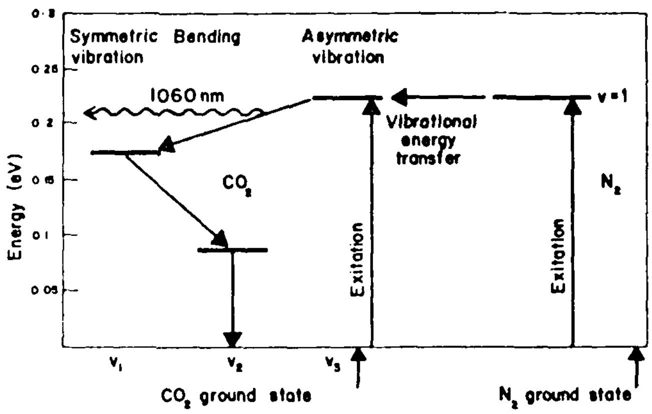

Figure 19. Level diagram for the first vibrational level of N_2 and some low lying vibrational levels of CO_2 which couple to N_2 (v = 1).

The Blumlein pulse generator will not be described here. It is sufficient to recognize that it can produce excitation currents of hundreds of kiloamperes at voltages of about [illegible] kV with a rise time near [illegible] ns. Because of the enormous power available from this generator LASER action has been observed in many systems in the VUV region.

j. Chemical Lasers[28] - Many exothermic chemical reactions lead to population inversion, primarily of the vibrational and rotational states of the ground electronic state of the diatomic product. This process has been studied by many, in particular [illegible] Polanyi and his associates [illegible] who proposed this mechanism for creating an inversion. Because chemical reaction energies can be very large compared with vibrational energy level spacing, a reaction can produce molecules which are excited to very high vibrational levels. In fact a major part of the energy that is liberated in many chemical reactions leads not to kinetic energy of the fragment products but rather to internal excitation.

One of the most important chemical lasers involves the production of excited HF or DF molecules. For example in the H + F_2 reaction [illegible] of the reaction energy appears in vibration so that the average vibrational level of the HF molecule [illegible]. Because the spacing between the vibrational levels of both the HF and DF molecules [illegible] from one vibrational level to another, a broad range of radiation wavelengths is emitted. In HF [illegible] nm, while in DF [illegible] 47 [illegible] nm. In addition each vibrational level has associated with it a large number of rotational sub-levels which lead to a large total number of different laser wavelengths. H_2 and F_2 do not undergo a rapid direct reaction. However in the presence of [illegible] hydrogen or fluorine they can react rapidly through the F+H_2 and H+F_2 elementary steps, which together form a chain of reactions leading to excitation. In most chemical LASERS operated thus far, it is necessary that free atoms be involved. These atoms can be formed in an electric discharge leading to cw operation in a [illegible] tube, or at high pressures in the TEA laser configuration, or in a flash photolysis apparatus where the chain of reactions is initiated by photo-dissociation.

6. APPLICATION OF LASER LIGHT[11]

Over twenty-five years ago at the time of the invention of the transistor one could predict essentially what has happened since that time. Because the transistor was an improved device for performing existing functions, its evolution was comparatively straightforward. The LASER on the other hand produces light that is different in its quality and intensity from light generated from any other source. [illegible] some of the more obvious uses of LASERS in existing [illegible], such as conventional interferometry will turn out to be less important than the development of new systems that take advantage of the unique characteristics of laser light. Perhaps the best example of this is found in the rapid development of the new field of *interferometry* known as holography, that is, the storage of three dimensional information in an interferogram. Though not a new idea the potentials of holography were realized only after the invention of the LASER.

Because of the highly specialized properties of the LASER which were discussed at length in comparison with other sources at the end of lecture I, properties such as brightness, spectral brightness, monochromaticity, spatial coherence, the fact that laser light effectively comes from a point source make possible applications and developments which had never previously been considered. Any list of applications prepared unquestionably will be out of date within a few years. The important point to remember is that laser light has now become an integral part of man's everyday experience, in the home, in the office, in the shopping centres, in manufacturing, communications and power production, in our military arsenal, and primarily in the research laboratory. The brightness of the source and the fact that it can deliver enormous power make it a hazard for man, particularly the most sensitive part of man, his eye. As we consider the various applications, try to keep in mind how and where this hazard exists and can be minimized. In subsequent lectures many aspects of this problem will be discussed.

a. LASERS in Metrology - Laser technology is important in the determination and maintenance of standards. However, the performance of He-Ne LASERS stabilized by saturated absorption in methane at 3390 nm

and iodine at 633 nm is such that they are being considered as frequency standards. These laser systems have shown a frequency stability comparable with the cesium-beam frequency standard now accepted and a reproducibility much better than the krypton-lamp length standard now universally used. Such reference systems are now commercially available. Based upon the accepted frequency and length standards, the velocity of light is now fixed at [illegible] m/sec. Even allowing for the improvement with LASERS, the value is not expected to change.

b. Communication and Information [illegible] LASERS will no doubt have their largest impact on the total human experience [illegible] information storage and retrieval. At optical frequencies the band width [illegible] transmitted through all telephone circuits, all radio [illegible] television [illegible] carried on one laser beam, provided the logic were available [illegible]. Besides the large information content that [illegible] advantage that an optical communication [illegible]. From the point of view of maintaining [illegible] interferences, such as from an electrical storm [illegible] an atomic blast, the optical communication [illegible]

Information [illegible] systems for short distances. However, [illegible] of such systems over long distances [illegible] communications [illegible] through small optical fibres [illegible] radio and television frequencies will [illegible]

The [illegible] the optical wavelength [illegible] in fibres [illegible] LASER [illegible] a high efficiency [illegible]

If the [illegible] rate and government files [illegible] the material [illegible] approach that [illegible] we have already [illegible] with [illegible] it is clear that [illegible] developed [illegible]

The heart of the [illegible]. The information [illegible] interference pattern is frozen within [illegible] LiNbO3 have [illegible] pattern [illegible] stored in one very [illegible] a [illegible] interference pattern. By transmission of [illegible] one can reconstruct the [illegible]. Written material [illegible] stored as a series [illegible] material. [illegible] library can then be transmitted to universities, companies, [illegible] a television receiver. Not only can information [illegible] and [illegible] be stored in multiple [illegible]. In the last few years [illegible] with digital [illegible] techniques, and television [illegible] understanding of the problem [illegible] retrieval [illegible]. Furthermore, it has made possible the active and continuing [illegible] that has never before been imagined.

c. Production and [illegible] power - The use of LASERS in power production is coupled intimately with nuclear [illegible] a large percentage of the cost is associated with a separation [illegible] demonstrated and will soon be the basis of commercial [illegible] LASERS can be [illegible] and subsequently [illegible] associated with a [illegible] the technical literature [illegible] LASERS, a large percentage [illegible] with [illegible] separation.

For the Canadian reactor, unlike the American system, the uranium that is used is unenriched. Nearly 40% of the total [illegible] associated with the production and handling of heavy water, the [illegible]. Normally, the heavy [illegible] deuterium, represents approximately [illegible] available in nature. [illegible] producing heavy water [illegible] with the first [illegible] LASERS are being used in an attempt [illegible] that are deuterium containing, in an attempt to especially separate them from the large bulk of material.

Probably the greatest call for high power laser technology is in the area of laser fusion. In order for fusion to [illegible] that either high powered gas or glass LASERS be developed that will deliver terawatts [illegible] watts [illegible] that is [illegible] seconds. [illegible] systems are nearing [illegible] high pressure gas LASERS are now working with efficiencies that approach [illegible]. It therefore [illegible] to imagine that laser systems can be [illegible] for the transmission of power over long distances and into awkward places. Unfortunately in the infrared, water vapour is a strong absorber, thus making it difficult to transmit power at these frequencies.

d. Lasers in the community - Besides the obvious application of laser technology to communications there are a number of other uses that are now being developed. Automated checkout for the supermarkets promises to be a multi-million dollar market for laser systems. At present the helium-neon LASER has assumed a place alongside the integrated circuit and the semi-conductor memory as a reliable electronic component in these systems.

Because of their high efficiency and brightness, LASERS are playing an increasingly important role in display systems. Furthermore, the possibility of eventually using injector LASERS for light bulbs is certainly real. For the moment, the LASERS that have been developed do not operate in the blue region of the spectrum. The efficiency of the present light bulb is approximately 10%, and their life is short. A blue diode LASER, such as SiC may be able to operate without being cooled with an efficiency approaching 25%. The coherent monochromatic radiation that would be produced could be converted to heterochromatic light by surrounding the LASER with the proper type of phosphor which would efficiently absorb the laser light, and reemit it over a broad band of frequencies. Such a system would be extremely simple, and long-lived. Before the application of infrared laser light to the cleaning of works of art, such as statues, and national monuments, the process has required many man years of painstaking labour to scrub the dirt from the surface with sand. Now with the aid of the high powered infrared LASER these objects d'art can literally be scrubbed with light. The light is preferentially absorbed by the soiled surface and the preferential heating of the dirt causes it to be boiled from the object. The same principle has been used with the laser eraser which is capable of vaporizing ink from paper without appreciably heating the paper. Museums have now included holographic techniques in their arsenal of weapons used in determining authenticity of works of art.

e. LASERS applied to pure and applied science - Lasers find their greatest application in scientific laboratories. The most obvious application of course is as a tunable light source reaching from the sub-millimeter range in the far infrared through down to the vacuum ultraviolet. The obvious primary use is of the tunable light source in conjunction with the standard spectroscopies. The spectral brightness of many laser sources makes them ideal for studying properties of atoms and molecules which otherwise could not be studied. With the aid of the LASER, investigation of non-linear optical phenomena has grown rapidly. Prior to the advent of the LASER in [illegible], the electric field strength associated with commonly occurring intense light sources might be in the vicinity of [illegible] volts/m. With the advent of the LASER, electric field strengths produced by LASERS are now well in excess of teravolts/m (10^{12} volts/m).

In much more modest fields multiphoton processes begin to occur within the material which lead to optical harmonic generation. The crystal potassium dihydrogen phosphate is one of the materials often used for this purpose. Often the efficiency for producing second harmonic frequency generation maybe in excess of 20%, although typical conversions are between 5 and 1 %.

As laser light interacts with gases, liquids and transparent solids, it is scattered both elastically or inelastically. Elastic scattering is called Raleigh scattering, while the inelastic scattering of light is called Raman scattering. Inelastically scattered light will contain lines corresponding to energy loss in exciting various rotational, vibrational and electronic states of the medium. If the light is intense enough it will also contain a series of lines corresponding to the addition of vibrational, rotational, electronic energy to the light of the LASER. This then becomes another very powerful tool for studying the internal structure of materials.

Essentially, Brillouin scattering in solids and liquids is the same process as Raman scattering. However replacing the vibrational rotational, electronic excitation is the motion of an acoustic wave within the material. The frequency of these acoustic waves can be added and subtracted from that of the laser light thus giving a rich spectrum reflecting their magnitude within the material.

Within the laboratory LASERS are often used as intense sources of radiation for pulse radiolysis, that is the time study of a system after energy has been rapidly introduced into it. Furthermore, the LASER is an excellent source of radiation for studying the interaction of non-ionizing radiation with living systems. For example in my laboratory, our primary interest is in studying laser radiation damage within the retina. We also use laser light to assist with detailed studies of basic mechanisms in colour vision.

The laser is now important in cellular microscopy. The effects of laser radiation upon the cell have been studied by a number of laboratories. The laser microscope also provides another instrument for micro-surgery of tissue cells and organelles. Laser radiation has now been used to monitor reactions in living systems involving brain cells, DNA, and RNA molecules. Because of the monochromaticity of the laser light and the small divergence of the beam, experiments can now be carried out down to sizes which approach one-half micron.

f. Industrial applications of LASERS - LASER technology is finding its way into virtually every aspect of industrial processing. The most dramatic application of LASERS of course is in industrial metal welding, drilling and cutting, ceramic machining and drilling, fabrication of high precision resistors, of printed circuitry, manufacturing standards control, package labelling, and so on. Let us consider a few more detailed examples.

This past year some of the underbodies for the Ford Montego and Torino are being welded with a 6 kw beam from a carbon dioxide LASER which was developed in the laboratories of United Aircraft. Similarly these high powered CO_2 systems are being developed for ship welding, thus cutting by ten the amount of time necessary for fabricating ship hulls. As with most laser systems used in industry, the welding system is invariably computer controlled. Laser beam welders are also important in the manufacture of automobile batteries (lead acid batteries) and in heat treating and surface hardening of such important parts as camshafts and valve seats. There appear to be definite advantages in using the LASER for heat treating since the rapid process leads to the minimum amount of part distortion.

As in the case of heavy manufacturing, the LASER is of importance in the chemical industry. As mentioned above, it is now effective in isotope separation of both uranium for fission reactors, potentially for producing heavy water as a moderator in the heavy water cooled reactors. Over the next few years its full potential will no doubt be developed.

g. Applications of LASERS to Medicine - The largest single use of LASERS in medicine is in therapeutic photocoagulation of ocular tissue. Up until the development of LASERS the greatest advancement has been the xenon Arc lamp. However, with LASERS one can now control the power, the spot size upon the retina, the irradiation time with the tunability of colour to match the absorption spectrum of the

material under irradiation.

Photocoagulation has now been extensively used in treating a number of diseases of the macula. For example, the majority of patients treated for serious central retinopathy have shown an improvement in visual acuity within three weeks. However, diabetic retinopathy is rapidly becoming a chief cause of blindness. It is now estimated that approximately 19% of the blindness in the U.S.A. is caused by such retinal changes. Coagulation of the retina is one of the major approaches to the control of this disease. Although the ruby LASER, which emits at 694 nm in the red, has been used, it has not been particularly successful. Instead, either the argon ion LASER which emits at 488 and 514 nm or the frequency-doubled neodymium doped YAG crystal which emits at 530 nm have more successfully been used. The relatively high absorption of the green wavelength by reduced or oxygenated hemoglobin makes these latter two lasers very attractive in the treatment of retinal vascular anomolies. Treatment of glaucoma, by poking a small hole in the iris with the LASER, has thus far been carried out in Russian laboratories.

In recent years, the LASER has become a surgical tool. Both the infrared CO_2(10,600 nm) and a green argon ion LASER (488 and 514 nm) have been effectively used as these radiations interact quite dramatically with tissue. The red ruby and He-Ne light are not appreciably absorbed by tissue, blood or water and consequently are of little use. The advantage of laser surgery is seen in the bloodless cut since vessels scar immediately. Attempts now are being made to use laser surgery in awkward places such as in the skull for the removal of cysts.

Because of the high power density and the monochromaticity which sets the defraction limit of the spot's size, the LASER is an excellent tool for microsurgery. Once again the choice of the critical wavelength is important since one is able to irradiate part of the subsystem of the cell with that frequency of light which is best absorbed by it.

The LASER is also being considered as a tool in dentistry. Thus far it has not readily been accepted but in the future it may be important in the treatment of special diseases and for mechanical construction in awkward places.

LASERS have also found extensive use in dermatology, particularly in those areas involving cosmetic changes such as the removal of tatoos, birthmarks, and growths. The early enthusiasm that developed around laser surgery associated with cancers has now lessened because it has been observed in many instances that treatment by the LASER has caused the diminishing of the original cancerous growth but has also caused it to spread to other areas.

h. Mining and Geological Applications of Lasers - One of the most common uses of LASERS now is in surveying. However, the monochromatic properties and its high spatial coherence have made it a superb tool for interferometric measurements of small earth crust movements. Extensive study has gone into the distortion of the earth's crust with the motions of tides and of earthquakes, and with the aid of the LASER, scientists throughout the world are now able to make predicitions as to when and where major earthquakes will occur.

The extreme power of the YAG, CO_2 gas LASER and some chemical LASERS make them excellent candidates for drilling and mining. Already LASERS are in the field in these areas.

LASER light was bounced from the moon. As a result, scientists have been able to determine very accurately the shape of the earth.

Laser radar or LIDAR is now playing a very important role in determining and monitoring pollutants in the lower atmosphere and the LASER is now playing a particularly important role in map-making.

j. Military applications of LASERS - Virtually every laser application thus far discussed finds a use within the military. Conversely, the hundreds of millions of dollars spent on laser-related research and development supported by military establishments not only finds application there, but has quickly found its way back into the community.

Information storage, processing and communications are of primary importance to the military. Integrated optic systems, which allow for coupling of the computers through optical fibres without electromagnetic interference are now commonly used in military systems. The use of holographic storage of information and the holographic techniques in map-making are now under consideration. The use of optical communicators between aircraft and between line posts are now under design. Some are presently in the field, as are laser range-finders and guidance systems.

The power associated with modern LASERS is sufficient for anti-personal weaponry. However, the main thrust will be in developing LASERS that can be used to ignite thermonuclear devices, and to detonate such devices in MERV war heads.

Although not strictly a military application, one of the "far-out" applications for the future will be the use of LASERS for space ship launching and propulsion in space. Such schemes are presently under study at NASA and have been proposed by such leading experts as Dr. Arthur Kantrowitz, Chairman of AVCO Research Laboratory. The magnitude of the LASERS necessary for such a scheme is mind-boggling; however Dr. Edward Teller, his teacher, was asked to comment upon the Kantrowitz proposal predicted: "It will happen before laser fusion will make a contribution in a practical sense. I am interested in... how soon the fusion energy we want to squeeze out of these microexplosions will really give economic power. And I believe propulsion of manned satellites will occur before that occurs."

7. REFERENCES

1. N.G. Basov and A.M. Prokhorov, Zh. Eksperim i Theor. Fiz 27, 431 (1954).
2. J.P. Gordon, H.J. Zeiger and C.H. Townes, Phys. Rev. 95, 282 (1954).
3. A.L. Schawlow and C.H. Townes, Phys. Rev. 112, 1940 (1958).
4. G. Chapline and L. Wood, Physics Today 28, No. 6 40 (1975)
   G.C. Baldwin and R.V. Khokhlov, Physics Today 28, No. 2 (1975).
5. F.J. McClung and R.W. Hellwarth, J.Appl. Phys. 33, 828 (1962).
6. R.J. Collins and P.P. Kisliuk, J.Appl. Phys. 33, 2009 (1962).
7. e.g., B.H. Soffer, J. Appl. Phys. 35, 2551 (1964).
8. e.g. P. Lallemand and N. Bloembergen, Phys. Rev. Lett. 15, 1010 (1965).
9. R.S. Adhav and A.D. Vlassopoulos, Laser Focus 10, 47 (1974).
10. D.J. Bradley, Endeavour 122, 90 (1975).
11. B.A. Lengyel, Lasers, (Wiley-Interscience: N.Y., 1971).
12. B. Lax, IEEE Spectrum, July 1965, p. 65.
13. e.g., P.P. Sorokin, J.R. Lankard, V.L. Moruzzi and E.C. Hammond, J.Chem. Phys. 48, 4726 (1968).
14. J.T. Warden and L. Gough, Appl. Phys. Lett. 19, 345 (1971).
15. L. Allen and D.G.C. Jones, Adv. in Phys. 14, 479 (1965).
16. A. Javan, W.R. Bennett and D.R. Herriott, Phys. Rev. Lett. 6, 106 (1961).
17. N.G. Basov, V.A. Danilychev, Yu.M. Popov and D.D. Khodkervich, JETP Lett. 12, 329 (1970).
18. W.B. Bridges, Appl. Phys. Lett. 4, 128 (1964), err 5, 39 (1964).
19. J.Wm. McGowan and R.F. Stebbings, Appl. Opt. (Chem.Lasers Sup.2), 68 (1965)
20. C.B. Collins, A.J. Cunningham and A.J. Stockton, Appl. Phys. Lett. 25, 6 (1974).
21. O.R. Wood, Proc. IEEE 62, 355 (1974).
22. A.J. Demaria, Proc. IEEE 61, 731 (1973).
23. A.J. Beaulieu, Appl. Phys. Lett. 16, 504 (1970).
24. M.C. Richardson, A.J. Alcock, K. Leopold and P. Burtyn, J.Quant. Electron QE-9, 236 (1973).
25. J.D. Daugherty, VII Quantum Electronic Conf., Montreal, 1972.
26. C.O. Brown and J.D. Davis, Appl. Phys. Lett. 21, 480 (1972).
27. e.g., W.J. Wiegano and W.L. Nighan, Appl. Phys. Lett. 22, 583 (1973).
28. A.N. Chester, Energia Nucleare 21, 23 (1972).
29. J.C. Polanyi, Appl. Opt. (Chem. Lasers Suppl.2) 109 (1965).
30. Modern Applications drawn from vol. 9, 10, and 11 Laser Focus.

ATE
LMED
8